AD

AD 747838

FRICTION WELDING OF MISSILE SYSTEMS HARDWARE

D. A. Seifert, K. E. Meiners, and
H. D. Hanes

BATTELLE
Columbus Laboratories

TECHNICAL REPORT AD

August, 1972

RESEARCH AND ENGINEERING DIRECTORATE
U. S. Army Missile Command
Redstone Arsenal, Alabama

Distribution of this document is unlimited

135

NOTICES

The findings of this report are not to be construed as an official Department of the Army position.

Destroy this report when no longer needed. Do not return it to the originator.

AD

FINAL REPORT

on

FRICTION WELDING OF MISSILE SYSTEMS HARDWARE

to

RESEARCH AND ENGINEERING DIRECTORATE
U. S. ARMY MISSILE COMMAND
REDSTONE ARSENAL, ALABAMA

by

D. A. Seifert, K. E. Meiners, and H. D. Hanes

Technical Report AD

August, 1972

BATTELLE
Columbus Laboratories
505 King Avenue
Columbus, Ohio 43201

Distribution of this document is unlimited

FOREWORD

This final technical development report was prepared by the Materials Processing Division of Battelle Memorial Institute, Columbus Laboratories, Columbus, Ohio, under the United States Army Contract No. DAAH01-71-C-0142. The work specified under this contract was under the monitorship of Mr. E. J. Wheelahan, AMSMI-RSM, Research and Engineering Directorate of the Army Missile Command, U. S. Army.

Authorization to print and distribute this report was given by Mr. S. A. Fedak, AMSMI-IPYB, Contracting Officer, U. S. Army Missile Command, Redstone Arsenal, Alabama.

Unclassified

Security Classification

DOCUMENT CONTROL DATA - R&D

(Security classification of title, body of abstract and indexing annotation must be entered when the overall report is classified)

1. ORIGINATING ACTIVITY (Corporate author) Battelle Columbus Laboratories	2a. REPORT SECURITY CLASSIFICATION Unclassified 2b. GROUP N/A

3. REPORT TITLE

Friction Welding of Missile Systems Hardware

4. DESCRIPTIVE NOTES (Type of report and inclusive dates)

Final Technical Report

5. AUTHOR(S) (Last name, first name, initial)

David A. Seifert, Kenneth E. Meiners, Hugh D. Hanes

6. REPORT DATE	7a. TOTAL NO. OF PAGES	7b. NO. OF REFS
	138	26

8a. CONTRACT OR GRANT NO. DAAH01-71-C-0142	9a. ORIGINATOR'S REPORT NUMBER(S)
b. PROJECT NO.	
c.	9b. OTHER REPORT NO(S) (Any other numbers that may be assigned this report)
d.	

10. AVAILABILITY/LIMITATION NOTICES

Distribution of this document is unlimited

11. SUPPLEMENTARY NOTES	12. SPONSORING MILITARY ACTIVITY
	Research and Engineering Directorate U. S. Army Missile Command Redstone Arsenal, Alabama

13. ABSTRACT

This report summarizes the program to establish cost-effectiveness criteria and to develop parametric data for friction welding of missile-systems hardware. A cost-effectiveness criteria checklist and summary of friction weldable materials are provided. Empirical models governing friction welding of thin-walled maraging steel structures were developed. Metallurgical, mechanical, and geometric aspects of friction welding 18Ni(250) maraging steel and 7075-T6 aluminum tubes are discussed. Mechanical property, friction-welding parameter, and thermal-history data are presented (26 references).

DD FORM 1 JAN 64 1473

Unclassified

Security Classification

14. KEY WORDS	LINK A		LINK B		LINK C	
	ROLE	WT	ROLE	WT	ROLE	WT
Friction Welding						
Maraging Steel - 18Ni(250)						
Aluminum Alloy - 7075						
Tubes						

TABLE OF CONTENTS

	Page
INTRODUCTION	1
EXPERIMENTAL APPROACH	2
Friction Welding Equipment and Facilities	2
Friction Welding Specimen Procurement and Fabrication	3
Phase I Investigations	8
Phase II Investigations	8
Phase III Investigations	11
Mechanical Testing	12
RESULTS AND DISCUSSION	18
Phase I Investigations	18
Phase II Investigations	23
Preliminary Investigations on Maraging Steel	23
Parametric Investigations of Friction Butt Welds Between Maraging Steel Tubes	30
Friction-Welding Investigations on 7075 Aluminum Tubes	45
Phase III Investigations	45
Half-Lapped Tube-to-Tube Joints	49
Half-Lapped Tube-to-Plate Joints	54
CONCLUSIONS	58
RECOMMENDATIONS	60
REFERENCES	61

LIST OF APPENDIXES

Appendix A.	Vendor's Analyses of Experimental Materials	63
Appendix B.	Summary of Materials Joined by Friction Welding	69
Appendix C.	Summaries of Friction-Welding Variables Investigated	73
Appendix D.	Thermal Histories of Friction-Welding Experiments	81

LIST OF APPENDIXES
(Continued)

		Page
Appendix E.	Summaries of Mechanical Properties	127
Appendix F.	Friction Welding Maraging Steel to Aluminum . . .	133

LIST OF FIGURES

Figure 1.	Friction-Welding Specimen Design for Half-Lap Tubular Joint Outer Component	5
Figure 2.	Friction-Welding Specimen Design for Half-Lap Tubular Joint Inner Component	6
Figure 3.	Flat-Plate Friction-Welding Specimen Design	7
Figure 4.	Design of Maraging Steel Tensile Specimen Fabricated From Longitudinal Section of Friction-Welded Tubes .	13
Figure 5.	Design of Aluminum-Alloy Tensile Specimen Fabricated From Longitudinal Section of Friction-Welded Tubes .	14
Figure 6.	Tensile Specimen Fabricated From Longitudinal Section of Maraging Steel Tube-to-Plate Joint	15
Figure 7.	Grip Assembly for Tensile Testing Tube-to-Plate Weld Joints	16
Figure 8.	Parent Metal Structure of 18Ni(250) Maraging Steel Tube Specimens	24
Figure 9.	Illustration of Grain Growth Adjacent to Friction Welds Caused by Prolonged Heating and/or Low Heat Generation Rates	25
Figure 10.	Illustration of Retention of Fine-Grain Structure and Grain Refinement Produced by Short Weld Cycles at Both High and Low Heating Pressures	26
Figure 11.	Illustration of the Effect of Increased Forging Pressure on the Microstructure of Maraging Steel Friction Welds	28

LIST OF FIGURES
(Continued)

Page

Figure 12. Microhardness of Friction Weld Between Maraging Steel Tubes Aged at 900 F for 3 Hours Prior to Welding . . . 29

Figure 13. Typical Test History for Friction Welding of Maraging Steel Tubes 31

Figure 14. Effect of Heating Pressure on Tensile Strength of Friction-Butt-Welded Maraging Steel Tubes 33

Figure 15. Effect of Axial Displacement During Heating on Tensile Strength of Friction-Butt-Welded Maraging Steel Tubes . 34

Figure 16. Effect of Forging Pressure on Tensile Strength of Friction-Butt-Welded Maraging Steel Tubes 35

Figure 17. Comparison of Strengths of Friction-Butt-Welded Maraging Steel Tubes With Those Derived From 168509-140703 exp $(-100V_H) + 703\ P_H + 2286\ P_F/P_H + 1.53\ S_L$ 37

Figure 18. Effect of Heating Pressure on Equilibrium Volumetric Displacement Rate for Friction Butt Welds Between 2.8-In.-Diameter Steel Tubes 39

Figure 19. Effect of Rotational Velocity on Change in Equilibrium Volume Displacement Rate With Axial Heating Pressure for Friction Butt Welds Between 2.8-In.-Diameter Maraging Steel Tubes 40

Figure 20. Microstructural Effects of the Greatest Differences in Cycle Variables for Friction Butt Welds Between Maraging Steel Tubes 42

Figure 21. Effect of Aging on Macrostructure and Hardness of Maraging Steel Friction Butt Welds 43

Figure 22. Microstructural Effect of Intermediate Anneal Prior to Aging of Maraging Steel Friction Welds 44

LIST OF FIGURES
(Continued)

Page

Figure 23. Typical Macrostructures of 7075-T6 Aluminum Friction-Welded Tubes 46

Figure 24. Typical Microstructure of 7075-T6 Aluminum Alloy Friction-Welded Tubes 47

Figure 25. Typical Microstructure of Half-Lap Joint Between Maraging Steel Tubes 49

Figure 26. Comparison of Strengths of Half-Lap Friction-Welded Maraging Steel Tubes With Those Derived From $319671-156489 \exp(-100V_H)-1866\sqrt{P_H} + 120774\sqrt{P_F/P_H}$. 52

Figure 27. Scanning Electron Micrographs of Tensile Fracture Surfaces of Half-Lap Friction-Welded Maraging Steel Tubes 53

Figure 28. Typical Interface Microstructures of Friction Welds Between Thin-Walled Tubes and Heavy Plates of Maraging Steel 56

Figure F-1. Microstructure of Friction Welded Joint Between Aluminum Alloy and Maraging Steel Tubes 137

LIST OF TABLES

Table 1. Characteristics of Battelle Mark II Friction-Welding Unit 3

Table 2. Experimental Matrices for Phase II Friction-Welding Investigations on Maraging Steel 9

Table 3. Conditions Investigated for Friction Welding 7075 Aluminum Tubes 10

Table 4. Experimental Matrix for Phase II Friction-Welding Investigations on Maraging Steel 11

Table 5. Criteria Checklist for Recognition of Potential Friction-Welding Applications 20

LIST OF TABLES
(Continued)

Page

Table 6. Empirical Relationship Between Strength and Independent Weld-Cycle Variables for Friction Butt Welds Between Thin-Walled Maraging Steel Tubes 36

Table 7. Empirical Relationship Between Strength and Independent Weld-Cycle Variables for Half-Lap Friction Welds Between Thin- and Thick-Walled Maraging Steel Tubes . 51

Table 8. Analysis Matrix of Factors Affecting the Quality of Half-Lap Friction Welds Between Thin-Walled Tubes and Heavy Plates of Maraging Steel 55

Table C-1. Friction-Welding Variables From Preliminary Phase II Studies on Maraging Steel 75

Table C-2. Friction-Welding Variables From Phase II Studies on Maraging Steel 76

Table C-3. Friction-Welding Variables From Phase II Studies on 7075 Aluminum 78

Table C-4. Friction-Welding Variables From Phase III Studies on Maraging Steel 79

Table E-1. Mechanical Properties of Maraging Steel Specimens From Phase II Studies 129

Table E-2. Mechanical Properties of 7075 Aluminum Specimens From Phase II Studies 130

Table E-3. Mechanical Properties of Maraging Steel Specimens From Phase III Studies 131

Table F-1. Summary of Conditions Used to Friction Weld Maraging Steel to Aluminum Tubes 136

INTRODUCTION

Recent improvements in the efficiency of solid rocket propellants have necessitated the use of stronger, more reliable materials for the construction of the various components, especially the motor cases, of small diameter ordinance missiles. Unfortunately these stronger materials such as the maraging steels and precipitation hardening stainless steels are considerably more expensive and difficult to fabricate than the older, more conventional materials. Since the missiles in question are not salvagable and are needed in large quantities, it would be highly desirable to reduce their overall cost by increased production efficiency and decreased material losses from machining and other production operations.

Friction joining presents itself as a particularly useful tool for the potential solution of these problems. This joining technique is not only fast and particularly amenable to high speed automated production operations, but offers joint properties approaching those of the parent materials with a high degree of reliability. Machining time and material losses can also be substantially reduced through friction joining by eliminating the need for internal machining of motor case components where thickness transitions are required solely to affect joining of various components by conventional fusion-welding techniques. Difficult forming operations might also be eliminated by the application of friction welding to fabrication of closed ended vessels from simple components rather than deep drawing or forging from sheet of billets.

It was, then, the purpose of this program to investigate and define those applications by which friction welding could increase the cost effectiveness of Missile Systems hardware production and to develop the engineering specifications necessary for the implementation of friction-welding technology by Missile Systems production contractors. A number of aspects associated with friction-welding technology were of interest to the sponsoring agency. First, it was important to define the values of the basic friction-welding parameters which would provide optimum material properties and production economics for a number of specific weld-joint configurations. Of particular interest were those configurations involving thin-walled tubes or hemispheres for at least one of the joined components. Also to be investigated were the feasibility of friction-welding component structures containing viscoelastic materials, and the need for internal support of thin-walled structures during friction welding.

EXPERIMENTAL APPROACH

A three-phased approach was used to define the applications and develop the engineering data pertinent to the incorporation of friction welding as a production tool in the fabrication of Missile Systems hardware. The initial phase of this study was directed toward identification of potential applications for friction welding in missile systems fabrication and the establishment of criteria to be used when considering the incorporation of friction welding into a particular missile-system fabrication process. Work under the second phase of the program was directed primarily toward determining the optimum friction-welding conditions and evaluating the effects of variations in these conditions for a joint configuration of primary interest to the Missile Command. The third phase of the program was concerned with application of the friction-welding technology gained during the second phase to two alternative joint configurations and to investigating the feasibility of friction welded joints between dissimilar materials.

Friction-Welding Equipment and Facilities

All friction-welding experiments in this program were carried out on the Battelle Mark II Friction Welder whose characteristics are shown in Table 1. The machine was fitted with two 4-jaw independent lathe chucks for holding and positioning both the rotating and stationary specimen components. Data output from the system were recorded on a Honeywell Model 1508 Visicoder Oscillograph capable of recording up to 24 channels of data directly on light-sensitive paper. This instrument was supplemented with the appropriate amplifiers and electronics for direct recording of axial force and torque through appropriately positioned load cells, axial displacement through two linearly variable differential transducers, linear and logarithmic rotational velocity through a tachometer-generator, and three independent temperature profiles through bimetal thermocouples. Time-base measurements were automatically recorded by the oscillograph. Permanent records of the friction-welding data were obtained by chemical processing of the photo-sensitive recording paper. Termination of the friction-welding cycle was triggered by axial displacement of the work pieces rather than by elapsed cycle time because of superior sensitivity of the displacement transducers (± 0.0005 in.) and because it was thought that this mode of termination would more accurately reflect the response of the workpieces to the friction-induced heating effects. Since the duration of the friction-welding cycle is directly connected with the economics of production operations involving the process and since most production operations utilizing domestically purchased equipment would necessarily be carried out by inertial rather than continuous drive friction welding, practically all of the experiments under this program were carried out with impulsive rather than gradual application of the axial heating pressure. This was accomplished by appropriate manual adjustment of the Data-Trak curve following programmer prior to initiation of the friction-welding cycle. In order to minimize the time necessary to stabilize the axial pressure when operating in this mode, an imbalance was permanently induced in the hydraulic system. This fixed the lower limits of applied axial load at about 2500 lb.

TABLE 1. CHARACTERISTICS OF BATTELLE MARK II FRICTION-WELDING UNIT

Rotational Speed - Linear control from 125 to 7500 rpm

Horsepower - Constant 25 hp delivered by a Synduction motor

Maximum Axial Load - 40,000 psi; can be programmed to follow any desired build-up

Braking System - Air-actuated, hydraulic disk brake

Specimen Size - Up to 8 inches directly in spindle up to 12 inches with face-plate attachment

Drive Mechanism - Constant-horsepower variable-speed drive

Methods for Terminating the Cycle - Time, torque, upset, and applied pressure

Friction-Welding Specimen Procurement and Fabrication

The materials of primary interest for this study were 18Ni(250) maraging steel, 17-7PH stainless steel, and 7075 aluminum alloy. Both the maraging steel and the precipitation hardening stainless steel were found to be unavailable in small quantities in tubular form. Approximately 12 feet of 7075-T6 aluminum-alloy tubing 3-in. OD by 0.250-in. wall thickness were, with considerable effort, found to be available from a surplus tubing dealer. Sufficient maraging steel sheet to complete both the Phase II and Phase III portions of the program was purchased from Teledyne-Vasco in compliance with MIL-S-46850-A. A copy of the vendor's certification is included in Appendix A. An eight-inch length of 18Ni(250) maraging steel bar stock 4-3/16 in. in diameter was purchased at the same time from the above vendor for use during the Phase III studies. Strict compliance with the MIL Spec was not required for this material. A copy of the vendor's analysis is included in Appendix A. The majority of the maraging sheet material was press-brake formed and seam welded into tube segments approximately 3 in. OD by 30 in. long by the Joining Technology Division of BCL using technology gained previously under Contract No. DAAHO3-69-C-0472 with the Army Missile Command. A small amount of approximately 3-in. -OD maraging steel tubing excess to that contract was obtained at no cost from the Joining Technology Division of BCL for preliminary welding studies so that an approximately six-week delay in the experimental program could be avoided. Because no source of 17-7PH stainless steel in tubular form could be found and development of the parameters for forming and welding sheets of this material into tubing was beyond both the scope and funding limitations of this program, this material was dropped from further consideration.

Fabrication of friction-welding specimens from the maraging steel tubes was begun by cutting them into approximately 3-in. lengths. Because these lengths were not perfectly round and contained residual stresses from the forming and seam-welding operations, they were pressed over stainless steel mandrels and annealed for approximately 15 min. after reaching a temperature of 1500 F. The difference between the thermal expansion coefficients of the stainless and maraging steels, 11.2 and 5.6 microinches/inch/deg F respectively, caused the maraging steel tube segments to be stretched into a nearly circular cross section which was retained upon cooling from the stress relief treatment. The segments were then machined to right circular cylinders having uniform wall thicknesses and ends perpendicular to their center axes. A square keyway was then milled across one end of each specimen for locking into the chucks of the friction welder. Each segment was given a number, thoroughly dimensioned, and the location of its seam weld was marked.

Most of the tubes for the Phase II study were machined to a diameter-to-wall-thickness ration (D/T) of approximately 30:1 but some were thinned to a ratio of 47:1 for studies to determine the effects of decreased wall thickness on welding parameters and properties. A number of 6-in.-diameter maraging steel specimens were fabricated from the remaining sheet material by rolling and TIG welding. These were given the same stress relief/stretch annealing treatment prior to machining as was described above. The diameter-to-wall-thickness ration (D/T) of these specimens was approximately 75:1 and they were used to evaluate the effects of increased diameter and D/T on welding parameters and resultant material properties.

The initial steps of tubular friction-welding specimen fabrication for the Phase III studies were carried out as described above. Additional machining was performed to produce the half-lap joint configurations shown in Figures 1 and 2. Flat disk specimens for the half-lapped tube-to-plate joint configuration studies were fabricated from the above mentioned 18Ni(250) maraging steel bar stock by sawing it into disks and then machining according to Figure 3. The tubular specimens for this study were the same as those shown in Figure 1 for the lapped tube-to-tube joint configuration.

Aluminum friction-welding specimens for both the Phase II and supplemental Phase III studies were prepared by cutting and machining the purchased tubing. The 7075 alloy specimens used in Phase II had a mean diameter of 2.83 in. and a diameter-to-wall-thickness ratio (D/T) of 23.8:1. The 6061 alloy specimens used for the supplemental Phase III investigations had a mean diameter of 2.79 in. and a D/T ratio of 14.4:1. The reason for the use of the

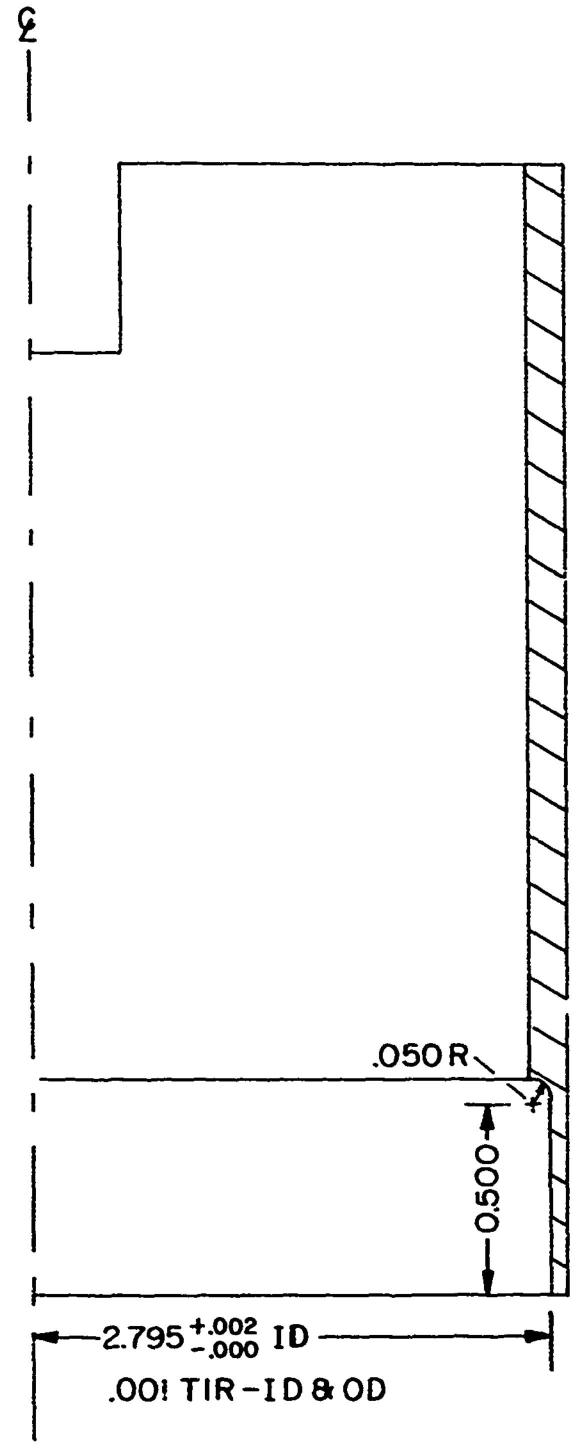

FIGURE 1. FRICTION-WELDING SPECIMEN DESIGN FOR HALF-LAP TUBULAR JOINT OUTER COMPONENT

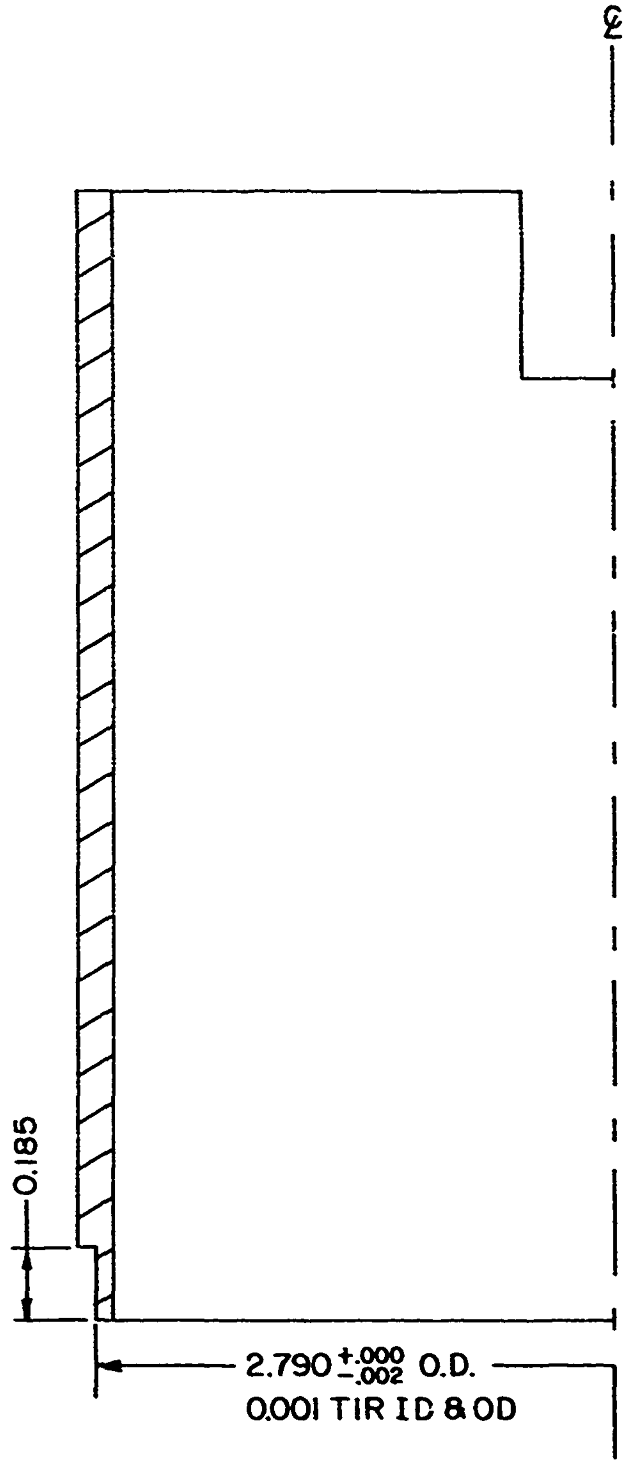

FIGURE 2. FRICTION-WELDING SPECIMEN DESIGN FOR HALF-LAP TUBULAR JOINT INNER COMPONENT

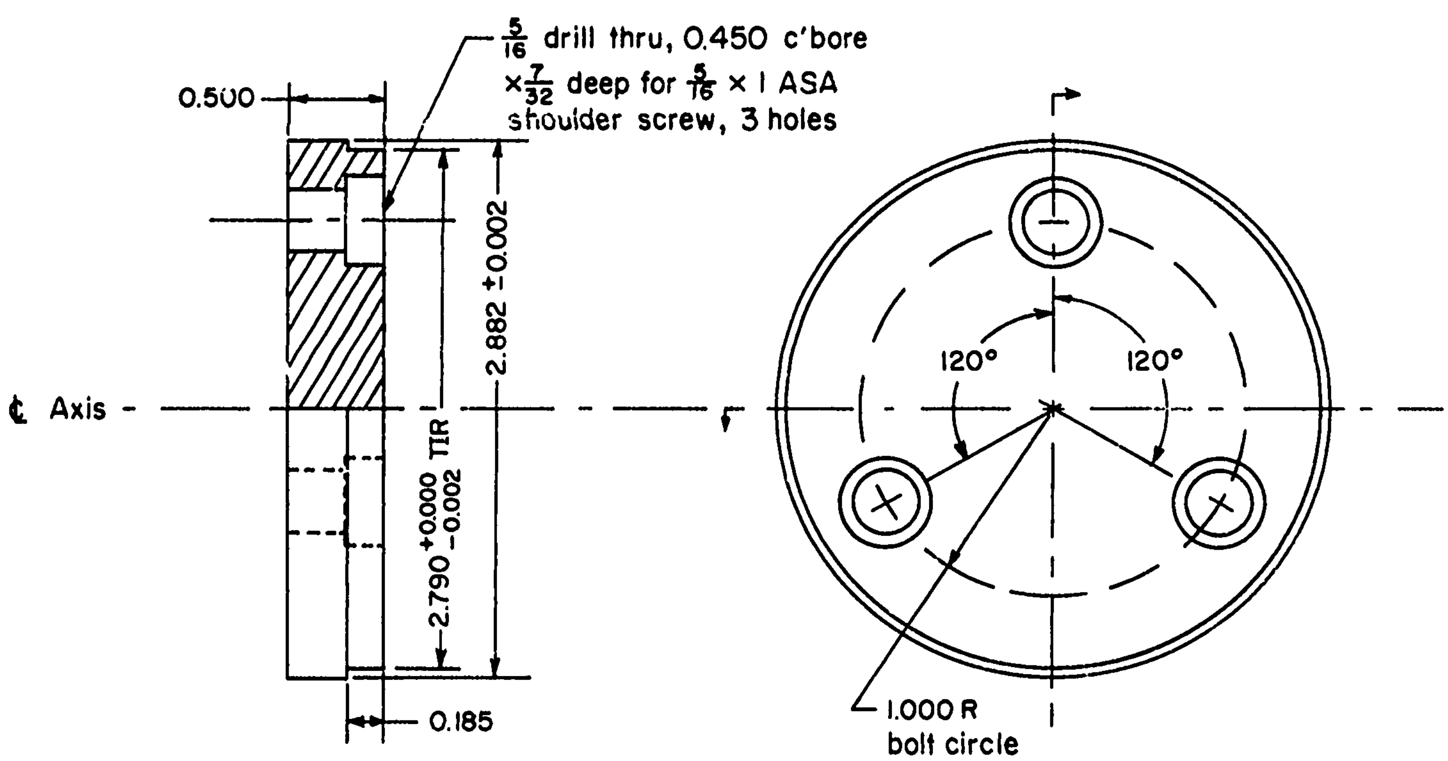

Note: Faces must be parallel and square with ℄ axis.

FIGURE 3. FLAT-PLATE FRICTION-WELDING SPECIMEN DESIGN

6061 alloy for this portion of the study will be explained in a later portion of this report.

Phase I Investigations

The initial phase of this study was directed toward identification of potential applications for friction welding in missile-systems fabrication and the establishment of criteria to be used when considering the incorporation of friction welding into a particular missile systems fabrication process. The search for potential applications of friction welding to missile-system fabrication was conducted through discussions with the Program Technical Manager and study of rocket motor designs presented in the Rocket Motor Manual.(1) Visits to prime missile systems contractors were deemed unnecessary by the Project Technical Manager and through mutual agreement with BCL, none were conducted. The establishment of criteria, both technical and economic, which must be considered when evaluating the potentials of incorporating friction welding into a missile-systems production process was undertaken through a survey of pertinent literature and by analyzing BCL's experience in the field.

Phase II Investigations

The second phase of the program was primarily concerned with optimizing the friction-welding parameters for a simple butt-type joint between thin-walled tube segments of like composition. Preliminary welding experiments were carried out using specimens fabricated from the 2.9-in.-OD maraging steel tubes obtained from the Joining Technology Division of BCL. It was the objective of these tests to determine the range of heating pressure, forging pressure, axial shortening (upset), rotational velocity, and braking which would produce contiguous welds in maraging steel tubes. Heating pressures between 3000 and 13,000 psi, rotational speeds of 1000, 1500, 2000, and 3000 rpm, preset axial shortening values between 0.002 and 0.040 in., and forging pressures between 3000 and 21,000 psi were tried with and without auxiliary braking. Evaluations were made by visual and metallographic inspection alone and neither temperature profiles nor mechanical properties were investigated.

The main portion of the Phase II experimental program was carried out using maraging steel tube specimens having a D/T ratio of about 30:1 and a mean diameter of about 2.83 in. Heating forces were arbitrarily set at 3000 lb, 5000 lb, and 8000 lb at rotational velocities of 1000, 2000, and 3000 rpm (surface velocities of 734, 1470, and 2200 sfm, respectively). Forging forces were varied from 6000 to 10,000 lb with axial displacements during heating being terminated at values ranging from 0.005 to 0.060 in. The actual conditions studied are summarized in matrix form in Table 2. Tensile properties in both the as-welded and maraged conditions were determined for all of these welding conditions. Free bend tests were also conducted in the as-welded condition for each of these welds. Temperature profiles at positions initially 1/16, 3/16, and 7/16 in. from the faying surfaces were also recorded for most of the welding experiments using Chromel-Alumel (Type K) thermocouples whose beads were securely resistance welded into shallow holes in the outer surface of the nonrotating specimen component. Studies to determine the scalability of the friction-welding process were carried out using maraging steel specimens having a mean diameter of about 2.80 in. with a D/T of about 47:1, and having a mean diameter of about 5.83 in. with a D/T of about 75:1. These experiments were carried out at conditions calculated to reproduce, as nearly as possible, the axial pressures, surface velocities, and axial displacements of those listed in the matrices below which had the best mechanical properties.

TABLE 2. EXPERIMENTAL MATRICES FOR PHASE II FRICTION WELDING INVESTIGATIONS ON MARAGING STEEL

A. Tests at 1000 rpm (743 sfm)

Forging Force (lbf) Applied After Upset U_H at Heating Force F_H

F_H \ U_H	0.010 in.	0.025 in.	0.035 in.	0.040 in.	0.061 in.
3000 lbf	18,000		12,000		6,000 18,000
5000 lbf	20,000	15,000		10,000	
8000 lbf	16,000	14,000		12,000	

B. Tests at 2000 rpm (1470 sfm)

Forging Force (lbf) Applied After Upset U_H at Heating Force F_H

F_H \ U_H	0.004 in.	0.010 in.	0.125 in.	0.015 in.	0.018 in.	0.025 in.	0.040 in.	0.055 in.
3000 lbf	18,000	12,000			6,000			
5000 lbf				15,000		12,500		10,000
8000 lbf			16,000			14,000	12,000	

C. Tests at 3000 rpm (2200 sfm)

Forging Force (lbf) Applied After Upset U_H at Heating Force F_H

F_H \ U_H	0.005 in.	0.010 in.	0.015 in.	0.020 in.	0.025 in.	0.035 in.	0.040 in.
3000 lbf	18,000	12,000		6,000			
5000 lbf			20,000		15,000	10,000	
8000 lbf			16,000		14,000		12,000

Friction-welding investigations on the 7075-T6 aluminum alloy tubes were carried out at 2000 rpm with heating pressures of approximately 2600, 3000, and 6000 psi, and forging pressures of 3000 and 6000 psi. Relative rotation was terminated at axial displacements of 0.010, 0.020, and 0.030 in. During the second experiment it was discovered that the initial torque peak accompanying impulsive loading to 3000 psi was enough to shear the safety pin in the friction-welder drive system and all remaining experiments using this material were carried out using pressure input rates of either 3000 or 6000 psi per second, a factor of 5 to 10 less than those experienced during impulsive loading. A summary of welding conditions investigated is given in Table 3. Temperature profiles were not recorded for these experiments. Metallographic, tensile, and bend-test evaluations were performed on these specimens.

TABLE 3. CONDITIONS INVESTIGATED FOR FRICTION WELDING 7075 ALUMINUM TUBES

Rotational Vel., rpm	Heating Force, lb	Forging force, lb	Preset Axial Upset, in.	Pressurization Rate, lb/sec
2000	2600	2600	0.035	Impulsive
2000	3000	3000	(a)	Impulsive
2000	3000	3000	0.035	3000
2000	0-5900	6600	0.030	6000
2000	0-5400	6000	0.030	6000
2000	0-3300	3600	0.030	3000
2000	0-3200	5800	0.010	3000
2000	0-3100	3200	0.030	3000
2000	0-3200	5800	0.010	3000
2000(b)	0-3100	3400	0.020	3000

(a) High initial torque generated by impulsive axial loading sheared friction welder drive pin causing premature cycle termination.

(b) Specimens heat treated 870 F, 50 min, water quenched prior to welding.

Phase III Investigations

The third phase of the program was concerned primarily with optimizing the friction-welding parameters for two different joint configurations using 18Ni(250) maraging steel components. The first of these was a half-lap joint between thin- and thick-walled tubular components while the other, also a half-lap type configuration, was a joint between a thin-walled tube and a relatively heavy plate. Both of these joint configurations were designed to prevent the formation of upset flash in the specimen bore and thus eliminate costly and time-consuming internal machining. The original intent that the parameters for a joint between dissimilar materials (e.g., 18Ni(250) maraging steel and 7075 aluminum) be rigorously investigated under this phase of the program was abandoned as a result of the Phase II investigations as will be explained in a later section of this report.

A two-factor, three-level experimental matrix, as shown in Table 4, was set up for both of these configurations and was based on information gained during the Phase II portion of this program. All tests were carried out at a relative rotational velocity of 2000 rpm with a heating pressure of approximately 9500 psi. The effects of forging pressure and axial displacement were studied. Tensile and metallographic properties were evaluated in both the as-welded and maraged conditions for all of these welding experiments. Temperature profiles for all of these weld cycles were recorded using a single Chromel-Alumel (Type K) thermocouple whose bead was securely resistance welded into a shallow hole in the stationary specimen at a distance of 1/16 in. from the original faying surface.

TABLE 4. EXPERIMENTAL MATRIX FOR PHASE III FRICTION WELDING INVESTIGATIONS ON MARAGING STEEL

All experiments conducted at relative rotational velocity of 2000 rpm (1470 sfm) and heating pressure of approximately 9500 psi.

Randomized order of performance for tube-tube/tube-plate configurations

U_H (b) \ P_F (a)	14,000	17,000	20,000
0.020	1/7	9/4	5/8
0.035	8/9	3/3	7/2
0.050	4/5	6/6	2/1

(a) Forging pressure, psi
(b) Predetermined upset for termination of weld cycle, in.

A cursory study of the ability to friction weld the maraging steel to 6061-aluminum alloy was also undertaken as part of this phase of the program. The tubular maraging steel specimens used were the same as those described above for the major part of the Phase II study and the aluminum specimens, machined from 3-in. -OD by 1/4-in. -wall drawn tubing, had a mean diameter of 2.79 in. and a D/T ratio of 14.3 for a distance of one inch from the faying surface. This heavier cross section of the aluminum specimens extending approximately equal distances past the surfaces of the mating steel tubes, was designed to eliminate or reduce the probability of the aluminum splitting and simply peeling away from the maraging steel during the friction-welding cycle. A discussion of the friction welding conditions investigated and the observations made during this cursory study will be presented in Appendix F of this report.

Mechanical Testing

Mechanical-property evaluations of friction-welded specimens were carried out in the Materials Processing Division's testing laboratory. Tensile testing was carried out on an Instron testing machine equipped with load/strain control. As far as possible, all testing was carried out in accordance with ASTM-E8-66 Tension Testing of Metallic Materials.[2]

Specimens for tensile testing friction welds between tubular components were fabricated according to Figure 4 for maraging steel specimens and Figure 5 for aluminum specimens. Wider grip sections were used on the maraging steel specimens to insure the availability of sufficient contact area with the flat wedge-type grips to prevent slippage. Fabrication of these specimens, both maraging steel and aluminum, was carried out by first sawing longitudinal sections from the friction-welded tubes. These were then stacked and clamped securely between heavy steel plates, cast in a rigid plastic, and ground to final dimensions. Tensile specimens for the tube-to-plate joint configurations were milled from the joined specimens according to Figure 6. A special grip for holding the plate side of these weld joints was designed and fabricated according to the sketch in Figure 7. As shown in the figure the stress axes of the upper and lower grips were offset some 0.022 in to eliminate the bending moment inherent in the specimen. This amount of offset, as determined by static moment analysis, brought the lower stress axis into alignment with the centroidal axis of the reduced thickness section of the specimen.

Whenever possible a 1-in. extensometer coupled to the testing machine data recorder was used to measure tensile strain as a function of tensile load until after yielding had occurred. Maraging steel specimens were tested at a free-running cross-head speed of 0.02 in. /min and aluminum alloy specimens at a speed of 0.01 in. /min. These extension rates, based on published elastic moduli of 26.3×10^6 psi[3] and 10.4×10^6 psi[4], respectively, were determined not to exceed the established maximum of 100,000 psi/min.[5]

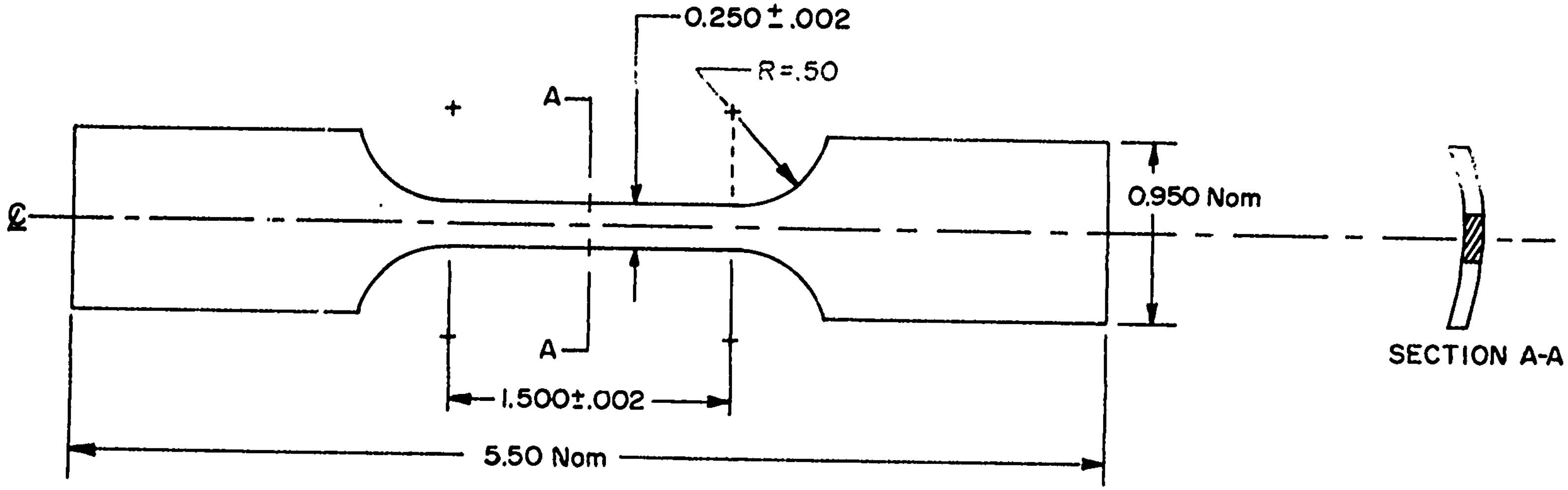

Notes
1. Blend radii-do not under cut.
2. Specimen edges are parallel to each other and perpendicular to plane tangent to specimen curved surfaces at ℄.

FIGURE 4. DESIGN OF MARAGING STEEL TENSILE SPECIMEN FABRICATED FROM LONGITUDINAL SECTION OF FRICTION-WELDED TUBES

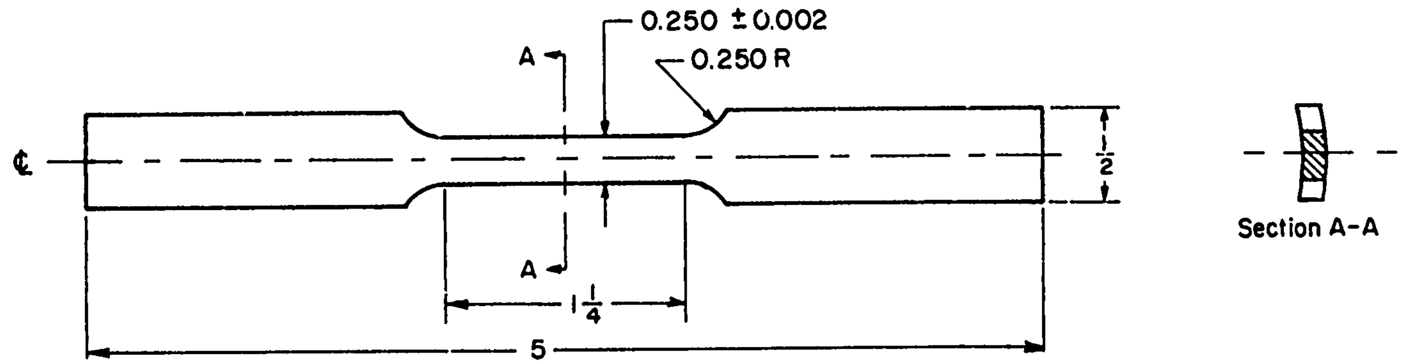

Notes:

1. Blend radii - do not undercut.
2. Specimen edges are parallel to each other and perpendicular to plane tangent to specimen curved surfaces at ℄.

FIGURE 5. DESIGN OF ALUMINUM-ALLOY TENSILE SPECIMEN FABRICATED FROM LONGITUDINAL SECTION OF FRICTION-WELDED TUBES

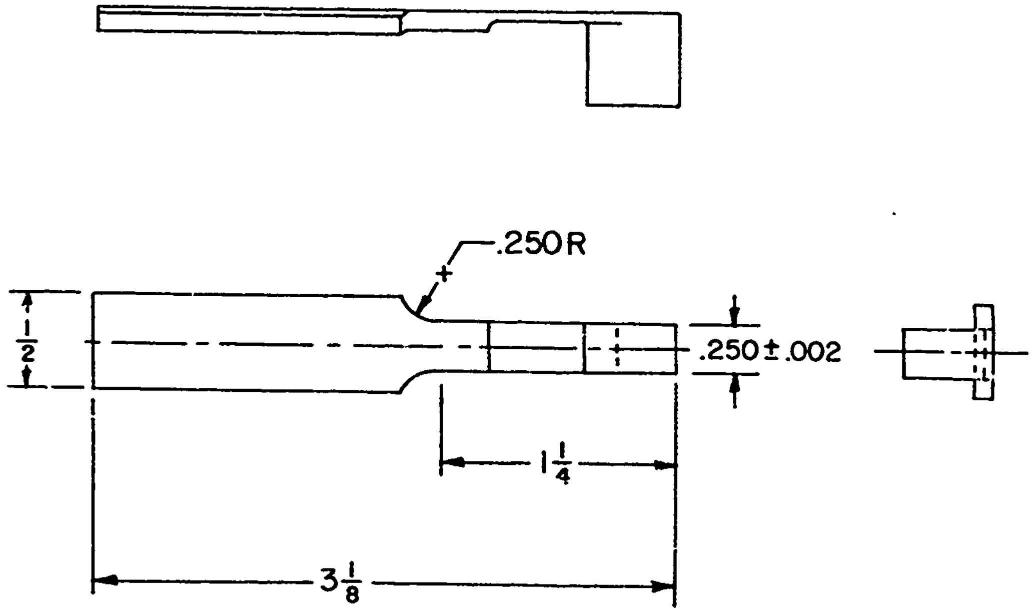

Notes:

1. Blend radii-do not under cut
2. Specimen edges are parallel to each other and perpendicular to plane tangent to specimen curved surfaces at ℄

FIGURE 6. TENSILE SPECIMEN FABRICATED FROM LONGITUDINAL SECTION OF MARAGING STEEL TUBE-TO-PLATE JOINT

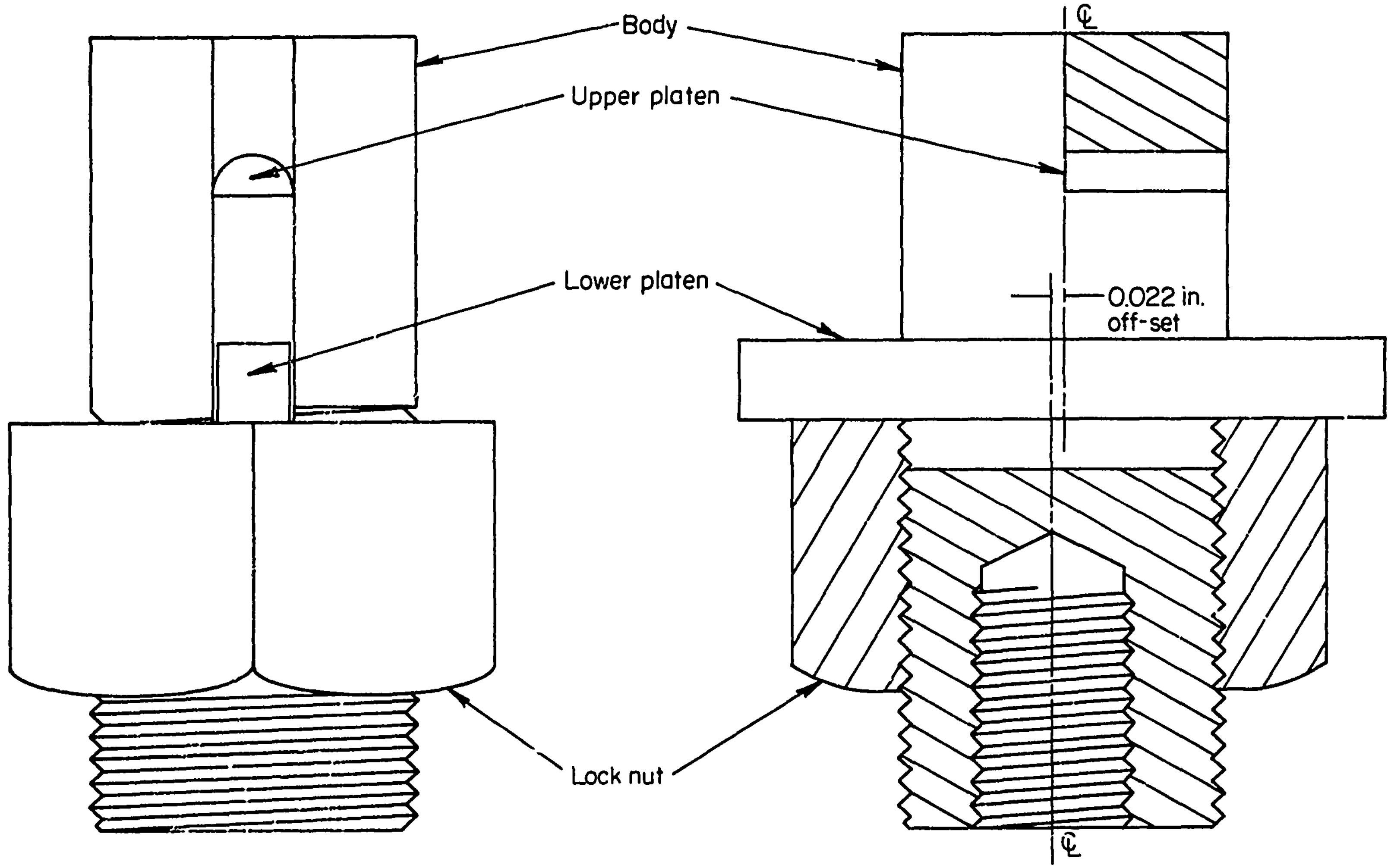

FIGURE 7. GRIP ASSEMBLY FOR TENSILE TESTING TUBE-TO-PLATE WELD JOINTS

Bend tests were conducted, as nearly as possible, in compliance with ASTM E16-64 Free Bend Test for Ductility of Welds.[6] Exceptions to this standard included use of a sharply veed ram during the initial bending. Neither were elongations measured as the tests were intended to be only qualitative in nature and were conducted only on the as-welded specimens. The approximate bend angle at rupture (when occurring) was measured. Specimens for this test were simply longitudinal sections approximately 1/2 in. in width sawed from the welded tubes.

RESULTS AND DISCUSSION

Phase I Investigations

The initial phase of this study of friction welding of missile systems hardware was concerned with identification of potential applications of friction welding to missile systems fabrication and to the establishment of criteria upon which the decision to incorporate friction welding into a specific missile-system production process might be based. These goals were accomplished principally through literature surveys and discussions of the needs of the Missile Command with the Program Technical Manager.

Several potential areas for the application of friction welding to missile-systems hardware fabrication were determined by careful study of designs presented in the Rocket Motor Manual.(1) Those missile systems such as XM-13 Shillelagh, MARC 16A1 Redeye, and M37A1 Improved Honest John Spin Rocket developed specifically for the Army were studied most carefully. In most instances the motor cases for these missile systems were fabricated by deep drawing or spin forging followed by machining of a suitable tool or alloy steel. The Honest John Spin Rocket had the simplest design and was fabricated from rolled and welded tubing.

Examination of the design sketches of each of the systems fabricated by deep drawing showed the motor cases to consist essentially of long thin-walled tubes with thickened end sections to permit attachment by either welding or mechanical fastening of end caps, nozzle assemblies, etc. One design even incorporated an intermediate thick-walled section for the support of internal hardware. Unless extremely sophisticated forming tooling and techniques were employed, fabrication of these motor cases would require a significant amount of costly and time consuming internal machining. Even the simplest design reviewed, that of the Honest John Spin Rocket, required the attachment of the head-end by welding.

The application of friction-welding technology to the fabrication of these rocket motor systems could greatly increase the cost effectiveness of their production by eliminating machining steps, speeding up production, and possibly by simplifying forming operations. Neither would the mechanical integrity of motor cases fabricated by this technique be sacrificed as friction-welded joints can be produced whose mechanical properties are as good as and sometimes better than those of the parent material. With the proper selection of joint configuration, essentially all internal machining could be eliminated from the production of wall-thickness transitions. Thick-and thin-walled tubular sections could simply be friction welded together in a matter of seconds using a half-lapped joint configuration. The need for deep drawing closed end tubes could also be eliminated by friction welding tubular case body sections to more easily formed separate end caps. Capital equipment expenditures might also be reduced somewhat by replacing deep drawing equipment, including associated heat-treat furnaces, with high production-rate friction welders. Tubing of the proper diameters and wall thicknesses could then be purchased in quantity from a commercial vendor, cut to the proper lengths, and friction welded together to form rocket motor-case bodies.

The assembly of other missile system components might also be facilitated through the use of friction welding. As shown in Appendix B, many dissimilar as well as similar materials have been successfully joined by various investigators.(7-14, 21, 22) Thus, the probability exists that guidance packages, warheads, guidance fins, and nozzle assemblies might be quickly and reliably joined to rocket motor cases by friction welding. These components, not required to withstand the extreme internal pressures of rocket engines could be fabricated from aluminum and other light-weight alloys.

The potential applications of friction welding to missile systems hardware presented above were discussed with the Program Technical Manager. On the basis of these discussions, three friction-welding joint configurations were chosen for study under the remaining two phases of this program. The joint configuration chosen for primary consideration was a simple butt-joint between thin-walled tube sections of similar materials while secondary joint configurations tentatively chosen for study under Phase III were a tube to plate or flange configuration utilizing similar materials, and a tube-to-tube configuration between dissimilar materials. Three materials of interest to the Army Missile Command, 18Ni(250) maraging steel, 7075 aluminum, and 17-7PH stainless steel, were chosen for study. Of these three, emphasis was to be placed on the maraging steel for all joint configurations between similar materials and on the maraging steel and aluminum alloy for dissimilar metal joints.

An additional result of the reviews of published literature and experience at BCL was the compilation of a "Criteria Checklist for Recognition of Potential Friction-Welding Applications". This checklist, as presented in Table 5, was oriented toward missile-systems applications and is intended to assist design and materials personnel in determining the technical feasibility and cost effectiveness of friction welding as a missile-systems production tool. The first two questions of the checklist are conceptual in nature and define the basic conditions necessary for the application of friction welding, on a cost effective basis, to the fabrication of missile-systems hardware. The third question presents a list of materials and configuration variables which must be compared when considering the technical feasibility of applying friction welding to the system in question.

Thermal conductivity and particularly thermal-expansion differences between the two components to be joined greatly influence friction weldability. Strength could also be an important factor. First, the strength of a friction welded joint between dissimilar materials is not likely to be much stronger than the weaker of the two. Second, and possibly more important, residual

TABLE 5. CRITERIA CHECKLIST FOR RECOGNITION OF POTENTIAL FRICTION-WELDING APPLICATIONS

SYSTEM ______________________________

This checklist is intended to assist designers and materials specialists in the recognition of potential applications where friction welding might simplify the fabrication of AMICOM hardware systems.

(1) Does system have rotational symmetry and/or are rotationally symmetric joints required between the various components?

(2) Would the incorporation of rotationally symmetric joints eliminate the need for extensive machining?

(3) Parametric considerations for evaluating merits of friction welding of components.

Parameter	Component A	Component B
Material		
Thermal Conductivity		
Thermal Expansion		
Strength		
Component Configuration		
Desired Diameter to Wall Thickness Ratio (D/T for tube configuration)		
Maximum D/T for Reliable Tube Joint		
Minimum Available Length (unsupported) for Design Considered – Tube Configuration		
Maximum Allowable Unsupported Length of Reliable Joint – Tube Configuration		
Maximum Allowable Upset (not removable) for Components Design		
Minimum Upset for Reliable Joint		

TABLE 5. (Continued)

Parameter	Component A	Component B
Maximum Allowable Temperature Rise at _______________ from Joint Interface		
Minimum Attainable Temperature Rise at _______________ from Joint Interface With/ Without Supplemental Cooling		

(4) Economic considerations for evaluating friction welding as a fabrication technique.

Factors Evaluated on a Per-Unit Assembly Basis	Fabrication Employing Friction Welding	Alternative Fabrication Technique
Capital and Tooling Costs		
Component Materials Costs		
Component Forming Costs (Machining, rolling, drawing, etc.)		
Joining Costs (including power requirements and time)		
Heat Treating Costs		
Overall Time to Fabricate One Assembly		
Overall Cost Per Assembly Produced		

stresses generated on cooling from the welding temperature by differences in thermal expansion could seriously weaken or even cause failure in some systems. Rigorous investigation of these factors may be, to some extent, bypassed if friction weldability of the two component materials in question has been previously established as given in Appendix B.

The physical design and shape of components to be friction welded could also influence the decision whether to incorporate friction welding in a production process, particularly where tubular components are involved. Such factors as diameter-to-wall-thickness ratios (D/T), area available for gripping the components, minimum proximity of faying surfaces to chucking devices, and allowable flash formation during welding must be considered.

Thermal considerations such as temperatures required at joint interfaces and allowable temperature distributions as a function of distance from joint interfaces may also be important for some applications. Several investigators(15-19) have provided mathematical models by which these factors may be estimated with reasonable accuracy once certain experimental information regarding heat-input rates, coefficient of friction, etc., are determined.

Information required for specification of friction-welding equipment for a particular joint configuration and materials combination can generally be determined only through experimental investigation. Power requirements are a prime example. The amount of torque generated at faying surfaces is highly dependent on coefficient of friction, a temperature and axial pressure dependent function, and configurations; e.g., for a given pair of materials and a fixed axial pressure, the torque generated during frictional heating is obviously greater for a tubular configuration than for a solid rod configuration having the same cross-sectional area. A Russian investigator(20) has suggested that a set of nomograms might be constructed for specifying the various friction-welding cycle variables based on a knowledge of the temperature dependence of the shear strength of the material being welded. The interrelationship between shear strength, speed of rotation, axial pressure, and time to reach equilibrium torque must still be experimentally determined for the configuration in question.

The fourth question of the "Criteria Checklist" provides a basis for comparison of the cost effectiveness of a fabrication process employing friction welding with an alternative fabrication technique. It is on this basis that a final decision regarding the applicability of friction welding to missile systems fabrication will be made. The comparison should, of course, be made on either a unit-time or a unit-assembly basis. Capital equipment and tooling costs should be averaged over the anticipated total production of the assembly required in the case of very specialized equipment or over the useful production lifetime of the equipment if it can be adapted to several applications. Materials costs for two processes under consideration should be comparable unless they are provided by the vendor in a more highly finished state for one of the processes. These materials-cost differences must, of course, be weighed against forming and joining costs. For example, the procurement of material in tubular form for a process involving friction welding, although initially more expensive on a unit-weight basis, would probably be less expensive than sheet material requiring numerous deep drawing, heat treating, and machining operations to bring it to the same state of completion as the friction welded components. Labor and overhead costs, usually a substantial portion of total fabrication costs, must also be considered on a unit-assembly basis. Any production operation requiring fewer process steps, and therefore fewer operators, and having a higher product output rate is then bound to be more cost effective than its competitor providing capital cost differences are not overwhelming.

Phase II Investigations

During the second phase of this program, friction-welding experiments were carried out using thin-walled tubular specimens of 18Ni(250) maraging steel and 7075-T6 aluminum alloy. Three series of experiments were carried out to evaluate the conditions which would produce optimum properties in butt welds between tubular segments of the above materials.

Preliminary Investigations on Maraging Steel

A series of some 30 friction-welding experiments were carried out using maraging steel tubes having a mean diameter of approximately 2.8 in. and a diameter-to-wall thickness ratio (D/T) of 30 to 34. The values of the friction-welding parameters (axial heating pressure, axial forging pressure, rotational velocity, axial displacement (upset), time, torque, and braking) used for these experiments are summarized in Appendix C.1. During the very first experiment it became apparent that the 4-jaw lathe chucks with which the Battelle friction welder is equipped, were not suitable for gripping friction-welding specimens of the type being studied in this program. Torque levels up to 270 ft/lb were generated at a relative rotational velocity of 1000 rpm and an axial pressure of 280 psi. This was sufficient to cause intermittent welding between the specimen components which in turn caused them to slip in the chucks. It was also found that the application of sufficient gripping force to prevent slippage in the 4-jaw chucks tended to cause significant distortion in the welding specimens which destroyed their rotational symmetry. These problems were overcome, for the purposes of this program, by milling a 1/2-in.-square notch diametrically across the rear face of each specimen and inserting a specially designed internal support structure which could be keyed to the friction welder chuck jaws and would prevent radial distortion of the specimens by the chuck jaws. These fixtures were used during all subsequent experiments. It is felt, however, that the use of such internal support would probably not be necessary in production situations where hydraulically actuated collets designed for the specific application and having significantly greater gripping surface areas would be used to hold the work pieces during friction welding. The purchase of collet type gripping fixtures especially for these studies was thought to be unnecessary in achieving the goals of this program.

Examination of the microstructures of these preliminary welds indicated that bonding is readily achieved over a wide range of welding conditions but that optimum microstructures, e.g., minimum perturbation of the parent metal structures, were considerably more difficult to produce. Since the parent metal had a very fine grain structure (about ASTM # 7) as shown in Figure 8, it was found that any set of welding conditions which generated more

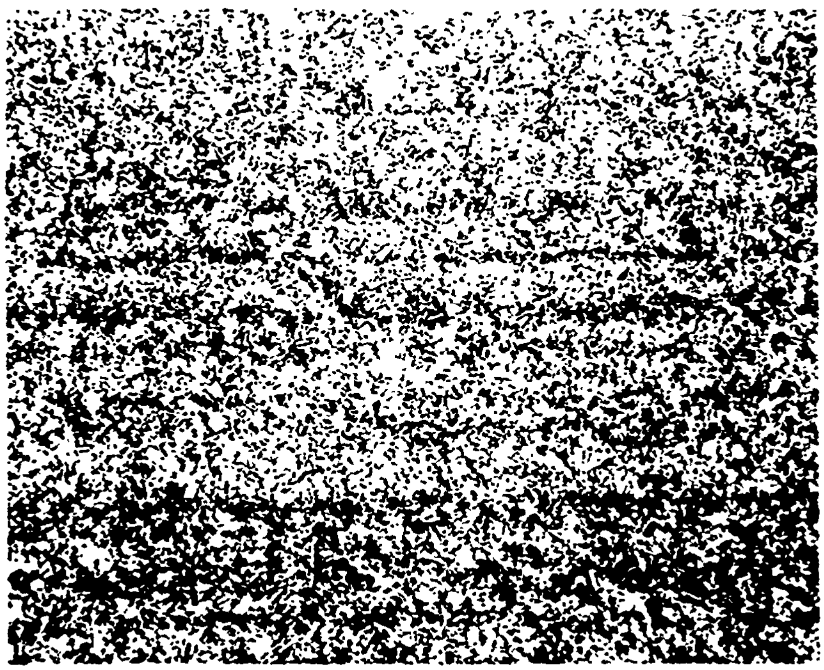

250X Vilella's Etch 1G535

FIGURE 8. PARENT METAL STRUCTURE OF 18Ni(250) MARAGING STEEL TUBE SPECIMENS

Aged 3 hr at 900 F.

than sufficient frictional heating tended to cause significant grain growth in the areas immediately adjacent to the weld interface. This was particularly true where heating rates were low and/or frictional heat generation times were long. This is illustrated in Figure 9, which shows the effects of (a) prolonged heating at moderate pressures and (b) heating at low contact pressures which increased the times required to achieve reasonable axial displacements. Excellent microstructures were achieved, on the other hand, at high heating and forging pressures and moderate speeds and at low heating pressures and speeds as shown in Figure 10. Unfortunately, however, those conditions

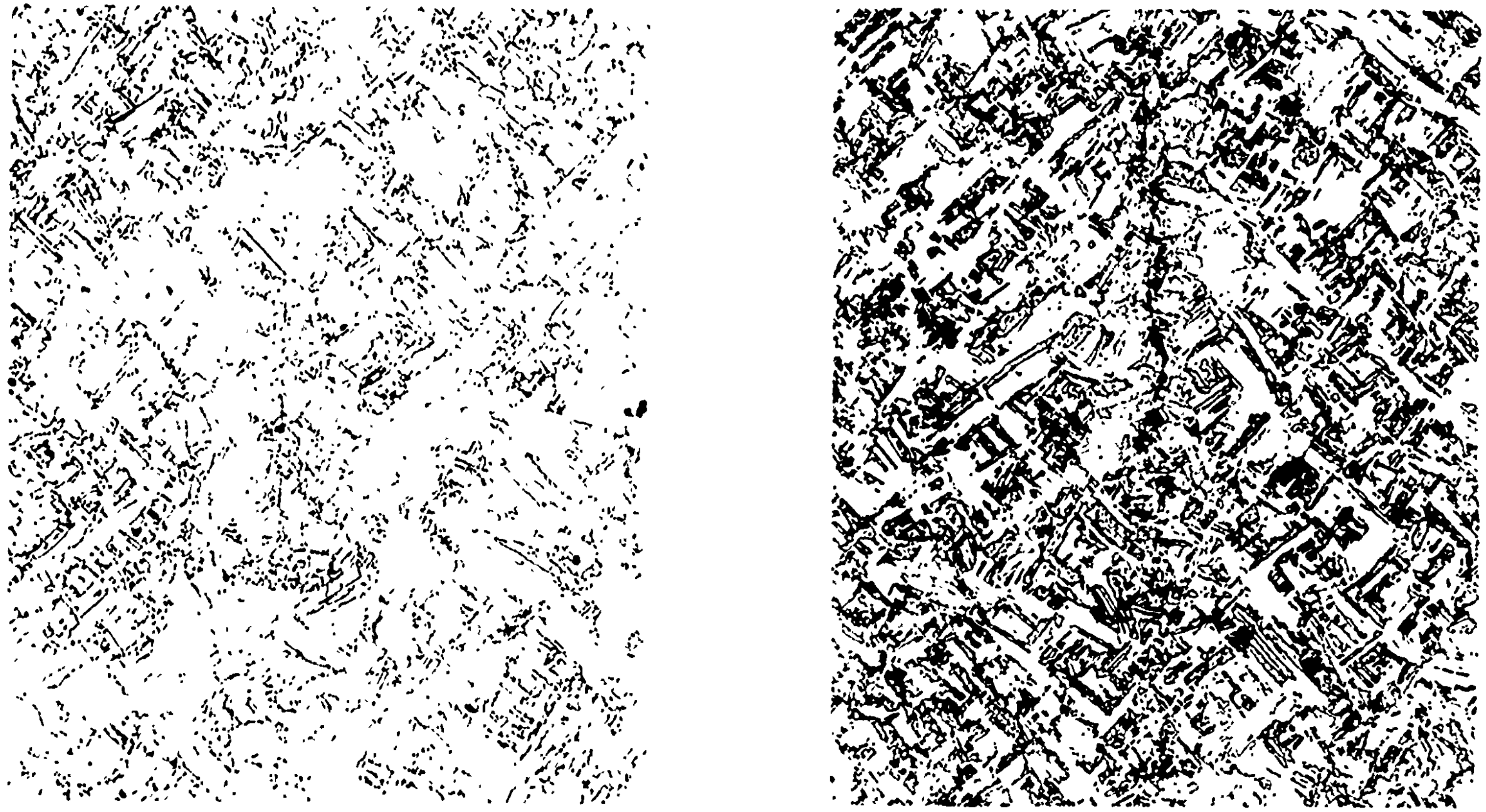

100X $2OH_2O$, $10HNO_3$, $20HCl$, 1/2 g $FeCl_3$ 5F433

(a) Welding conditions: 1000 rpm; 5840 psi heating pressure; 6360 forging pressure; approximately 0.4 in. upset; 21 sec (as welded).

100X 100 Picral, 2HCl, $2HNO_3$ 6F939

(b) Welding conditions: 1500 rpm; 3880 psi heating pressure; 6700 psi forging pressure; 0.044 in. upset; 5.1 sec (as welded).

FIGURE 9. ILLUSTRATION OF GRAIN GROWTH ADJACENT TO FRICTION WELDS CAUSED BY PROLONGED HEATING AND/OR LOW HEAT GENERATION RATES

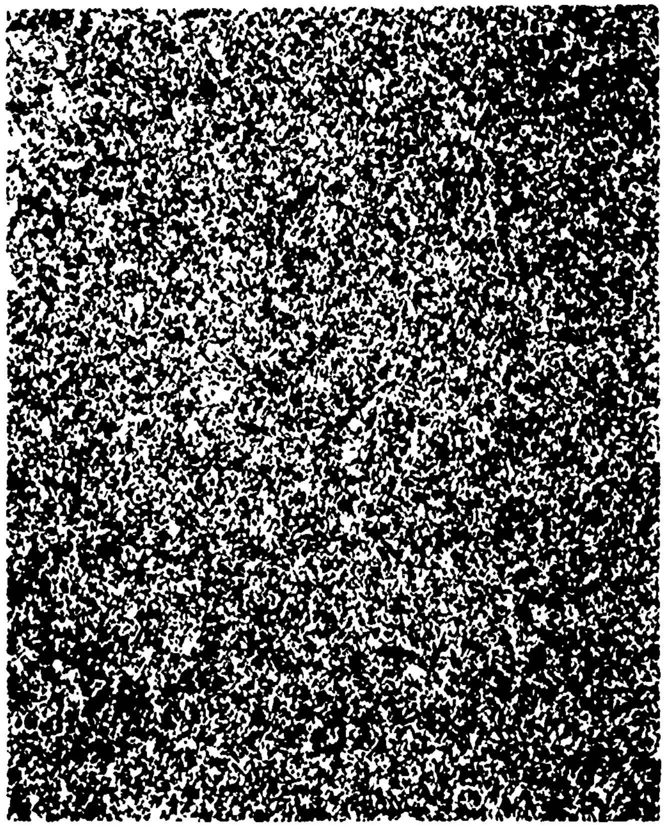

100X 100 Picral, 2HCl, $2HNO_3$ 6F936

(a) Welding conditions: 2000 rpm; 11,960 psi heating pressure; 21,290 psi forging pressure, 0.045 in. upset; 0.88 sec (as welded).

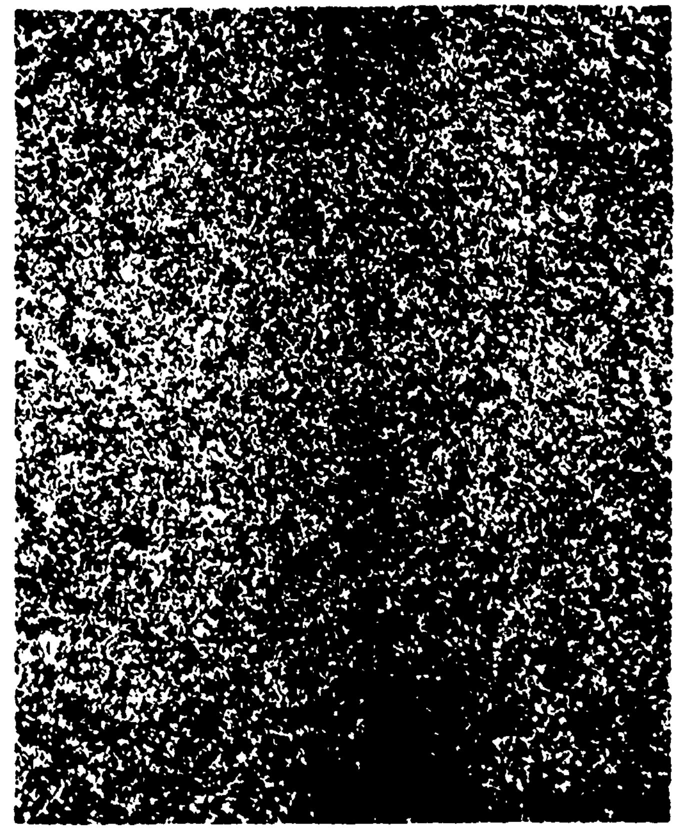

100X $20H_2O$, $10HNO_3$, 20HCl, 1/2 g $FeCl_3$ 5F431

(b) Welding conditions: 1000 rpm; 3880 psi heating pressure; 3880 psi forging pressure; 0.003 in. upset; approximately 1 sec (as welded).

FIGURE 10. ILLUSTRATION OF RETENTION OF FINE-GRAIN STRUCTURE AND GRAIN REFINEMENT PRODUCED BY SHORT WELD CYCLES AT BOTH HIGH AND LOW HEATING PRESSURES

which produced good microstructures at low axial pressure and rotational speeds did not achieve axial displacements sufficient to insure bonding over the entire faying surface areas.

Preliminary studies on the effects of forging pressure indicated that, in general, increasing the forging pressure above the level of the heating pressure tended to reduce the width of heat affected zones and to produce some grain refinement at the weld interfaces, particularly where relatively low (3000 to 5000 psi) heating pressures were used. This is illustrated in Figure 11, where, after heating for approximately 3.7 sec. at an axial pressure of 4800 psi and a rotational speed of 2000 rpm, axial pressure was (a) not significantly increased and (b) was approximately doubled at termination of the weld cycle. Some disadvantages to the use of high axial forging pressures were also found as the possibility of axial misalignment in the welded specimens was increased, particularly where heat inputs were high and prolonged and/or specimen support was relatively distant from the faying surfaces.

Investigation of the effects of braking or stopping time on weld integrity were undertaken but were discontinued when it was discovered that the main result of failure to use auxiliary braking was to increase the probability of axial misalignment and destruction of axial or rotational symmetry in the welded tubes. This was most apparent where high forging pressures were used and was probably more a result of the friction-welder design than any other factor. Since the application of both auxiliary braking and forging pressure are triggered by microswitches activated when the spindle drive system is disengaged, failure to use auxiliary spindle braking produces a significant increase in axial pressure while rotational speeds are still relatively great. This results in increased torque which tends to cause distortion of the specimens' axial symmetry. These tendencies could, in retrospect, be overcome either by redesigning the friction welder so that forging pressure is not applied until after rotation completely ceases or by providing rigid support for the work pieces in close proximity to the faying surfaces. It was found during the course of this investigation that, for the specimen geometries under consideration, rigid support of the work pieces at a distance of about 1/2 in. from the faying surfaces was, for all practical purposes, sufficient to eliminate the tendency of the forging force to cause axial misalignment and distortion.

One of the objectives of this program was to determine the feasibility of friction welding together missile-systems components which contained certain viscoelastic materials. In the case of maraging steel this would mean friction welding together previously maraged components. A single experiment was conducted to investigate this possibility by welding together two tube segments which had been previously maraged for 3 hr at 900 F. Welding conditions which had previously been shown to yield satisfactory weld microstructures were used for this experiment. After welding, the specimen was examined metallographically and a microhardness trace across the weld interface made. As shown in Figure 12, a distinct loss of

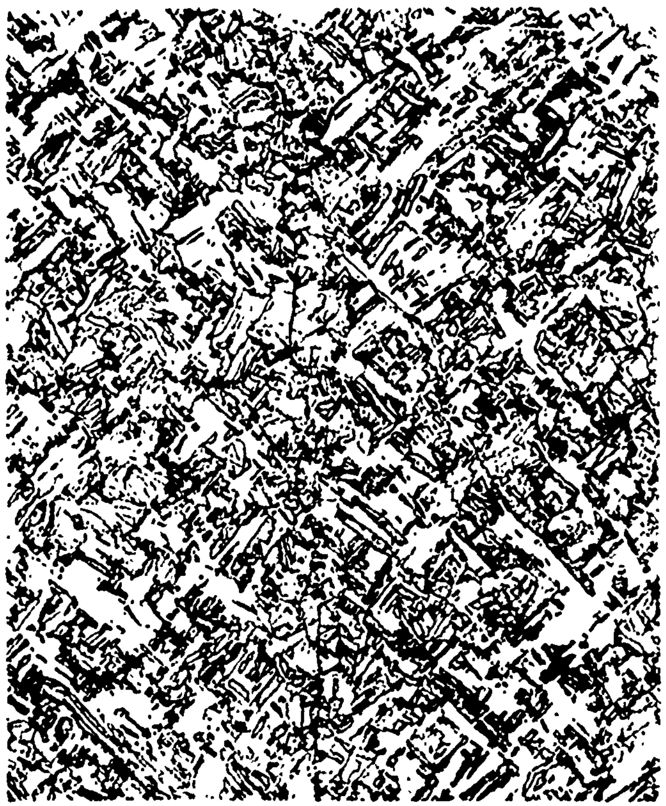

100X 100 Picral, 2HCl, $2HNO_3$ 6F414

(a) Welding conditions: 2000 rpm; 4830 psi heating pressure; 5160 psi forging pressure; 0.033 in. upset; 3.73 sec.

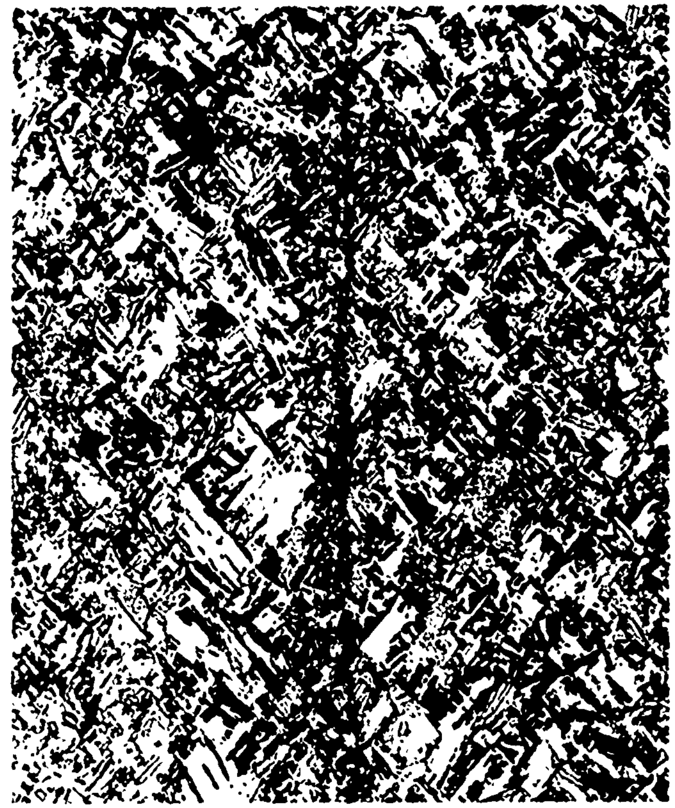

100X 100 Picral, 2HCl, $2HNO_3$ 6F413

(b) Welding conditions: 2000 rpm; 4740 psi heating pressure; 9360 psi forging pressure; 0.038 in. upset; 3.72 sec.

FIGURE 11. ILLUSTRATION OF THE EFFECT OF INCREASED FORGING PRESSURE ON THE MICROSTRUCTURE OF MARAGING STEEL FRICTION WELDS

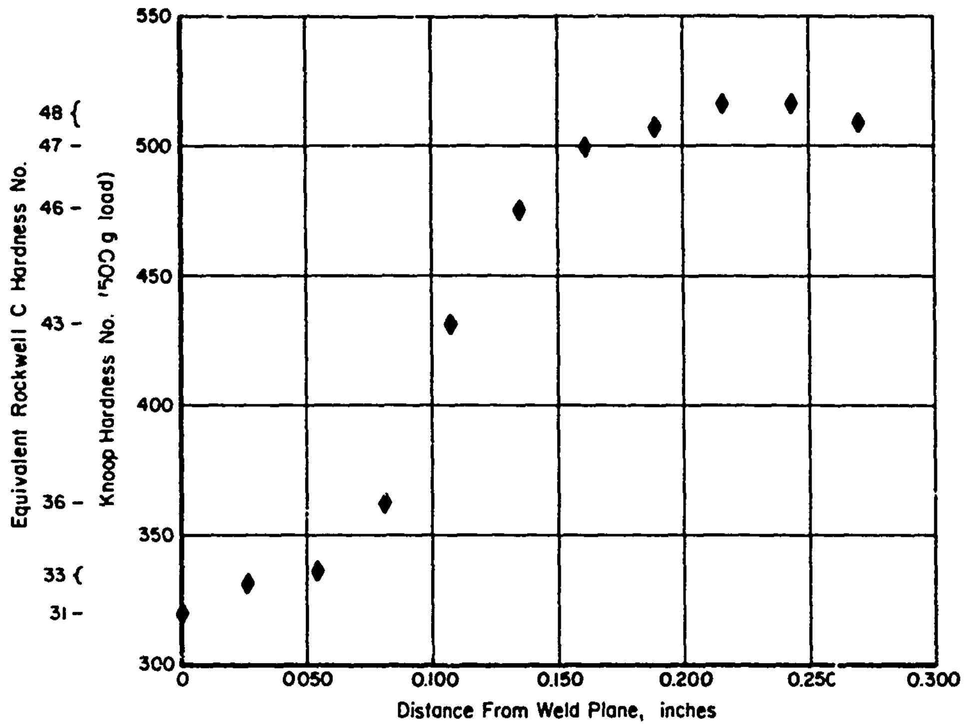

FIGURE 12. MICROHARDNESS OF FRICTION WELD BETWEEN MARAGING STEEL TUBES AGED AT 900 F FOR 3 HOURS PRIOR TO WELDING

hardness was evident at the weld interface. This, as was not unexpected, was probably caused by rapid resolutioning of the Ni_3 Ti and Fe_2Mo precipitates which give maraging steel its extraordinary strength and toughness(23, 24). A band of decreased strength commensurate with the band of reduced hardness was probably therefore generated. This would have to be removed by an additional maraging treatment to realize the optimum properties of maraging steel. Such a heat treatment would, in the very least, be detrimental to any contained viscoelastic material as well as requiring two maraging heat treatments for each component produced. In view of these results it was decided that further friction-welding studies involving previously maraged specimens would be unwarranted. This and a previous experiment had already indicated that the conditions needed to weld maraged tubes did not differ significantly from those needed to weld maraging steel tubes in the solution annealed condition.

Parametric Investigations of Friction Butt Welds Between Maraging Steel Tubes

Based on the information gained from the preliminary investig tions discussed above, an experimental program was set up to study the effects of the independently controlled weld-cycle variables on the mechanical and microstructural properties of friction butt welds between thin-walled maraging steel tubes. It was initially intended that a total of nine experiments encompassing three levels of heating force, three levels of forging force, and three levels of axial displacement would be performed at each of three rotational velocities using tubular specimens having a mean diameter of about 2.8 in. and a diameter-to-wall thickness ratio of about 30:1. The experimental matrices, shown in Table 2, did not follow the original plan because of several factors. First, the limit of sensitivity of the friction-welding machine did not always result in exact duplication of applied forces; and second, mechanical difficulties with the clutch mechanism did not always permit termination of the weld cycle at the prescribed axial displacement. Neither were differences in specimen cross-sectional areas accounted for when performing the elding experiments. Additional experiments, using specimens having mean diameters of about 2.8 in. and D/T's of 45 to 49 and specimens having mean diameters of about 5.8 in. and D/T's of 75 to 85 were performed to investigate the scalability of those weld-cycle variables proven by mechanical-property tests to have produced acceptable welds in the 2.8 in. in diameter, 30:1 D/T specimens. All of the weld-cycle variables and specimen geometries from the Phase II study are summarized in Appendix C.2. A typical friction-welding test history, from which these data were derived, is shown in Figure 13. Time-temperature profiles for each of the Phase II friction-welding experiments were determined from thermocouples embedded in the surfaces of the nonrotating specimen components at distances initially 1/16 in., 3/16 in., and 7/16 in. from the faying surfaces. These data are summarized graphically in Appendix D but will not be treated rigorously because of the complex relationships involved[17, 18, 19] and because the property changes discussed above which occur during the welding cycle have essentially necessitated subsequent heat treatment to achieve full properties and therefore precluded the possibility of friction-welding components containing those viscoelastic materials which were the primary reason for concern over heat generation. Bend and tensile-property data in both the as-welded and subsequently maraged conditions for these friction-welding experiments are summarized in Appendix E, along with base-metal property data. Microstructural ariations resulting from changes in welding conditions were more subtle and will not be presented in summary form but rather will be described in general terms later in this discussion.

It was the primary purpose of this program to determine the interrelattionships among the independent (controllable) friction-welding cycle variables, e.g., rotational speed, axial heating pressure, axial forging pressure, and axial displacement (or, alternatively, heating time), and their effects on resultant weld quality for the purpose of enabling engineers and

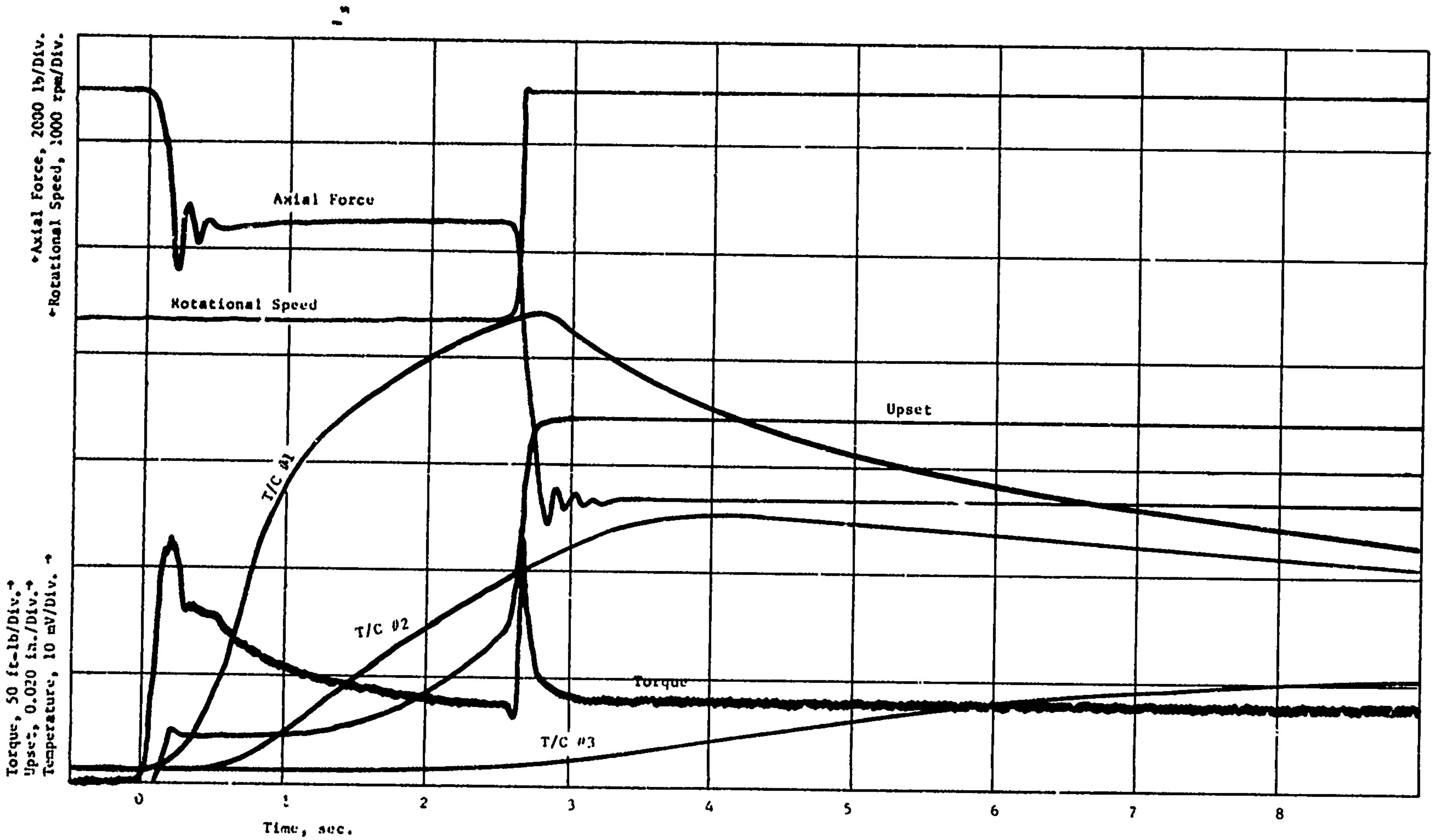

FIGURE 13. TYPICAL TEST HISTORY FOR FRICTION WELDING OF MARAGING STEEL TUBES

designers to specify the equipment and process characteristics necessary for the reliable and economical incorporation of friction welding into missile systems production operations. In order to accomplish this end, the mechanical properties, specifically tensile strengths, were first examined with respect to each of the independent variables individually. This was done graphically as shown in Figures 14 through 16. It was immediately apparent from these representations of the data that no single independent variable was particularly predominant in controlling the tensile strength of friction butt welded maraging steel tubes. Similar correlations between ductility (elongation at rupture) and the independent cycle variables were considerably less conclusive while those involving either strength or ductility with rotational speed were decidedly inconclusive. It was therefore decided that a relatively complex relationship in which each of the independent variables contributes to the attainment of the resultant weld properties must exist.

Multiple correlation/regression techniques using a relatively broad but powerful statistical analysis computer program[25] were applied to all of the data generated during the Phase II investigations in order to determine the influence of each of the independent weld-cycle variables on the strength of friction-welded maraging steel tubes. Examination of the data as presented in Figures 14, 15, and 16, suggested that axial displacement and heating pressure had a stronger influence on mechanical properties than did forging pressure or relative rotational velocity. Further, the trends suggested by these data indicated that the functional relationship between tensile strength and both upset and heating pressure should be either exponential, logarithmic, or parabolic in form and that forging pressure should have a weak parabolic relationship with tensile strength. All combinations of these functional relationships along with linear and logarithmic functions of surface velocity were fit to the data and evaluated statistically. The most satisfactory statistics, e.g., multiple correlation coefficient, standard error, and F-ratio, were obtained for a polynomial describing tensile strength as dependent on the exponential of axial displacement, U_H, the square root of heating pressure, P_H, the square root of the ratio of forging pressure, P_F, to heating pressure, and on linear surface velocity. The relationship was statistically improved by normalizing the axial displacement values based on specimen cross-sectional areas in terms of volume of material displaced from the faying surfaces. The relationship thus obtained is presented in Table 6, along with the relevant statistics. This relation is taken to be valid for butt-welded maraging steel tubes having mean diameters between 2.8 and 5.8 in. with D/T ratios between 30:1 and 85:1. According to the statistics presented in the table, the regression model accounts for some 55 percent of the variance observed in the tensile strengths and strength data predicted from the model should not be in error more than 10 percent of levels greater than 218,000 psi. A comparison of actual tensile strengths with those predicted from the regression equation is presented in Figure 17. It can be seen from this relation that most of the experimentally determined strength data fall within the standard error limits of the model except at the lower strength levels where the density of experimental data points is much lower. The solid

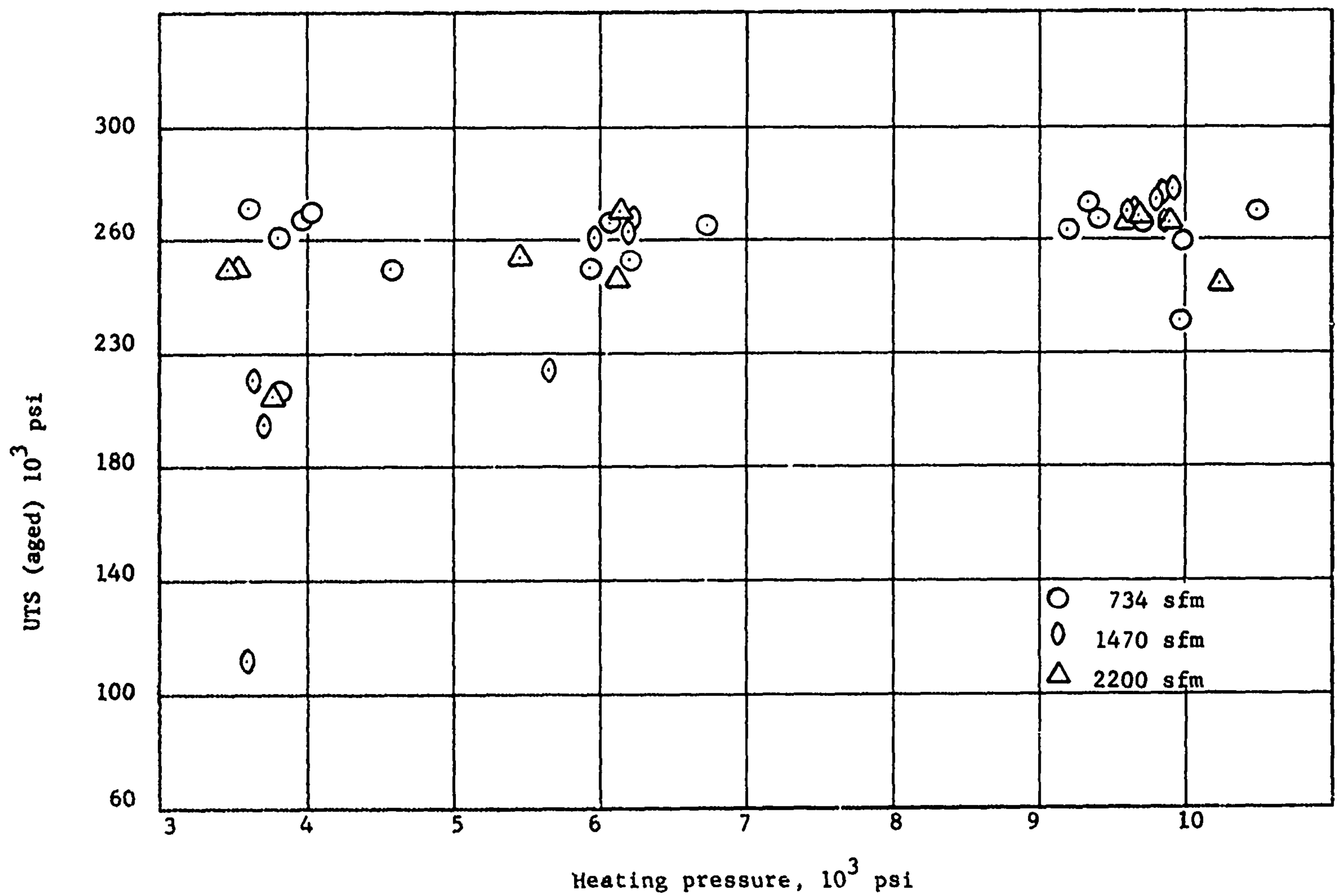

FIGURE 14. EFFECT OF HEATING PRESSURE ON TENSILE STRENGTH OF FRICTION-BUTT-WELDED MARAGING STEEL TUBES

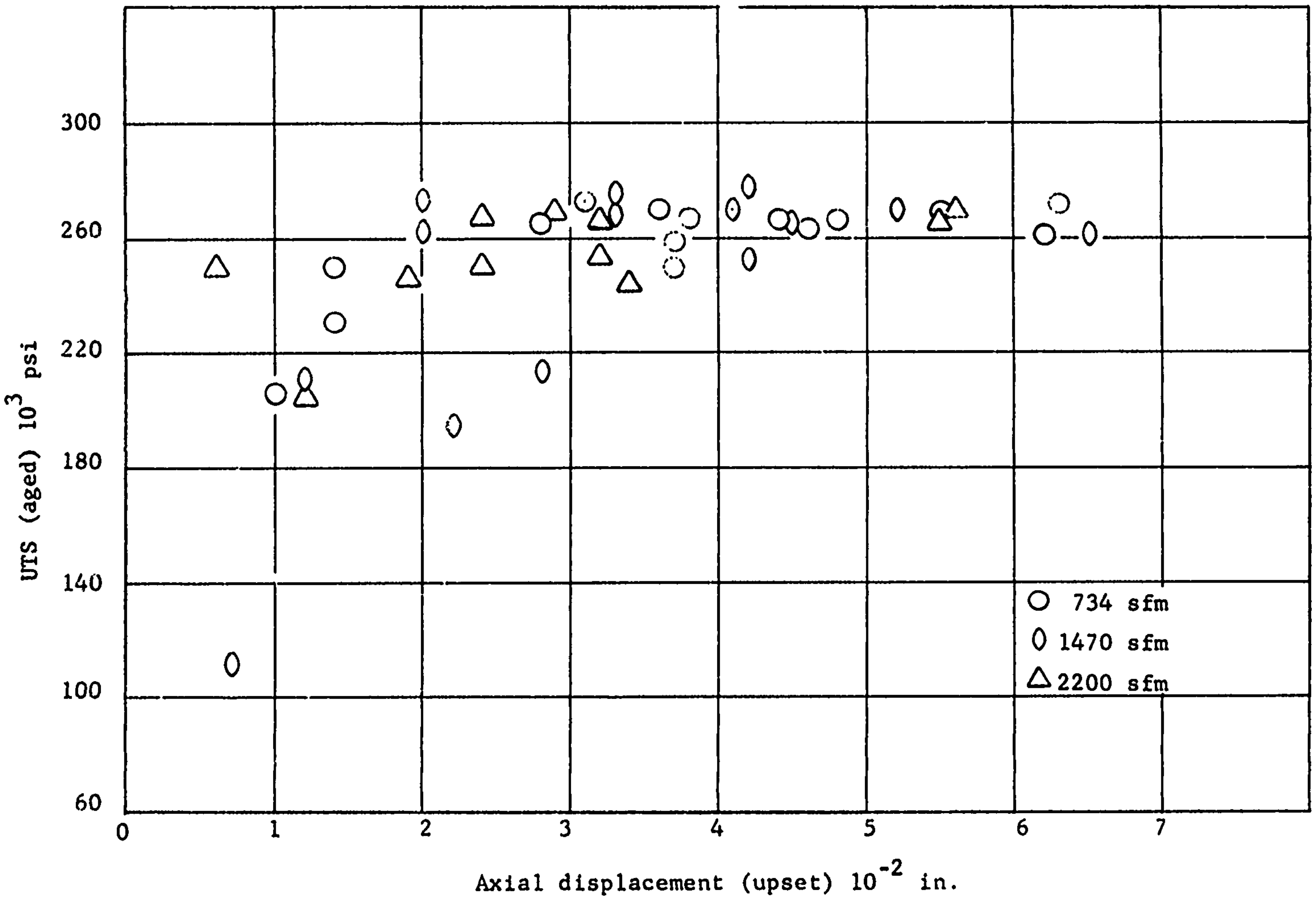

FIGURE 15. EFFECT OF AXIAL DISPLACEMENT DURING HEATING ON TENSILE STRENGTH OF FRICTION-BUTT-WELDED MARAGING STEEL TUBES

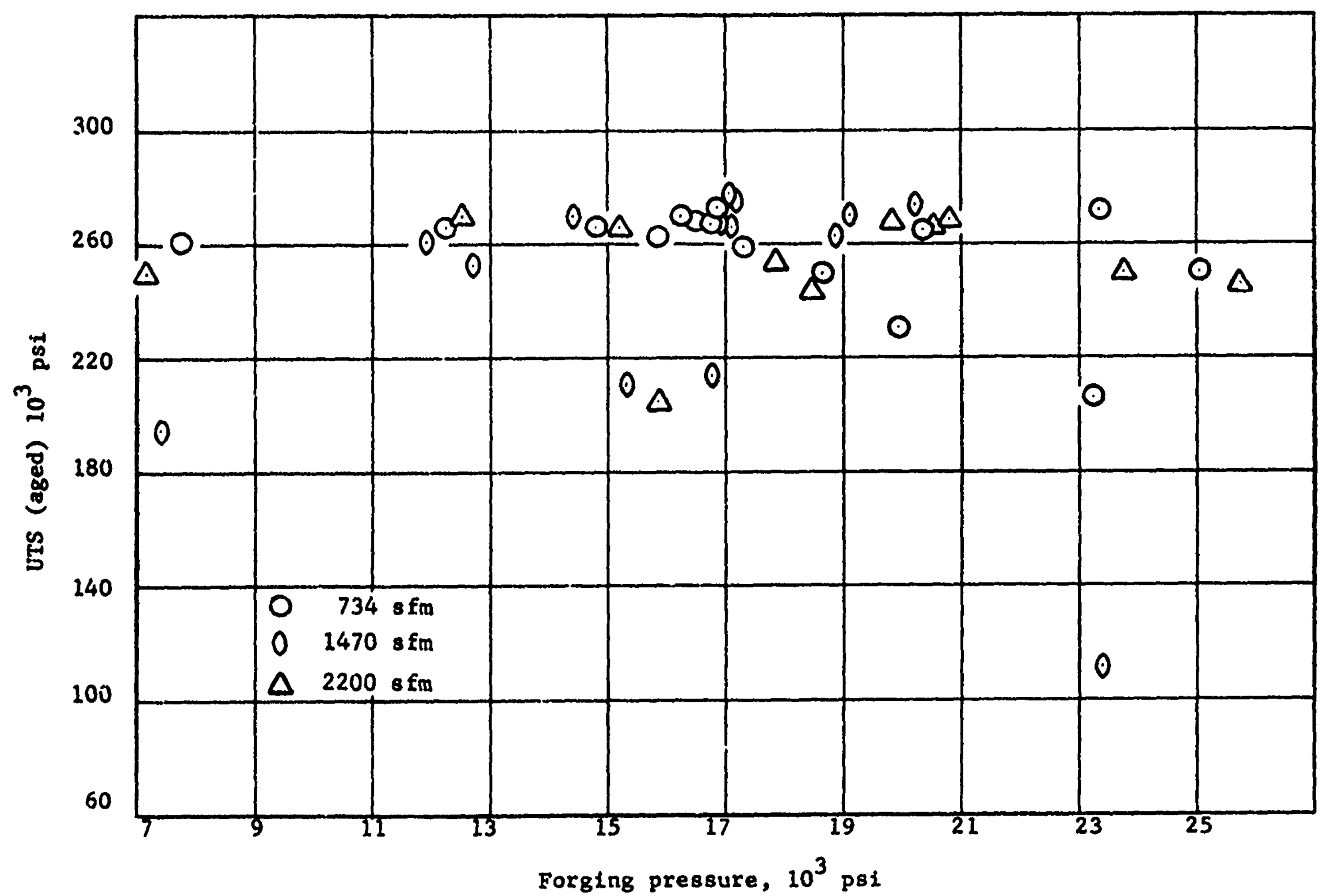

FIGURE 16. EFFECT OF FORGING PRESSURE ON TENSILE STRENGTH OF FRICTION-BUTT-WELDED MARAGING STEEL TUBES

TABLE 6. EMPIRICAL RELATIONSHIP BETWEEN STRENGTH AND INDEPENDENT WELD CYCLE VARIABLES FOR FRICTION BUTT WELDS BETWEEN THIN-WALLED MARAGING STEEL TUBES

$$UTS = 163509 - 140703 \exp(-100\ V_H) + 783 \sqrt{P_H} + 22861 \sqrt{P_F/P_H} + 1.53\ S_L$$

UTS = Tensile strength, psi

V_H = Volume of material expelled from faying surface, in.^{3}

P_H = Axial heating pressure, psi

P_F = Axial forging pressure, psi

S_L = Relative surface velocity of sliding components taken at the mean tube diameter, standard ft per min.

Statistics:

Multiple correlation coefficient, R	0.74470
R squared (portion of variance in dependent variable accounted for by regression eqn.)	0.55458
Standard error	21,879
Degrees of freedom in regression	4
Degress of freedom in residual	35
F ratio	10.89453

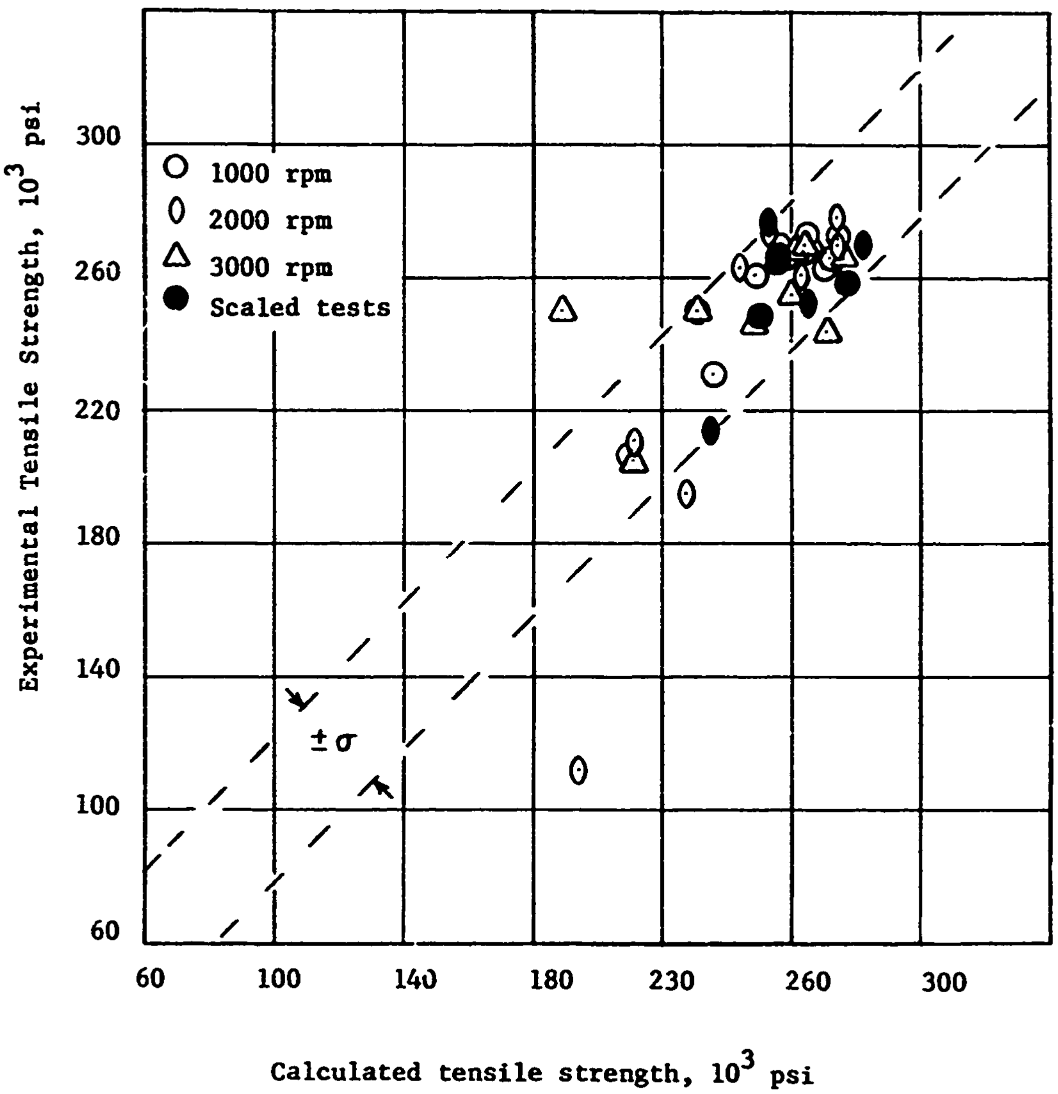

FIGURE 17. COMPARISON OF STRENGTHS OF FRICTION-BUTT-WELDED MARAGING STEEL TUBES WITH THOSE DERIVED FROM $168509 - 140703 \exp(-100V_H) + 703\ P_H + 2286\ P_F/P_H + 1.53\ S_L$

symbols represent values for experiments using specimens having larger mean diameters and higher D/T's whose welding conditions were derived by scaling based on specimen cross-sectional area. This indicates, then, that the model derived here is adequate for use by designers in specifying the conditions for friction-butt-welding thin-walled maraging steel tubes.

According to the model presented above, acceptable friction butt welds can be obtained over a relatively wide range of speeds, heating pressures, axial displacements, and forging pressures. In order to determine what combinations of these variables might provide the most cost-effective welding conditions, the relationship between equilibrium axial displacement rates, axial heating pressure, and rotational velocities was studied. Equilibrium displacement velocities for welds between 2.8 in. in diameter, 30:1 D/T tubes, when reached prior to weld-cycle termination, were determined from the displacement versus time curves on the weld-cycle records. Equilibrium volumetric displacement velocities are presented in Figure 18 as a function of heating pressure for three rotational speeds. Several interesting points can be derived from these relationships. First, it would appear that there is little effect of rotational velocity on displacement rates at low heating pressures and that displacement velocity increases with increasing axial pressure at a rate that is greater at higher rotational speeds. Also, the pressure versus displacement velocity relationships appear to be nonlinear at 1000 and 2000 rpm but approach linearity at intermediate pressures at 3000 rpm. This is somewhat contrary to the findings of Ellis[14] for similar investigations using mild steel bars and may, for the most part, be due to differences in specimen geometry. It would appear from Figure 18, that while higher displacement rates, and therefore welding rates, are attained at increased heating pressures, there is little effect of differences in speed above 2000 rpm. Graphical differentation of these curves with respect to heating presssure, shown in Figure 19, as a function of rotational speed, would indicate that welding is more efficient at 2000 rpm than at 3000 rpm at the higher heating pressures. Furthermore, the figure suggests that peak welding efficiency occurs at lower rotational speeds as heating pressure is increased within the range of these investigations.

Based on these relationships and the above welding model it would appear that friction-butt-welding maraging steel tubes would be most effectively performed at heating pressures in the range of 9000 to 10,000 psi and surface velocities of 1470 sfm using any combination of axial displacement and forging pressure that would yield the desired joint strength. Using the peak torque values listed in Appendix C, and the relation

$$HP = \frac{2\pi\tau\eta}{33,000} ,$$

where HP is horsepower, τ is torque in foot-pounds, and η is rotational speed in rpm, machines designed to friction butt weld 5.8 in. in diamter, 0.075 in. wall thickness maraging steel tubes at these conditions should be capable of

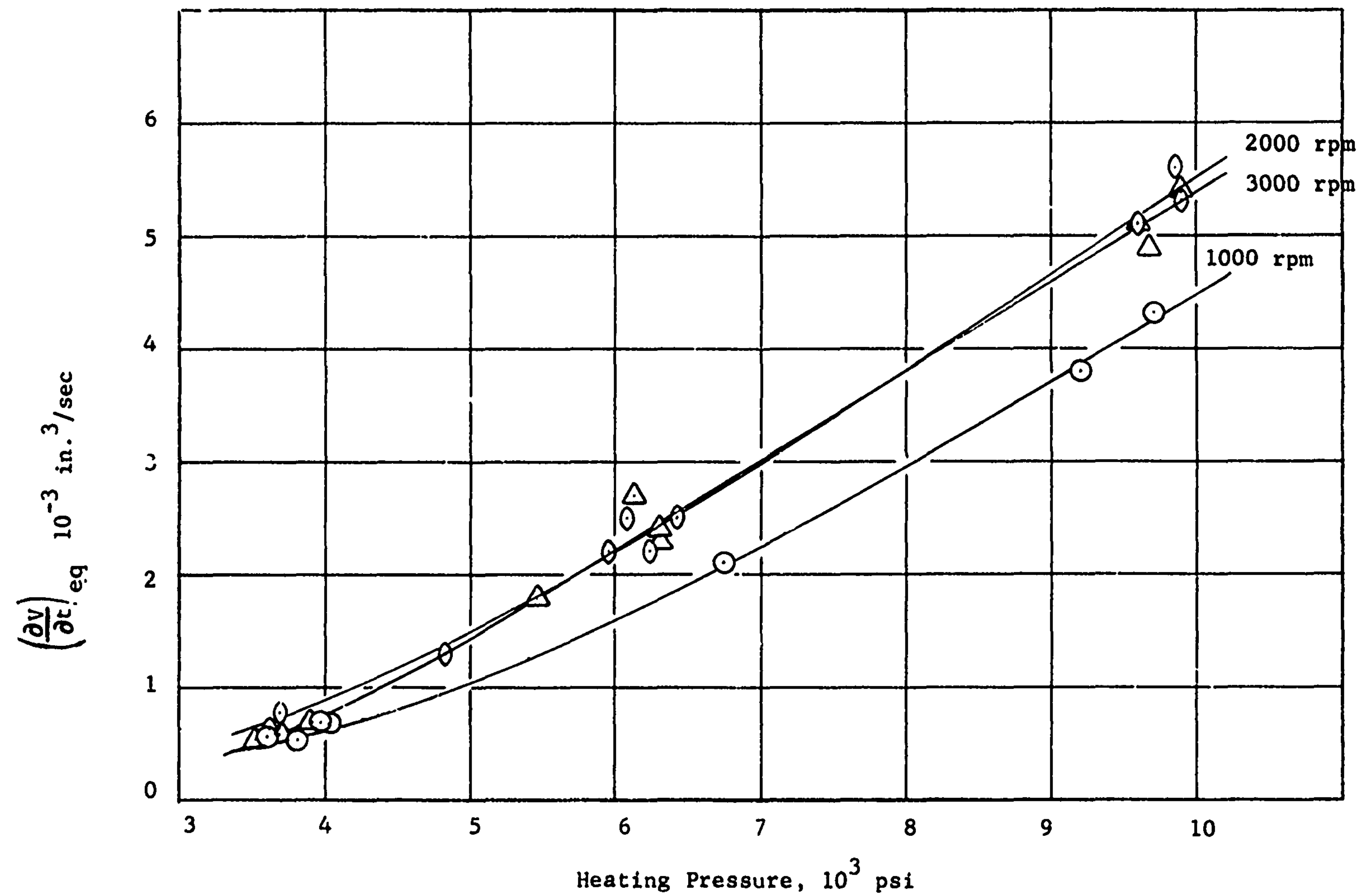

FIGURE 18. EFFECT OF HEATING PRESSURE ON EQUILIBRIUM VOLUMETRIC DISPLACEMENT RATE FOR FRICTION BUTT WELDS BETWEEN 2.8-IN.-DIAMETER STEEL TUBES

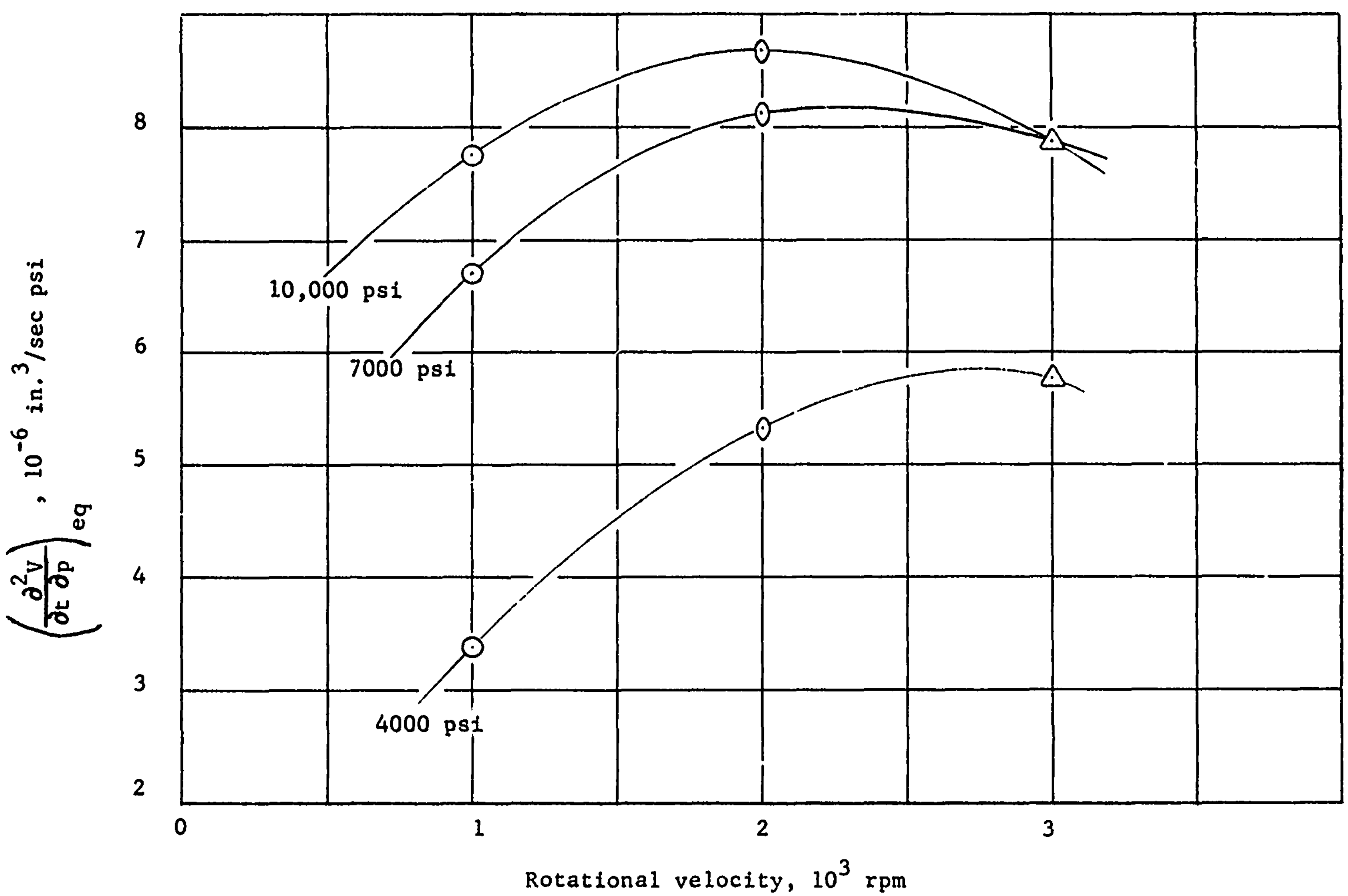

FIGURE 19. EFFECT OF ROTATIONAL VELOCITY ON CHANGE IN EQUILIBRIUM VOLUME DISPLACEMENT RATE WITH AXIAL HEATING PRESSURE FOR FRICTION BUTT WELDS BETWEEN 2.8-IN.-DIAMETER MARAGING STEEL TUBES

delivering at least 80 horsepower to the workpieces. Similarly, machines designed to weld 2.8 in. in diameter tubes having 0.095 in. and 0.060-in.-thick walls should be capable of delivering 60 horsepower and 40 horsepower to the respective workpieces.

Microstructural changes of the maraging steel friction welds due to variations in welding conditions during the parametric studies were considerably less obvious than those discussed above for the preliminary welding study. Differences in grain size of the heat affected zone and character of the weld interfaces were discernable, however, as shown in Figure 20, which essentially represents the extremes of the welding conditions studied. Changes which might be associated with differences in mechanical properties were usually less obvious and occasionally not discernable at all. A brief study of fracture mechanisms was undertaken during the Phase III studies and will be discussed later.

The effects of the maraging heat treatment (900 F for 3 hr) on both microstructure and hardness of maraging steel friction welds were studied for a number of welding conditions which caused significant differences in mechanical properties. Again, variations due to differing welding conditions were not particularly discernable. The maraging heat treatment did have a significant effect on both microstructure and hardness as shown in Figure 21. Longitudinal hardness and structure variations across the interfaces as a result of welding can probably be attributed to both heating and mechanical working effects. The narrow region of increased hardness at the weld interface, as shown in Figure 21, was probably caused by mechanical work introduced by the applied forging pressure. The adjacent areas were probably softened by the high temperatures generated during frictional heating while the regions of high hardness toward the outer edges of the heat affected zone probably result from a partial aging effect on the solution annealed workpieces. Maraging subsequent to welding not only served to increase overall hardness and to flatten the hardness profile as shown by the figure, but also accentuated the texture of the material by preferential precipitation of what appeared to be carbides in longitudinal bands which flare outward toward the specimen surfaces at the weld. This longitudinal banded structure is thought to have been introduced during fabrication of the material from which the specimens were made. Because of the axial shortening during welding, some of these carbides have a tendency to become concentrated at the weld interface and may have contributed to lack of strength in some specimens. Solution treatment of the weld prior to aging tended to reduce the carbide precipitate concentration at the weld interface as well as to produce some grain refinement as shown in Figure 22. Hardness profiles were not significantly affected by this treatment. It should be noted here that while this practice is usually undesirable after conventional welding because of possible distortion due to uneven stress fields, no such distortion would be expected in friction welds because of the completely uniform heating and welding which occurs simultaneously over the entire weld cross section.

100X 100 Picral, 2HCl, $2HNO_3$ 9F227

a. Welding Conditions: 1000 rpm; 3800 psi heating pressure; 7730 psi forging pressure; 0.091 in. upset; 9.83 sec.

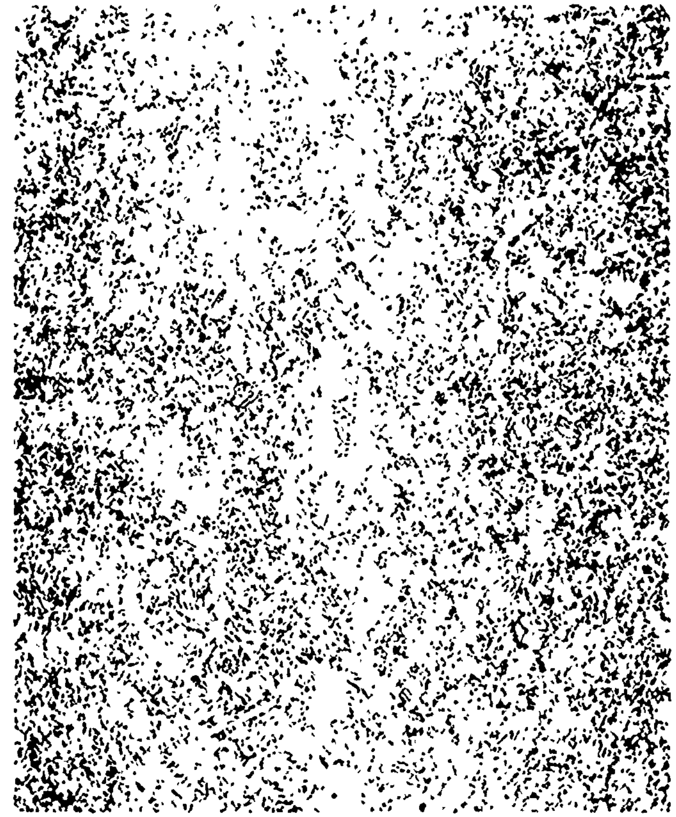

100X 100 Picral, 2HCl, $2HNO_3$ 9F060

b. Welding Conditions: 3000 rpm; 9680 psi heating pressure; 19,850 psi forging pressure; 0.065 in. upset; 1.23 sec.

FIGURE 20. MICROSTRUCTURAL EFFECTS OF THE GREATEST DIFFERENCES IN CYCLE VARIABLES FOR FRICTION BUTT WELDS BETWEEN MARAGING STEEL TUBES

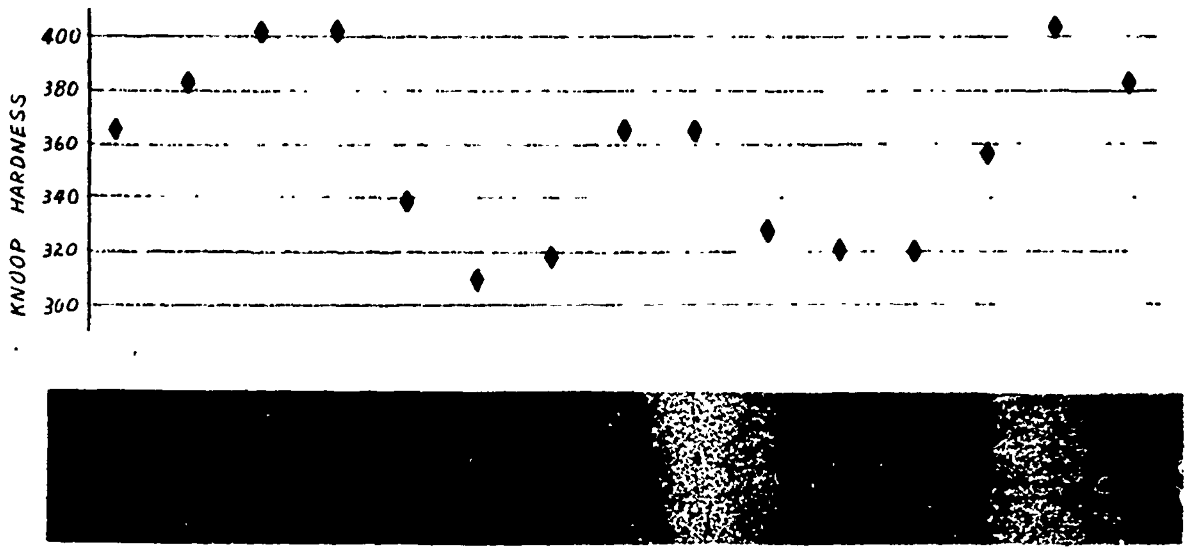

20X Vilella's Etch 9F755

a. Knoop Hardness and Macrostructure as Friction Welded

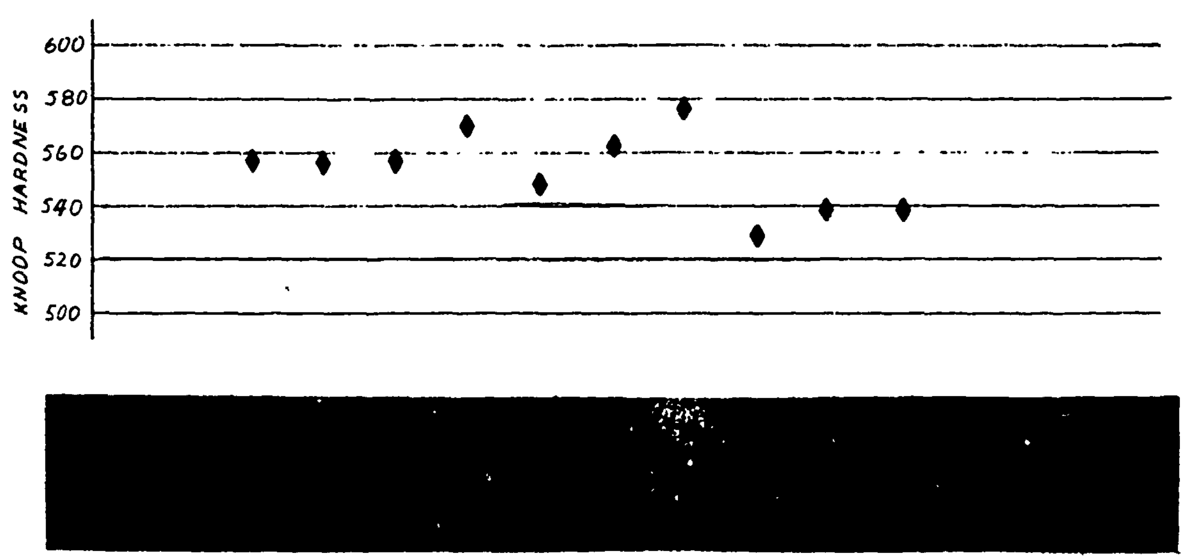

20X Vilella's Etch 9F761

b. Knoop Hardness and Macrostructure After Aging 3 Hr at 900 F

FIGURE 21. EFFECT OF AGING ON MACROSTRUCTURE AND HARDNESS OF MARAGING STEEL FRICTION BUTT WELDS

Reduced 23 Percent in Reproduction

100X Vilella's Etch 9F785

a. Maraged 3 Hr at 900 F After Welding

100X Vilella's Etch 9F786

b. Solution Treated at 1500 F for 15 Min, After Welding, Then Aged 3 Hr at 900 F

FIGURE 22. MICROSTRUCTURAL EFFECT OF INTERMEDIATE ANNEAL PRIOR TO AGING OF MARAGING STEEL FRICTION WELDS

Friction-Welding Investigations on 7075 Aluminum Tubes

A total of ten friction-butt-welding experiments was carried out between 7075-T6 aluminum tube segments approximately 2.83 in. in diameter with about 0.120-in.-thick walls. The results of these experiments are summarized in Appendix C. As might be expected, this material was found to behave very differently from maraging steel during welding. First, it was found that impulsive application of axial loads of as little as 3000 lb at the beginning of the weld cycle created enough torque to shear the spindle drive pin in the friction welder. Therefore, the application of heating pressures greater than about 2500 psi had to be programmed at rates no greater than about 4500 psi per sec. As is noted, two axial heating pressures are listed in the appendix summary. This is a result of the material's high resistance to axial deformation at low temperatures during friction welding. The high thermal conductivity of the material considerably delayed frictional heating at the faying surfaces and thereby delayed axial deformation. As interfacial temperatures increased, however, a sudden loss in strength permitted axial deformation at a rate that could not be matched by the friction welder's hydraulic system. A sudden drop in axial heating pressure, as listed in the summary, was therefore experienced at the end of the welding cycles.

Mechanical-property evaluations conducted on the aluminum friction welds are summarized in Appendix E, along with experimentally determined properties for the base material. As can clearly be seen from the data, no satisfactory welds were obtained for this material as the maximum joint strength attained was only about 57 percent of that of the base material. The reasons for this apparent lack of weldability of 7075-T6 extruded aluminum tubing were revealed by microstructural examination. As can be seen in Figure 23, the structure of the alloy is highly directional in nature having a layered structure. Considerable delamination of this structure due to the applied axial forces occurred during all friction-welding experiments. The most likely reasons for the weakness of these friction welds were probably the observed delamination and the transformation of the high directional structure of the alloy to an equiaxed structure at the joint interface as shown in Figure 24. If the mechanical properties of extruded shapes of this alloy are dependent to a large degree on the directionality of their microstructures, then it can be reasonably concluded that friction welding is not a suitable joining technique where full base metal properties are required. For these reasons friction-welding studies on extruded 7075 aluminum tubes were discontinued.

Phase III Investigations

This phase of the program was concerned with optimizing the parameters for friction-welded joints between maraging steel tubes having significantly different wall thicknesses using a half-lap design and for similar

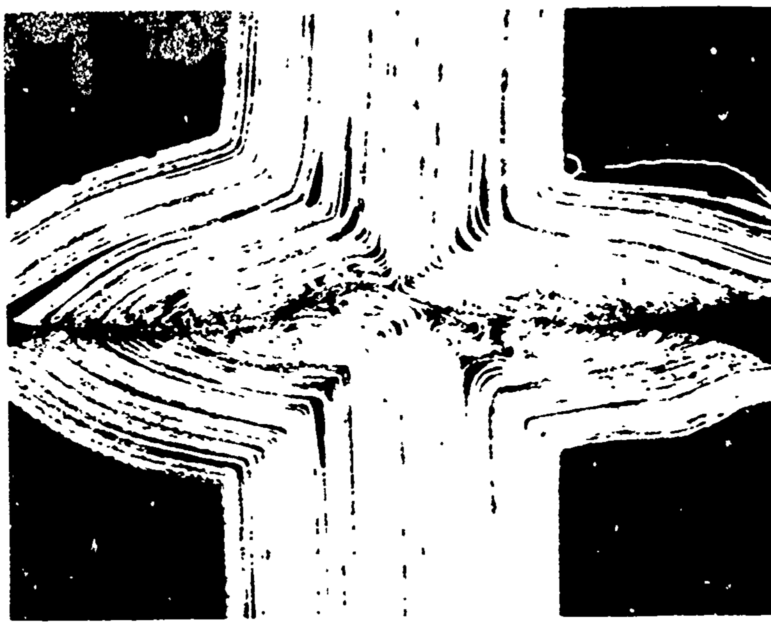

15X Keller's Etch 9F094

a. Transverse Section

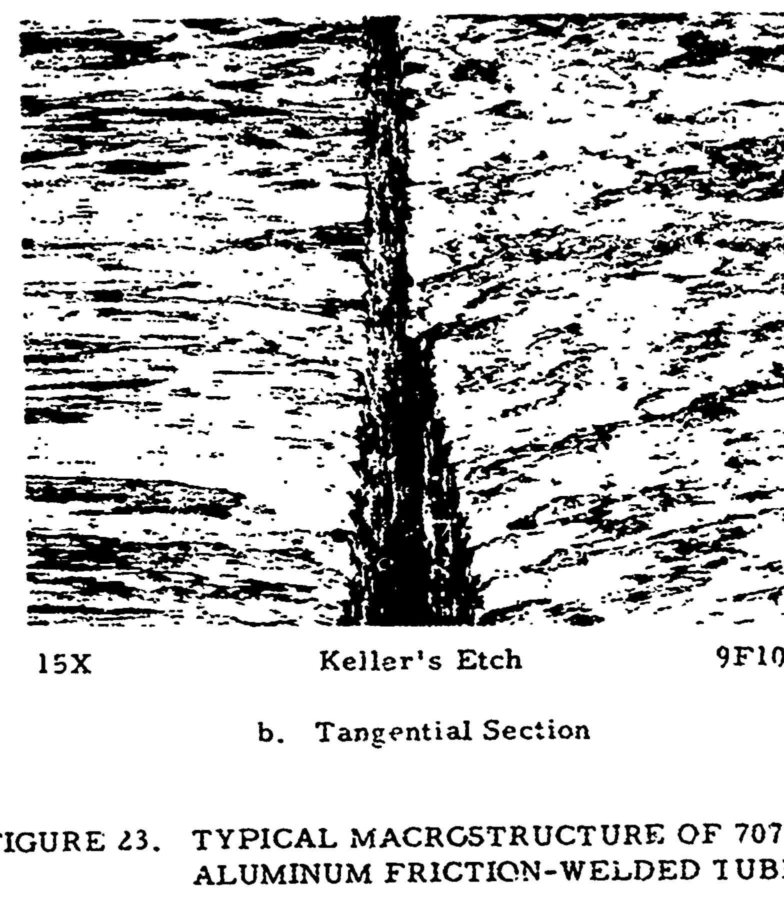

15X Keller's Etch 9F100

b. Tangential Section

FIGURE 23. TYPICAL MACROSTRUCTURE OF 7075-T6 ALUMINUM FRICTION-WELDED TUBES

500X Keller's Etch 9F069

FIGURE 24. TYPICAL MICROSTRUCTURE OF 7075-T6 ALUMINUM ALLOY FRICTION-WELDED TUBES

joints between thin-walled maraging steel tubes and relatively heavy plates. The results of the Phase III studies on tubular butt welds were used as a base for these investigations. Dissimilar metal welds between the maraging steel and 7075 aluminum alloy were not studied because, as discussed above, the morphology of the aluminum tubing rendered it unsuitable for friction welding.

A two factor-three level experimental matrix, as shown above in Table 4, was set up to study the effects of forging pressure and axial displacement on friction welds between thin- (D/T = 60 to 75) and thick- (D/T = 30) walled maraging steel tubes having the same outside diameter and between similar thin-walled tubes and 1/2-in. -thick plates. A heating pressure of 9500 psi at a rotational velocity of 2000 rpm (1470 sfm), determined to be optimum by the Phase II work, was to be used for all of these experiments, which were performed in a randomized order.

The welding data recorded for the Phase-III experiments are summarized in Appendix C. As can be seen from this summary, a total of eleven rather than nine experiments were required using the tube-to-tube half-lap joint configuration as a significant problem developed which caused two of the experiments to be repeated. Examination of the first joint in this series revealed the tendency for the thin-walled component to flare outward at the joint interface. This situation had to be rectified because machining away the external weld flash would cause a significant decrease in the wall thickness of the thin-walled component immediately behind the weld joint which would result in a region of decreased strength in the joined components. It was at first thought that the flaring was caused by restraint of the internal weld flash by the lap step machined in the thick-walled component. To test this hypothesis a recess or flash trap was machined in the lateral wall of the lap step for the second experiment. When flaring of the thin-walled component again occurred without restraint of the internal weld flash it was concluded that the flaring was probably due to increased heat dissipation, and therefore a narrower plastic region, at the root of the lap step in the thicker walled component than at its outer edge. This variation in the thickness of the plastic zone across the faying surface of the heavier walled component could then act as a wedge forcing the thinner walled component to flare outward. Subsequent microstructural examination of the Phase III weld joints supported this conclusion. As indicated by Figure 25, all of the weld interfaces were inclined with respect to the specimen axes instead of perpendicular to them as would be expected for a true butt type joint.

Three alternative approaches were considered for solution of the flaring problem. Two of these, one being to increase the outside diameter of the thick-walled component and the other being elimination of the lap step, would effectively have eliminated the joint design being studied and were therefore unsatisfactory. A third alternative, adopted for the remainder of this study, was to provide rigid external support for the thin-walled component in very close (less than 1/8 in.) proximity to its faying surface. This was accomplished during this study with a restraining collar but the same effect could

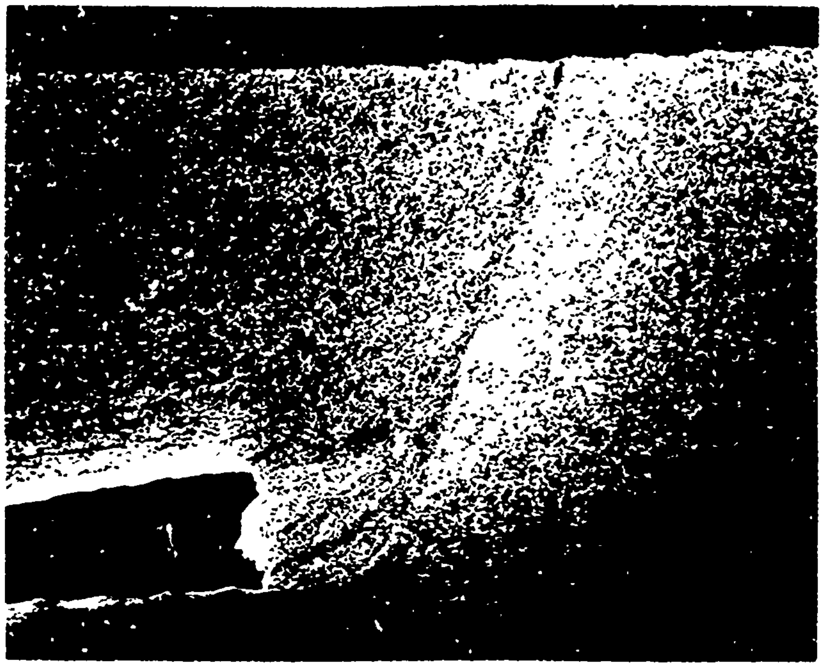

75X Vilella's Etch 1G506

FIGURE 25. TYPICAL MICROSTRUCTURE OF HALF-LAP JOINT BETWEEN MARAGING STEEL TUBES

be achieved in production simply by chucking the workpiece very close to its faying edge during friction welding. The restraining collar also provided an additional heat sink for the thin-walled components, which permitted them to heat at a rate more commensurate with those of heavier walled components.

Temperature histories were, as a matter of course, determined for each of the Phase III experiments and are included in Appendix D but, as before, will not be treated rigorously. In those cases where the thin-walled component was held stationary as well as for all experiments involving plates, fixturing prevented the use of more than one thermocouple. This, as before, was resistance welded into a shallow hole drilled in the specimen outer surface at a distance of 1/16 in. from the faying edge. Tensile properties of the friction-welded joints for both Phase III configurations were determined in the as-welded and subsequently maraged conditions. These data are summarized in Appendix E. Microstructural effects were, again, not summarized but will be discussed.

Half-Lapped Tube-To-Tube Joints

Examination of the data presented in Appendixes C and E revealed several interesting aspects of friction welds between thin- and thick-walled tubes. First, some very high tensile strengths were obtained, especially in comparison with the results of the Phase II study. This may, to some extent, be accounted for by the design of the tensile specimens. Because a slight amount of flaring of the thin-walled components was still able to occur, as can be seen in Figure 25 above, and because the lap step was machined away from the ID surface of the thick-walled components for about 1/2 in. adjacent to the welds, a virtual notched tensile specimen design was created and fractures were essentially confined to the weld interface rather than being permitted to occur in the base metal as was the case for the Phase II studies. This would suggest that joint strengths in excess of base metal strengths are possible through friction welding.

Because of the limited sensitivity of the friction-welder hydraulic system, it was not possible to reproduce the same axial heating pressure for all of the experiments in the matrix as shown in Appendix C. This complicating factor essentially precluded a simplistic analysis of the effects of axial displacement and forging pressure on weld quality. A comparison of the tensile strengths of these friction welds with values calculated using the model derived from the Phase II studies indicated that although the observed strengths were higher than predicted by the model, a similar relation between strength and the independent weld cycle variables should exist. Multiple correlation/regression techniques were then used to generate the model presented in Table 7. Although this model shows a reasonably good correlation between independent weld-cycle variables and tensile strengths of the welds, as indicated by the correlation coefficient presented in the table and by Figure 26, a comparison of the F ratio with tabulated values[26] would indicate a greater than 5 percent probability of obtaining a better fit to the data by chance alone. This may be due, in part, to the small number of experimental data points considered in the regression. It is interesting to note that although this model suggests a higher dependence of tensile strength on forging pressure than the model developed under Phase II (probably because of the small range of variation in heating pressure), axial or volumetric displacement, as before, exerts the greatest influence on friction-weld tensile strengths. Rotational velocity was eliminated from this model because it was held constant throughout this series of experiments. Requirements for power delivered to the work pieces were about the same for this joint configuration as for the butt joints studied under Phase II.

Metallographic examination of these joints was carried out in both the as-welded and subsequently maraged conditions. Joint microstructures appeared very similar to those presented above for the Phase II studies except there appeared to be a higher incidence of agglomerated carbides or oxides trapped in the weld interfaces. This may have resulted from the restraining influence of the lap step machined in the heavier walled component. Scanning electron micrography of the tensile specimen fracture surfaces from two of the welds, as shown in Figure 27, indicated that failure was ductile in welds exhibiting both high and low tensile strengths. Those areas of Figure 27b which are not representative of fracture surfaces, either ductile or brittle, are thought to be a result of carbides or oxides trapped in the weld interface. This would suggest that loss of tensile strength in these friction welds was at

TABLE 7. EMPIRICAL RELATIONSHIP BETWEEN STRENGTH AND INDEPENDENT WELD-CYCLE VARIABLES FOR HALF-LAP FRICTION WELDS BETWEEN THIN- AND THICK-WALLED MARAGING STEEL TUBES

$$UTS = 219671 - 156489 \exp(-100V_H) - 1866\sqrt{P_H} + 120774\sqrt{P_F/P_H}$$

UTS = Tensile strength, psi

V_H = Volume of material expelled from faying surface, $in.^3$

P_H = Axial heating pressure, psi

P_F = Axial forging pressure, psi

Statistics:

Multiple correlation coefficient, R	0.82482
R squared (portion of variance in dependent variable accounted for by regression eqn.)	0.68033
Standard error	25,650
Degrees of freedom in regression	3
Degrees of freedom in residual	4
F ratio	2.83759

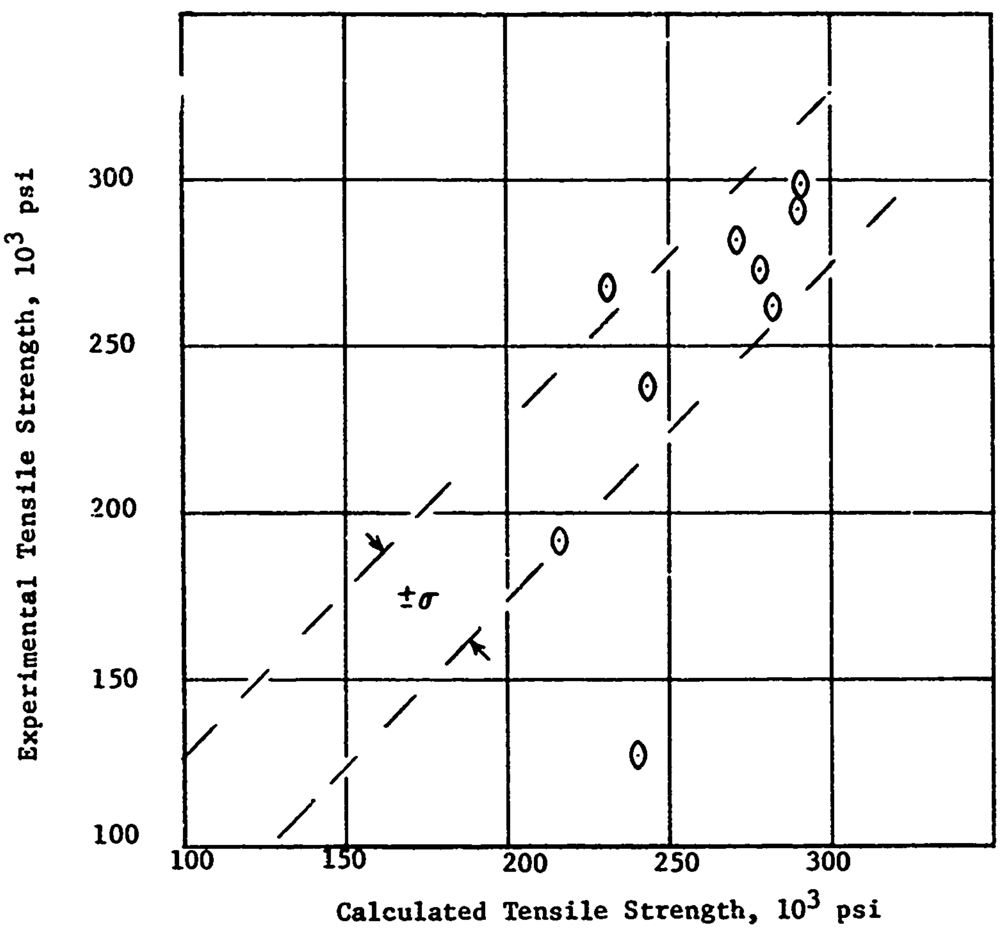

FIGURE 26. COMPARISON OF STRENGTHS OF HALF-LAP FRICTION-WELDED MARAGING STEEL TUBES WITH THOSE DERIVED FROM $319671-156489 \exp(-100V_H)-1866\sqrt{P_H}+120774\sqrt{P_F/P_H}$

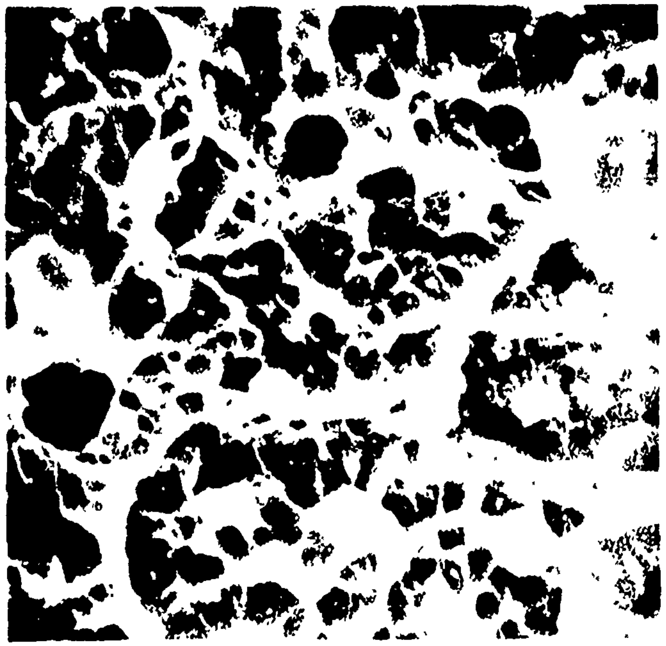

5000X

a. Weld No. 95 Fracture Surface

0.2 percent offset yield strength	294,000 psi
Ultimate tensile strength	299,000 psi
Elongation	1.68 percent

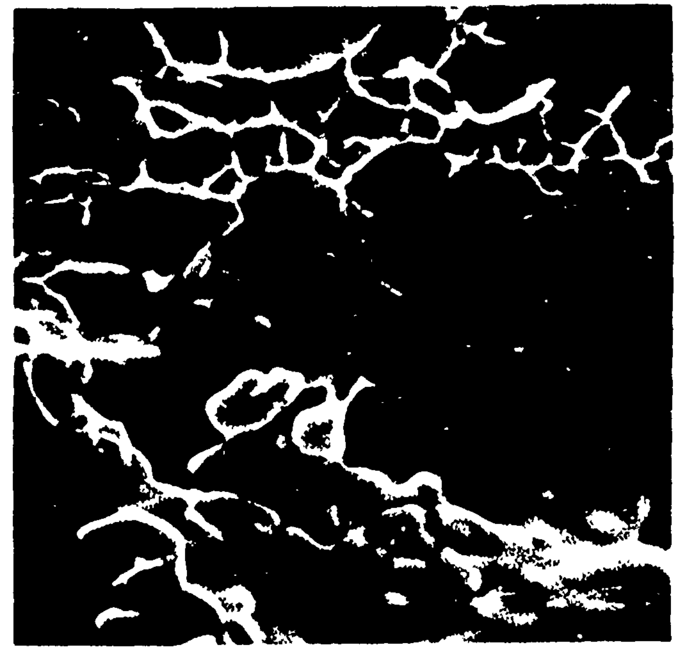

6600X

b. Weld No. 92 Fracture Surface

0.2 percent yield strength	Undetermined
Ultimate tensile strength	192,000 psi
Elongation	0.58 percent

FIGURE 27. SCANNING ELECTRON MICROGRAPHS OF TENSILE FRACTURE SURFACES OF HALF-LAP FRICTION-WELDED MARAGING STEEL TUBES

least partially due to reduction of the effective cross-sectional area of the weld interface by the included particles; thus inferring that the best friction welds between maraging steel tubes will be produced at conditions of heating pressure and speed which will least perturb the morphology of the components but at axial displacements great enough to expel any oxides or carbides that might be initial'y trapped in the faying surfaces.

Half-Lapped Tube-to-Plate Joints

Examination of the strength data presented in Appendix E for friction welds between thin-walled tubes and heavy plates of maraging steel indicates that the tube-to-plate welds generated during this portion of the investigation are generally inferior to those created between thin- and thick-walled tubes at similar conditions of pressure, speed, and upset. Alternatively it may be said that satisfactory friction welds between tubular specimens having small cross-sectional areas and heavy sectioned plates are considerably more difficult to achieve than similar welds between components whose cross-sectional areas immediately adjacent to the faying surfaces are more nearly equal. Analysis of these strength data with respect to the factorially designed experimental matrix, as shown in Table 8, indicated that, on the average, the best mechanical properties were achieved at heating-phase upsets of about 0. 037 in. and high forging pressures, but that satisfactory properties might also be achieved at low forging pressures. Very little correlation was discernable between weld mechanical properties and any of the independent friction-welding variables and multiple correlation/regression analysis techniques were unable to produce a model with sufficient statistical significance to have any value as a design tool.

Microstructurally the tube-to-plate welds were somewhat different from either of the two tube-to-tube weld designs in that the grain size of the plate material was approximately ten times that of the tube material. The effects on heat dissipation of the differences in mass between the two specimen components are also readily recognizable. As can be seen by comparing the microstructures of Figure 28 with those of Figures 20 and 25, the heat sink provided by the massive plate component served to essentially prohibit any significant plastic deformation by this component during frictional heating. This is evidenced by the comparative lack of inclination of the weld interface with respect to the axis of rotation and the lack of perturbation of the adjacent plate component grain structure. Structural differences in the trapped internal weld flash between the two Phase III joint configurations also indicate that the plate components remained relatively cool and acted as heat sinks. The flash trapped in the tube-to-tube joints has a structure very similar to the surrounding material while that trapped in the tube-to-plate joints is extremely fine grained and in some instances appears somewhat austenitic in character, indicative of quenching. From these discussions it would appear, then, that although friction-welded joints having satisfactory properties are possible between thin-walled tubes and heavy plates, the probability of obtaining

TABLE 8. ANALYSIS MATRIX OF FACTORS AFFECTING THE QUALITY OF HALF-LAP FRICTION WELDS BETWEEN THIN-WALLED TUBES AND HEAVY PLATES OF MARAGING STEEL

All welds were performed at a relative rotational velocity of 2000 rpm (1470 sfm). Values in the matrix blocks represent the following factors:

Heating Pressure, psi	Forging Pressure, psi
Heating Upset, in.	Total Upset, in.
Ultimate Tensile Strength, psi	

							Horizontal Averages	
	9410	13,920	9090	16,580	8440	19,260	8980	16,590
	0.023	0.036	0.022	0.037	0.024	0.043	0.023	0.039
	142,000		202,500		150,000		154,000	
	8710	13,460	8930	16,960	9230	20,500	8960	16,820
	0.039	0.054	0.036	0.052	0.036	0.050	0.037	0.052
	169,000		122,500		279,000		190,000	
	9040	13,970	8920	16,490	9770	19,660	9240	16,710
	0.055	0.063	0.056	0.067	0.056	0.072	0.056	0.067
	144,500		53,100		67,800		88,470	
Vertical Averages	9050	13,780	8980	16,680	9150	19,660		
	0.039	0.051	0.038	0.052	0.039	0.055		
	152,000		126,000		165,600			

100X Vilella's Etch 1G508

a. Welding Conditions: 2000 rpm; 9230 psi heating pressure; 20,500 psi forging pressure; 0.050 in. upset; 1.51 sec strength 279,000 psi (aged).

100X Vilella's Etch 1G514

b. Welding Conditions: 2000 rpm; 8440 psi heating pressure; 19,260 psi forging pressure; 0.043 in. upset; 1.06 sec strength 150,000 psi (aged).

FIGURE 28. TYPICAL INTERFACE MICROSTRUCTURES OF FRICTION WELDS BETWEEN THIN-WALLED TUBES AND HEAVY PLATES OF MARAGING STEEL

satisfactory welds at a wider variety of conditions would be enhanced by preheating the heavier component to reduce heat losses and promote plastic deformation at the faying surfaces during welding.

CONCLUSIONS

(1) In general, it can be concluded from this study that friction welding can be effective in decreasing costs and increasing efficiency in missile systems production operations. Its incorporation would result in simplification of component forming operations, reduction in the number of machining steps, and increased speed and reliability in joining operations which would thereby increase the cost effectiveness of missile systems production.

(2) An empirical model has been derived which will permit specification of the conditions of rotational speed, axial heating and forging pressures, and axial displacement necessary to achieve high-quality friction butt welds between 18Ni(250) maraging steel tubular components having mean diameters between 2.8 and 5.8 inches and diameter to wall-thickness ratios between 30 and 80. The greatest welding efficiencies were found to occur at rotational velocities equivalent to 1470 sfm and axial heating pressures between 9000 and 10,000 psi. Machines for producing these welds should be capable of delivering between 40 and 80 horsepower to the work pieces.

(3) An empirical model similar to that for friction butt welding was found to define the conditions of axial heating and forging pressures and displacement at 1470 sfm necessary to achieve satisfactory half-lap friction welds between thin and thick walled maraging steel tubes. Similar efforts for half-lap joints between thin walled tubes and heavy plates were unsuccessful, indicating that differences in geometry adjacent to the faying surfaces between the components to be joined can have a pronounced effect on the optimum conditions for successful friction welding. It is therefore concluded that the proper conditions for friction welding one joint configuration cannot necessarily be inferred from studies on another joint configuration and that, at the present state of the art, a certain amount of parametric development is necessary for each joint design of interest.

(4) Friction welds between work pieces of a given material having significantly different cross sections are considerably more difficult than those between components more nearly equal in cross section but may be facilitated by preheating the heavier component.

(5) It was found from this study that the quality of friction welded joints between maraging steel tubes has, in terms of welding variables, a greater dependence on axial pressure and displacement during the heating phase of the weld cycle than on either forging pressure or relative rotational velocity. Microstructural investigations have indicated that high joint integrity is most likely when frictional heating is evenly

distributed between the components to be joined, is limited to the immediate vicinity of the weld interface, and is sufficient to permit plastic deformation of the interfacial material but not prolonged enough to cause significant grain growth in the areas adjacent to the weld. Tensile failure of friction welds was found to be ductile in nature with weakness being at least partially due to included carbides and/or oxides which act to reduce the effective bond area.

(6) Rigid support for the thin walled tubular work pieces was found to be necessary within 1/2 inch of the faying surfaces to prevent distortion during the forging phase of friction butt welds. Thin walled components of half-lap joints were found to require rigid external support to within 1/8 in. of the faying surfaces to prevent flaring during the weld cycle and subsequent loss of component wall thickness during removal of the external weld flash.

(7) Auxiliary braking is desirable for conventional friction welds between thin-walled components because it serves to decrease the probability of radial distortion in the welded joint and reduces the torque peak generated during deceleration of the rotating component.

(8) Maraging steel components should be friction welded in the solution-annealed condition as the heat generated during welding is sufficient to cause re-solution of the strengthening precipitates, thus requiring additional aging to achieve full maraged properties.

(9) Solution treatment of friction-welded maraging steel components prior to aging was found to be beneficial to joint quality by irreversibly dissolving carbides concentrated at the weld interface and causing refinement of the grain structure in the bond zone.

(10) It is not feasible to friction weld maraging steel components containing viscoelastic materials because of the subsequent heat treatment required to achieve optimum properties. Maraging steel components containing viscoelastic materials could, however, be friction welded to dissimilar materials where re-solution would not affect the overall joint strength.

(11) Because of their highly directional, almost fibrous, grain structures, it is not feasible to achieve fully efficient friction welds between extruded 7075-T6 aluminum alloy tubes. It is logical to assume, then, that this conclusion would also hold true for other materials, similarly fabricated, whose mechanical properties are dependent on their highly directional grain structures.

RECOMMENDATIONS

(1) It is realized that the expense of converting present missile-systems production operations or those in the latter stages of development to friction-welding technology would be prohibitive but based on the work performed under this contract and the findings presented in this report, it is recommended that the process be seriously considered as a cost-effective tool for use in the production of all future missile systems.

(2) This study has produced empirical relationships applicable to the friction welding of thin-walled maraging steel components of circular cross section. It is not felt, however, that these relationships can necessarily be translated to other materials and joint configurations without suitable experimental development. Similar efforts, possibly more limited in scope, should be directed toward other materials and friction-welding joint configurations of specific present or possible future interest to the Missile Command to provide design experts with the information necessary to consider the application of friction-welding techniques to future missile systems-fabrication concepts.

(3) During the course of literature surveys performed in connection with this program, very little information was found regarding nondestructive techniques for verifying the quality of friction welds. It is recommended therefore, that consideration be given to the development of nondestructive inspection techniques capable of evaluating friction-weld quality. Such an effort might be directed toward eventual automated production usage, providing either full or partial inspection as needs may require.

REFERENCES

(1) Rocket Motor Manual (U), Chemical Propulsion Information Agency, The Johns Hopkins University Applied Physics Laboratory, Silver Springs, Maryland, CPIA/MI, March, 1969 (CRD).

(2) "1968 Book of ASTM Standards, Part 31", American Society for Testing and Materials, May, 1968, pp 202-221.

(3) "High-Strength Steel 18 Ni Maraging", Defense Metals Information Center, Battelle Memorial Institute, Columbus, Ohio, September 1, 1968, p V-2.

(4) Metals Handbook, Vol 1, 8th Ed., American Society for Metals, Metals Park, Ohio, 1961, p 948.

(5) ASTM Standards, Op Cit, p 218.

(6) Ibid, pp 249-252.

(7) Hazlett, T. H., "Properties of Friction Welds Between Dissimilar Metals", Welding Journal, 41 (10), 448-505 (1962).

(8) Hazlett, T. H., and Gupta, K. K., "Friction Welding of High-Strength Structural Aluminum Alloys", Welding Journal, 42, 4905-4945 (1963).

(9) "Friction Welding Spins Its Way Onto the Production Floor", Iron Age, 194 (14), 59-61 (1964).

(10) Hodge, E. S., "Friction Joining", Battelle Technical Review, 14 (8-9), 10-13 (1965).

(11) Rao, M., and Hazlett, T. H., "A Study of the Mechanisms Involved in Friction Welding of Aluminum Alloys", Welding Journal, 49 (4), 1815-1885 (1970).

(12) Nessler, G. G., et al, "Friction Welding of Titanium Alloys", Welding Journal, 50 (9), 3795-3855 (1971).

(13) Moore, T. J., "Friction Welding", Welding Journal, 51 (4), 253-262 (1972).

(14) Ellis, C.R.G., "Continuous Drive Friction Welding of Mild Steel", Welding Journal, 51 (4), 1835-1975 (1972).

(15) Cheng, C. J., Thermal Aspects of the Friction Welding Process (Part I), American Machine and Foundry Company, CRL, TR 296 (July 7, 1961).

(16) Cheng, C. J., Thermal Aspects of the Friction Welding Process (Part II), American Machine and Foundry Company, CRL, TR 334 (August 15, 1962).

(17) Cheng, C. J., "Transient Temperature Distribution During Friction Welding of Two Similar Materials in Tubular Form", Welding Journal, 41 (12), 542S-550S (1962).

(18) Wang, K., and Nazappan, P., "Transient Temperature Distribution in Inertia Welding of Steels", Welding Journal, 49 (9), 419S-426S (1970).

(19) Rich, T., and Roberts, R., "Thermal Analysis for Basic Friction Welding", Metal Const. and Brit. Weld. Jour., 3 (3), 93-98 (1971).

(20) Voinov, V. G., "Mechanism of Joint Formation in Friction Welding", Svarochnoe Proizvodstvo (Welding Production), 15 (1), 8-13 (Translation).

(21) Metals Handbook, Vol. 6, 8th Ed., American Society for Metals, Metals Park, Ohio, 1971, p 511.

(22) Paprocki, S. J., et al, "Joining Zircaloy-Stainless Steel and SAP Alloys by Friction, Rolling, and Explosive Techniques", BMI-1594, Battelle Memorial Institute (September 4, 1962), pp 8, 20.

(23) Miller, G. P., and Mitchell, W. I., "Structure and Hardening Mechanisms of 18-Percent Nickel-Cobalt-Molybdenum Maraging Steels", J. Iron and Steel Inst., 203, 899-904 (1965).

(24) Marcus, H., Schwartz, L. H., and Fine, M. E., "A Study of Precipitation in Stainless and Maraging Steels Using the Mossbauer Effect", Trans. ASM, 59, 468-478 (1966).

(25) Nie, N., Bent, D. H., and Hull, C. H., "Statistical Package for the Social Sciences", McGraw-Hill, New York, 1970.

(26) Weast, R. C., Ed., "Handbook of Chemistry and Physics", 48th Ed., Chemical Rubber Company, Cleveland, 1967, pp A-163 to A-165.

APPENDIX A

VENDOR'S ANALYSIS REPORTS ON MARAGING STEEL MATERIALS

FORM V1669 5M-9-69

VASCO

A TELEDYNE COMPANY

LATROBE, PA. 15650

ANALYSIS REPORT

Customer: Battelle Memorial Institute
505 King Avenue
Columbus, Ohio 43201

Your Order No. A 9116 Part

Our Order No. V 451848

Brand: CVM Vascomax 250

SIZE	BARS	WEIGHT	HEAT No.	DATE SHIPPED
36 x .100 x 36	7 pcs	285	1870-A	3-24-70

Analysis

Heat No.	C	Si	Mn	S	P	W	Cr	V	Mo	Co	Ni
1870-A	.023	.03	.03	.005	.003				4.90	8.19	18.43

Heat No.	Al	Ti	B	Zr	Ca
1870-A	.10	.44	.002	.013	.05 (added)

Sworn and subscribed to before me
this 26 day of February 1971

JAMES E. KLOOS, Notary Public
My Commission Expires Jan. 31, 1972
Derry Township, Westmoreland County

Certified Correct

FORM V1868 8M-3-70

TELEDYNE VASCO

LATROBE, PA. 15650

ANALYSIS REPORT

Customer: Battelle Memorial Institute
505 King Avenue
Columbus, Ohio 43201

Your Order No. C 7943

Our Order No. V-408122

Brand: CVM VascoMax 250 Sheet MIL-S-46850-A

SIZE	BARS	WEIGHT	HEAT No.	DATE SHIPPED
.108" x 12"	20 pcs	285	04853	4-6-71

	Longitudinal	Transverse
Tensile Strength, psi	274,400	262,700
Yield Strength, psi 0.2% Offset	271,500	258,800
Elongation %	3.3	4.0

Hardness - 50.7 Rc
Annealed Hardness - 29/32 Rc
Grain Size - 7.1
Aging Time & Temperature - 900° - 3 hours

JK Rating:

	A Thin	A Heavy	B Thin	B Heavy	C Thin	C Heavy	D Thin	D Heavy	E Thin	E Heavy
T	0	0	0	0	0	0	1	0	1	0
B	0	0	0	0	0	0	1	0	1	0

Analysis

Heat No.	C	Si	Mn	S	P	W	Cr	V	Mo	Co	Ni
04853	.021	.05	.04	.008	.005				4.93	8.48	18.61

Heat No.	Al	Ti	B	Zr	Ca
04853	.14	.48	.002	.010	.05 (added)

Sworn and subscribed to before me
this 12 day of April 1971
JAMES T. KCOCS, Notary Public
My Commission Expires Jan. 31, 1972
Derry Township, Westmoreland County

Certified Correct

FORM V1668 8M-3-70

TELEDYNE VASCO

LATROBE, PA. 15650

ANALYSIS REPORT

Customer: **Battelle Memorial Institute**
505 King Ave.
Columbus, Ohio 43201

Your Order No. **C 7943 Part**

Our Order No. **V 408117 S**

Brand: **CVM VASCOMAX 250**

SIZE	BARS	WEIGHT	HEAT No.	DATE SHIPPED
4-3/16" round	1	33-3/8#	1453-A	2/25/71

Analysis

Heat No.	C	Si	Mn	S	P	W	Cr	V	Mo	Co	Ni
1453-A	.010	.01	.02	.005	.004	—	—	—	4.76	8.50	18.60

Heat No.	Al	Ti	B	Zr	Ca
1453-A	.15	.50	.003	.013	.05 Added

Sworn and subscribed to before me
this 26 day of February 1971

JAMES F. KLOSS, Notary Public
My Commission Expires Jan. 31, 1972
Derry Township, Westmoreland County

Certified Correct

J. F. McAuliffe

APPENDIX B

SUMMARY OF MATERIALS JOINED BY FRICTION WELDING

APPENDIX B

SUMMARY OF MATERIALS JOINED BY FRICTION WELDING

Material Joined	Configuration	Relative Velocity, rpm	Contact Pressure, ksi: Heating Phase	Contact Pressure, ksi: Forging Phase	Upset, in.	Time, sec	Reference
			Similar Metal Joints				
Aluminum (comm. pure)	3/4-in. rod	3800	4	6.5		6	10
1100 Aluminum	1-in. bar	5200[a]	7.6	7.6	0.150	1	21
2024 Aluminum	1/4-in. rod	3200	43	180	0.005		7
6061 Aluminum	1/4-in. rod	1000-1500	6-12	6-12		2-6	22
	3/8-in. rod	1000-1500	3-6	3-6		2-9	22
	1-in. bar	5700[a]	8.9	8.9	0.150	1	21
Copper (comm. pure)	1-in. bar	8000[a]	6.4	6.4	0.150	0.5	21
Copper (ETP)	1-in. bar	6000	5	10		18	10
Copper	1-1/2-in. bar	5400	6.4	10		8.5	9
Cartridge brass	1-in. bar	7000[a]	6.4	6.4	0.150	0.7	21
Magnesium	1/4-in. rod	3200	57	113	0.010		7
Nickel	1/4-in. rod	3200	86	169	0.010		7
Inconel 718	1-in. bar	1500[a]	63.6	63.6	0.150	3	21
Udimet 700	1/2-in rod	3600[a]	41	41	0.150		13
Carbon steel	1/2-in. rod	3000	5	5		7	10
	1-in. bar	1500	7.5	7.5		15	10
1018 Steel	5/16-in. rod	4400	8	18		3	9
	1-in. bar	4600[a]	15.3	15.3	0.100	2	21
1037 Steel	1-11/16-in. bar	2200	12	24		21	9
1045 Steel	1-in. bar	4600[a]	17.8	17.8	0.100	2	21
4140 Steel	1-in. bar	4600[a]	19.1	19.1	0.100	2	21
SAR 8620 steel	3-1/16-in. bar	2500	28	60		11	9
T-1 Tool steel	3/4-in. bar	4000	15	20		10	10
Maraging steel	1-in. bar	3000[a]	25.5	25.5	0.10	2.5	21
18 Ni (250) maraging	3-in. thin-wall tube	2000	9.5	17	0.075	1.6	This work
18 Ni maraging	2.36-in.^{2} tube	2500	16	30		12.5	9
302 Stainless	1-in. bar	3500[a]	22.9	22.9	0.10	2.5	21
304 Stainless	1/4-in. rod	3200	86	169	0 070		7
300 and 400 Series S.S.	1-in. bar	3000	12	16		7	10
	5.5-00 x 1/2-wall tube	800	20	20		35	10
410 Stainless	1/4-in. rod	1500	10	10		2-4	22
	1-in. bar	3000[a]	22.9	22.9	0.10	2.5	21
Ti-6Al-4V	1-in. bar	6000[a]	10.2	10.2	0.10	2	21
Ti-13Al-11V	3/4-in. bar	10,000	0.4	8.5		20-25	10
Ti-6Al-4V	22-in.-diam ring	1500[a]	50	50			12
Zirconium	1/4-in. rod	3200	31-86	31-169	0.030		7
Zircoloy-2	1/4-in. rod	500-1000	10-26	10-26		18-3	22
			Dissimilar Metal Joints				
1100 Aluminum to copper	1-in. bar	2000[a]	96	96	0.200	1	21
2024 Aluminum to copper	1/4-in. rod	3200	114	114	0.015		7
6061 Al - 302 S.S.	1-in. bar	5500[a]	6.4	19.1	0.200	3	21
Cu - 1018 Steel	1-in. bar	8000[a]	6.4	6.4	0.150	1	21
Inconel 718 - 1045 Steel	1-in. bar	1500[a]	51	51	0.150	2.5	21
Sintered high-carbon steel - 1018 steel	1-in. bar	4600[a]	15.3	15.3	0.100	2.5	21
1141 Steel to 1020 steel	13/16-in. rod	4400	12	17		4	9
3140 Steel to 21Cr-4Ni-9mn Steel	3/8-in. rod	5000	25	40		10	10
4140 steel - 1035 steel	1-3/4-OD x 1/4-wall tube	6800	2.5	6		42	10
	4-1/2-OD x 5/8-wall tube	3000	5.5	16		26	10
5120 Steel - 1026 steel	3/4-in. bar	2200	7.5	18		8	9
5130 Steel - Sint. Fe	5/15-in. rod	5600	8	16		10	9
M-2 Tool St. - 1045 steel	1-in. bar	3000[a]	51	51	0.100	3	21
Stainless - carbon steel	3/4-in. bar	3000	7.5	15		10	10
302 S.S. - 1020 steel	1-in. bar	3000[a]	22.9	22.9	0.100	2.5	21
Zr to 1020 steel	1/4-in. rod	3200	28.6	169	0.020		7
Zr to 304 S.S.	1/4-in. rod	3200	28.6	116	0.025		7
Zircoloy-2 to 410 S.S.	1/4-in. rod	1000	10	10		4	22

(a) Initial relative velocity - inertia welding process.

APPENDIX C

SUMMARIES OF FRICTION-WELDING VARIABLES INVESTIGATED

APPENDIX C

SUMMARIES OF FRICTION-WELDING VARIABLES INVESTIGATED

TABLE C-1. FRICTION-WELDING VARIABLES FROM PRELIMINARY PHASE II STUDIES ON MARAGING STEEL

Weld Cycle	Mean Specimen Diam, in.	D/T Ratio	Faying Area, in.^{2}	Rotational Velocity, rpm	Heating Pressure, psi	Initial Peak Torque, ft-lb	Conditions at Cycle Termination: Torque, ft-lb	Conditions at Cycle Termination: Upset, in.	Forging Pressure, psi	Spindle Brake, psi	Total Upset, in.	Weld Energy, Btu/in.^{2}	Cycle Time, sec
1	2.798	34	0.751	1000	400	Specimen components seized together on contact and slipped in chucks							
2	2.798	34	0.721	1000	3,880	235	90	--	--	--	0.008	--	~1[a]
3	2.802	32	0.761	1000	Clutch failed to disengage to terminate cycle					--	0.344	--	--[a]
4	2.800	33	0.748	1000	5,880	170	60	0.040	6,150	Off	0.056	--	9.3[a]
5	2.800	32	0.[illegible]	1000	5,840	70	50		6,360		0.40	--	21[a]
(Aged)								Clutch failed to disengage to terminate cycle					
6	2.800	33	0.748	2000	2,960	150	60	0.025	6,950	30	0.042	37.1	1.3[illegible]
7	Weld not completed because of failure of clutch to disengage to initiate cycle termination												
8	2.805	31	0.789	2000	6,340	200	47	0.030	15,650	30	0.039	49.6	2.[illegible]4
9	2.805	32	0.780	2000	4,740	162	30	0.026	9,360	30	0.038	60.8	3.72
10	2.802	32	0.766	2000	4,830	160	30	0.027	5,160	30	0.033	62.6	3.73
11	2.802	33	0.[illegible]53	2000	4,980	155	35	ND	9,630	30	0.035	No	No
12	2.802	32	0.761	2000	7,100	170	52	ND	12,480	30	ND	42.3	No
13	2.802	32	0.761	2000	11,96[illegible]	165	92	0.030	21,290	30	0.045[c]	32.1	0.88
14	2.802	33	0.753	2000	13,550	No	ND	0.019	13,810	30	0.034	No	0.8[illegible]
15	2.802	32	0.761	1500	3,880	188	30	0.029	6,700	30	0.044	66.8	5.1
16	2.802	32	0.761	1500	6,240	200	50	0.034	11,430	30	0.045[c]	15.2	2.28
17	2.805	31	0.789	1500	8,750	207	90	0.037	16,220	30	0.046	31.0	1.55
18	2.802	33	0.753	1500	11,290	160	48	0.049	12,350	30	ND	44.7	2.55
20	2.805	32	0.780	2000	6,540	155	45	0.014	16,540	30	0.045[c]	39.0	1.85
21	2.802	32	0.766	2000	6,330	155	44	0.012	16,060	30	0.044[c]	36.6	1.65
22	2.201	33	0.748	2000	6,420	180	40	0.030	16,840	Off	0.048[c]	56.0	2.57
23	2.805	31	0.789	2000	6,080	160	40	0.031	15,720	60	0.045[c]	46.4	2.5
24	2.805	31	0.789	1500	5,070	250	No	ND	5,070	30	0.005	9.9	0.47[b]
25	2.805	32	0.780	1500	4,940	195	40	0.025	13,080	30	0.071	52.2	3.6
27	2.801	32	0.766	2000	6,140	150	43	0.032	17,230	30	0.122	62.3	[illegible] 96
(Aged)													
28	2.802	3[illegible]	0.766	3000	3,920	75	20	0.029	3,920	60	0.035	94.1	5.9
29	Weld not completed because of failure of clutch to disengage to initiate cycle termination												
30	2.802	32	0.761	3000	6,310	75	28	0.031	13,270	60	0.063	53.1	2.42
31	2.805	31	0.789	3000	3,680	105	15	0.028	7,600	60	0.055	97.7	7.45
32	2.802	33	0.753	3000	9,300	130	43	0.023	19,120	60	0.050	38.6	1.22

(a) Programmed ramp axial pressure buildup.

(b) Friction welder drive pin sheared, causing effective cycle termination.

(c) Total upset questionable because of limits of readout linearity.

TABLE C-2. FRICTION-WELDING VARIABLES FROM PHASE II STUDIES ON MA[illegible]ING STEEL

Weld Cycle	Mean Specimen Diam, in.	D/T Ratio	Faying Area, in.^{2}	Rotational Velocity, rpm	Heating Pressure, psi	Initial Peak Torque, ft-lb	Conditions at Cycle Termination: Torque, ft-lb	Conditions at Cycle Termination: Upset, in.	Forging Pressure, psi	Spindle Brake, psi	Total Upset, in.	Weld Energy, Btu/in.^{2}	Cycle Time, sec
26	2.802	32	0.758	2000	6,340	120	40	0.033	16,750	30	0.100	59.7	2.85
35	2.804	30	0.811	2000	3,700	122	24	0.022	7,400	60	0.048	84.8	6.90
36	2.804	30	0.830	2000	5,960	118	37	0.065	11,920	60	0.119	24.5	4.55
37	2.809	30	0.816	2000	9,800	143	60	0.020	20,200	60	0.053	33.9	1.14
38	2.807	31	0.798	2000	3,630	120	34	0.012	15,300	60	0.095	76.2	6.00
39	2.806	31	0.779	2000	3,590	115	20	0.007	23,440	60	0.130	62.2	4.87
40	2.804	30	0.806	2000	6,200	115	38	0.020	18,850	60	0.079	48.1	2.58
41	2.306	30	0.833	2000	9,610	145	59	0.052	14,400	60	0.079	44.3	1.82
42	2.804	31	0.797	2000	9,910	113	65	0.042	17,050	60	0.074	41.2	1.53
43	2.808	31	0.812	3000	3,450	79	17	0.024	7,140	60	0.058	95.6	7.71
44	2.801	32	0.770	3000	3,765	75	17	0.012	15,850	60	0.103	62.4	4.90
45	2.804	33	0.766	3000	3,525	67	19	0.006	23,750	60	0.149	67.6	4.34
46	2.802	32	0.783	3000	6,130	77	29	0.056	12,500	60	0.110	68.2	3.32
47	2.808	31	0.807	3000	5,450	88	26	0.032	17,850	60	0.103	56.5	3.00
48	2.802	31	0.784	3000	6,120	100	33	0.019	25,750	60	0.105	59.1	2.23
49	2.800	31	0.787	3000	9,900	115	54	0.055	15,250	60	0.089	54.7	1.72
50	2.800	31	0.801	3000	9,610	75	50	0.060	17,850	60	0.191	79.0	2.74
51	2.805	33	0.753	3000	10,230	100	57	0.034	18,450	60	0.074	44.4	1.19
52	2.801	31	0.805	3000	9,680	100	55	0.024	19,850	60	0.065	43.5	1.23
60	2.774	46	0.513	2020	5,650	85	28	0.028	16,760	60	0.084	48.4	1.43
61	2.773	47	0.513	2020	9,840	104	45	0.033	17,150	60	0.064	34.4	1.17
65	2.805	32	0.777	1000	3,800	230	35	0.062	7,730	60	0.091	93.3	9.83
66	2.801	31	0.805	1000	3,600	195	35	0.063	23,350	60	0.282	91.4	10.35
67	2.801	33	0.757	1000	4,030	205	43	0.036	16,250	60	0.107	64.1	5.55
68	2.801	31	0.805	1000	3,790	245	65	0.010	22,350	60	0.028	27.4	1.65
69	2.802	31	0.791	1000	6,070	270	62	0.044	12,260	60	0.073	47.7	3.20
70	2.795	33	0.742	1000	6,740	225	80	0.028	20,350	60	0.049	27.9	1.40
71	2.803	30	0.810	1000	5,930	232	84	0.014	25,060	60	0.036	23.8	1.27
72	2.803	31	0.803	1000	9,710	235	98	0.048	14,810	60	0.067	32.4	1.61
73	2.802	30	0.814	1000	9,340	275	98	0.031	16,840	60	0.052	29.9	1.48
74	2.802	30	0.823	1000	9,970	270	112	0.014	19,930	60	0.027	4.8	0.80
75	5.738	78	1.346	675	6,680	460	310	0.016	16,950	60	0.022	21.1	0.82

TABLE C-2. (Continued)

Weld Cycle	Mean Specimen Diam. in.	D/T Ratio	Faying Area, in.²	Rotational Velocity, rpm	Heating Pressure, psi	Initial Peak Torque, ft-lb	Conditions at Cycle Termination Torque, ft-lb	Conditions at Cycle Termination Upset, in.	Forging Pressure, psi	Spindle Brake, psi	Total Upset, in.	Weld Energy, Btu/in.²	Cycle Time, sec
76	5.802	83	1.282	610	9,990	415	340	0.037	12,300	60	0.047	21.2	1.03
77	5.786	81	1.291	1088	6,200	410	125	0.042	12,700	60	0.064	37.3	2.29
78	5.796	71	1.493	1088	10,500	295	215	0.041	19,100	60	0.054	23.9	1.08
79[a]	5.793	74	1.420	683	6,340	570	600	0.001	17,040	60	0.022	15.6	0.53
80	2.780	48	0.510	1010	9,410	165	63	0.038	16,7[illegible]0	60	0.066	26.7	1.19
81	2.773	47	0.514	1010	4,575	205	30	0.037	18,670	60	0.117	45.9	3.78
82	2.799	32	0.769	1000	3,965	175	35	0.055	16,510	60	0.167	68.2	8.04
83	2.797	33	0.750	1000	9,200	265	80	0.046	15,850	60	0.070	36.0	1.71
84	5.793	82	1.263	958	10,050	278	178	0.064	17,300	60	0.079	40.4	1.33
85	2.796	33	0.755	2000	6,230	125	33	0.033	16,960	60	0.097	49.1	2.94
86	2.798	3[illegible]	0.760	2000	9,870	108	64	0.045	17,110	60	0.076	35.8	1.44
87	2.796	33	0.745	3000	9,660	78	37	0.029	20,810	60	0.069	30.2	1.22
88	2.772	45	0.531	3030	9,600	47	27	0.032	20,530	60	0.079	23.7	0.86
89	5.800	81	1.315	1235	9,320	230	>750	ND	9,320	Off[b]	0.004	14.3	0.5

(a) Friction-welder drive system disengaged prematurely, probably due to chatter in the specimens.
(b) Friction-welder drive pin sheared, causing effective cycle termination.

TABLE C-3. FRICTION-WELDING VARIABLES FROM PHASE II STUDIES ON 7075 ALUMINUM

Weld Cycle	Mean Specimen Diam, in.	Faying Area, in.^{2}	Rotational Velocity, rpm	Pressurization Rate, psi/sec	Heating Pressure, psi	Initial Peak Torque, ft-lb	Conditions at Cycle Termination		Forging Pressure, psi	Spindle Brake, psi	Total Upset, in.	Weld Energy, Btu/in.^{2}	Cycle Time, sec
							Torque, ft-lb	Upset, in.					
19	2.829	[illegible]	1500	Impulsive	2460	157	15	0.035	2460	30	0.043	25.2	4.9
33	2.829	1.058	1000 avg	Ditto	2740	185	7375	ND	2840	Off(a)	0.016	ND	0.5
34	2.828	1.057	2000	2840	2840-2080(c)	65	36	0.057	3030	60	0.131	36.2	3.5
53	2.829	1.058	2000	5670	5580-3120(c)	65	50	ND(b)	6240	60	1.226	ND	5.4
54	2.828	1.057	2000	4460	5110-3880(c)	57	48	0.066	5680	60	0.166	28.7	3.05
55	2.829	1.053	2000	2850	3130-2370(c)	60	41	0.071(b)	3420	60	0.418	48.1	4.36
56	2.829	1.049	2000	2860	3050-2380(c)	60	38	0.071(b)	5530	60	0.505	ND	4.65
57	2.829	1.049	2000	2860	2960-1910(c)	65	37	0.050	3050	60	0.123	41.1	3.92
58	2.829	1.058	2000	2840	3020-2550(c)	61	38	0.014	5480	60	0.021	35.8	3.4
59(d)	2.831	1.041	2000	2880	2980-2310(c)	60	37	0.034	3270	60	0.094	36.9	3.32

(a) Friction-welder drive pin sheared, causing effective cycle termination.
(b) Friction-welder clutch failed to disengage automatically, causing excessive axial upset unreliable displacement transducer readings at cycle termination.
(c) Experienced loss in axial heating pressure due to sudden softening of specimens, and hydraulic rams were unable to keep up with displacement of material from faying surfaces.
(d) Specimens stress-relief annealed 870 F, 50 minutes, water quenched prior to welding.

TABLE C-4. FRICTION-WELDING VARIABLES FROM PHASE III STUDIES ON MARAGING STEEL

Weld Cycle	Mean Specimen Diam. in.	D/T Ratio	Faying Area, in.^{2}	Rotational Velocity, rpm	Heating Pressure, psi	Initial Peak Torque, ft-lb	Condition at Cycle Termination		Forging Pressure, psi	Spindle Brake, psi	Total Upset, in.	Weld Energy, Btu/in^2	Cycle Time, sec.
							Torque, ft-lb	Upset, in.					
						Tube-to-Tube Half-LAP Joint Configuration							
90	2.838	65	0.392	2000	8930	122	41	.041	14,920	60	0.061	43.3	1.14
91	2.837	61	0.401	2000	9230	100	37	.028	17,330	60	0.054	31.3	0.89
92	2.840	65	0.388	2000	9410	100	50	.021	13,920	60	0.034	42.9	1.24
93	2.838	69	0.366	2000	9840	89	36	.056	20,770	60	0.080	93.4	2.64
94	2.838	65	0.392	2000	9310	106	49	.041	16,840	60	0.055	53.1	1.42
95	2.838	63	0.401	2000	9100	110	40	.064	16,080	60	0.081	62.4	1.62
96	2.840	64	0.397	2000	9320	118	51	~.020	20,030	60	0.045	38.5	0.99
97	2.839	68	0.374	2000	9630	100	40	.057	16,980	60	0.075	65.1	1.67
98	2.839	65	0.392	2000	9060	88	43	.036	19,770	60	0.060	47.8	1.37
99	2.831	75	0.338	2000	9620	94	45	.039	13,910	60	0.052	45.2	0.99
100	2.831	75	0.333	2000	9320	97	50	.023	17,160	60	0.043	40.1	0.83
						Tube-to-Plate Half-LAP Joint Configuration							
101	2.839	66	0.384	2000	9770	89	51	.056	19,660	60	0.072	60.3	1.53
102	2.838	67	0.379	2000	9230	127	49	.036	20,050	60	0.050	58.8	1.51
103	2.839	65	0.392	2000	8930	99	48	.036	16,960	60	0.052	57.4	1.50
104	2.837	68	0.374	2000	9090	99	48	.022	16,580	60	0.037	50.5	1.18
105	2.835	69	0.365	2000	9040	92	42	.055	13,970	60	0.063	90.4	2.55
106	2.837	68	0.370	2000	8920	82	41	.056	16,490	60	0.067	101.9	3.08
107	2.841	65	0.388	2000	9410	94	54	.023	13,920	60	0.036	44.0	1.09
108	2.838	67	0.379	2000	8440	113	53	.024	19,260	60	0.043	46.6	1.06
109	2.839	67	0.379	2000	8710	106	48	.039	13,460	60	0.054	59.3	1.50

APPENDIX D

THERMAL HISTORIES OF FRICTION-WELDING EXPERIMENTS

APPENDIX D

SUMMARY OF FRICTION WELDING THERMAL HISTORIES

Friction welding specimen thermal histories are presented here as a collection of graphs showing specimen temperatures as a function of time from the start of the weld cycles. These representations were obtained directly from the respective weld cycle oscillograph records of thermocouple potentials.

The dashed vertical line on each graph represents the point in time at which the weld cycle was terminated (relative rotation between the specimen components was halted). In most cases three time-temperature traces were obtained from thermocouples imbedded in the nonrotating specimen components at distances of 1/16, 3/16, and 7/16 inch from the original faying surfaces. In those cases where only one time-temperature trace appears, a single thermocouple imbedded in the nonrotating specimen component at a distance of 1/16 inch from the original faying surfaces was all that could be accommodated because of limitations imposed by special chucking fixtures. The erratic behavior of some of the highest reading thermocouples was, in some cases (Cycles 44, 47, 60, 65, 70, 72, 73, 85, 105, 106, and 109), caused by failure to remain in intimate contact with the specimen. This contact was in some instances restored by mechanical action of the weld flash. During Cycle 82, however, the thermocouple apparently opened at its bead and was later rejoined by the curling weld flash, with the specimen itself acting as the junction.

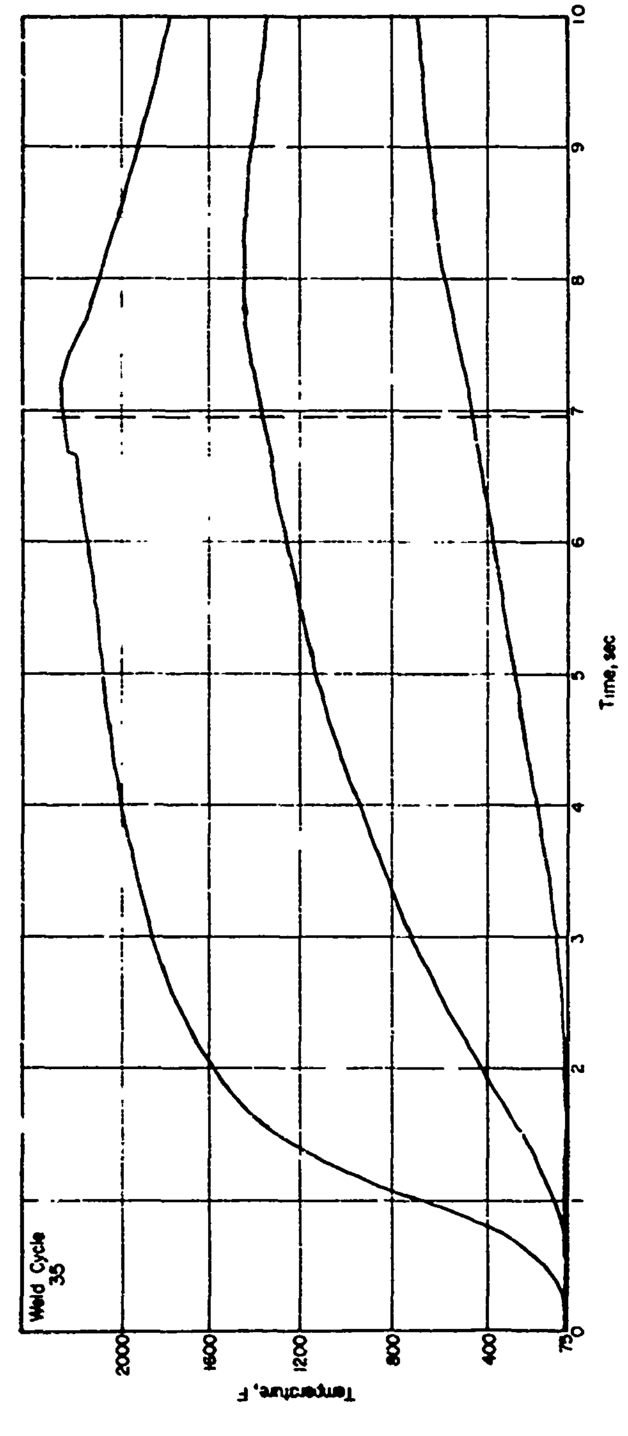
Weld Cycle
35
2000
1600
1200
800
400
75
Temperature, F
0
1
2
3
4
5
6
7
8
9
10
Time, sec

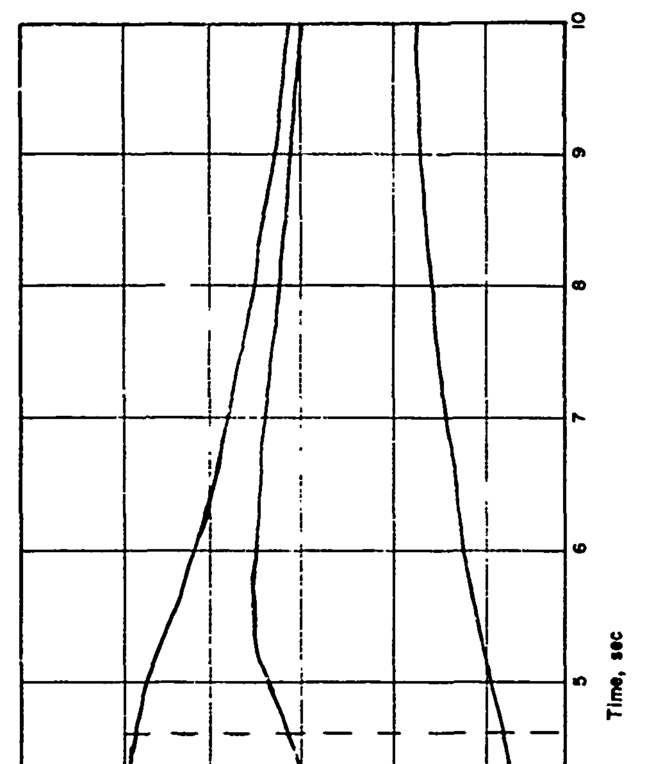
Weld Cycle
36
Temperature, F
2400
2000
1600
1200
800
400
32
0
1
2
3
4
5
6
7
8
9
10
Time, sec

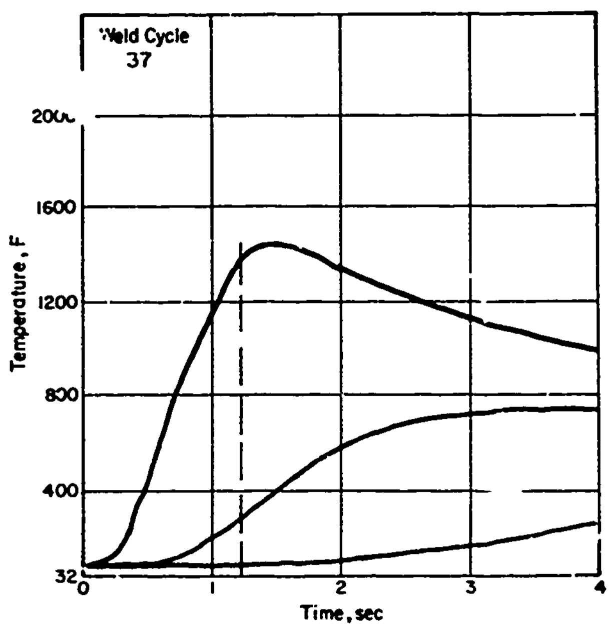

Weld Cycle
37
2000
1600
1200
800
400
32
Temperature, F
0
1
2
3
4
Time, sec

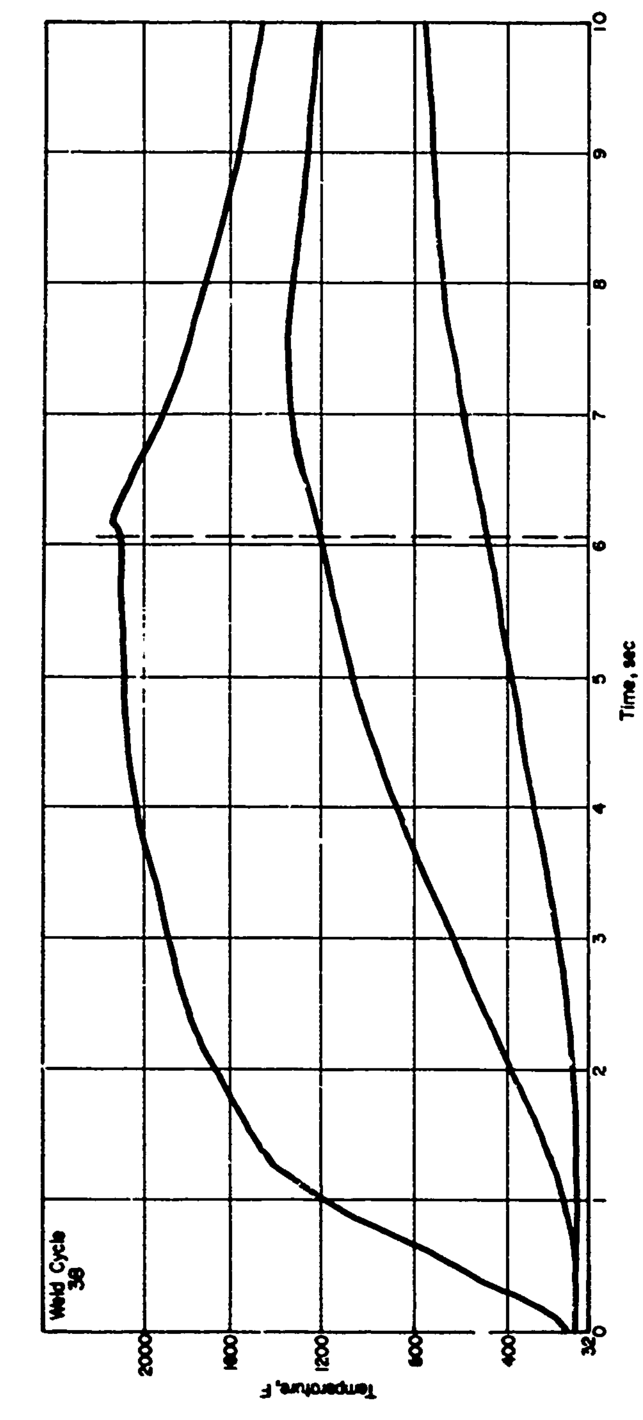

Weld Cycle 38
Temperature, F
32
400
800
1200
1600
2000
Time, sec
0
1
2
3
4
5
6
7
8
9
10

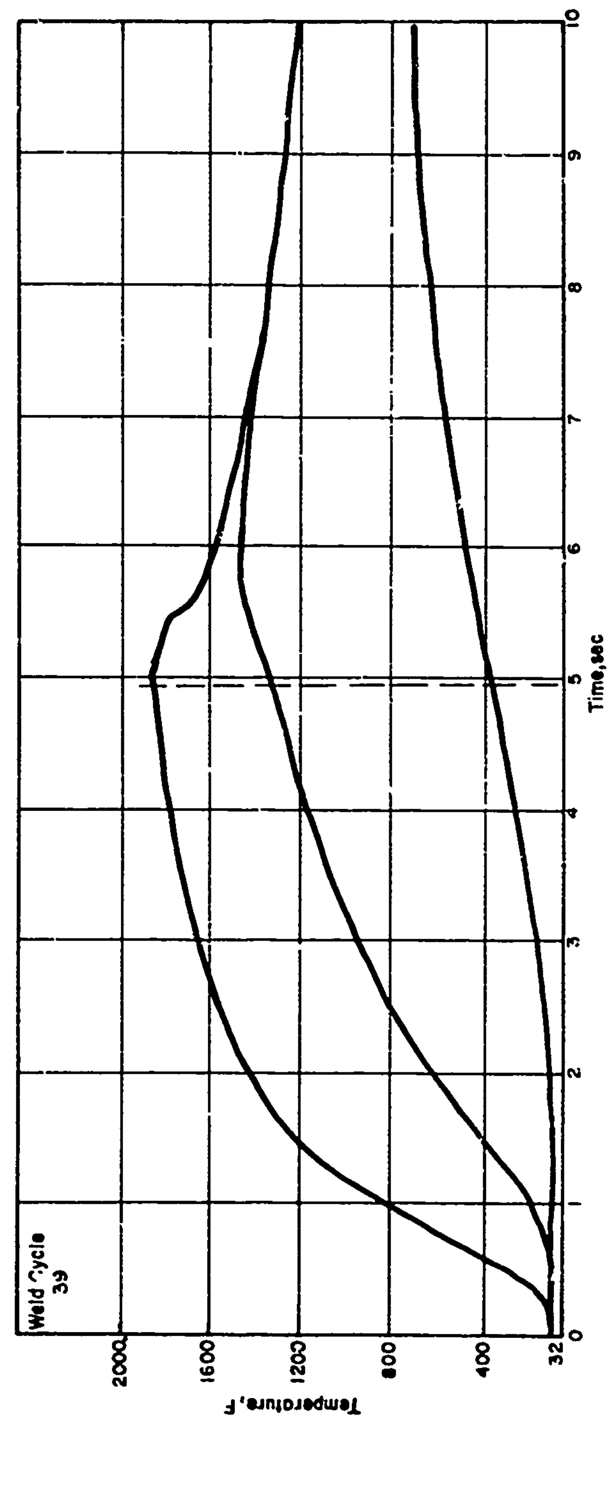
Weld Cycle 39
Temperature, F
2000
1600
1200
800
400
32
Time, sec
0
1
2
3
4
5
6
7
8
9
10

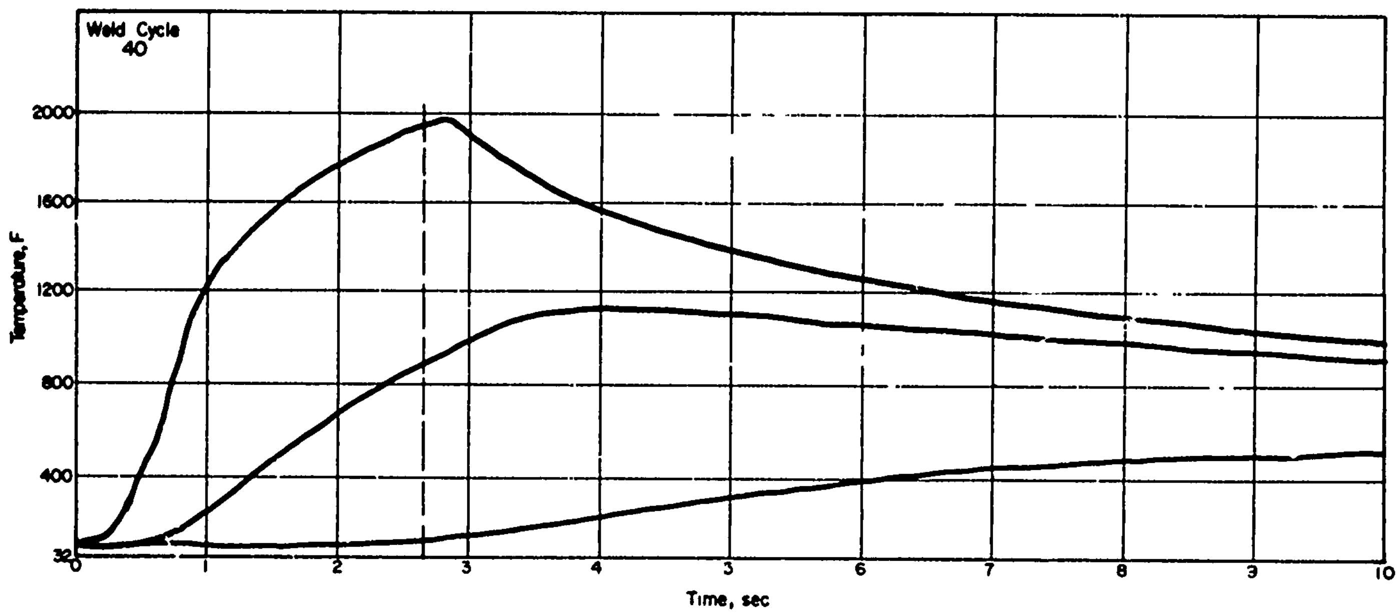
Weld Cycle
40
Temperature, F
32
400
800
1200
1600
2000
Time, sec
0
1
2
3
4
5
6
7
8
9
10

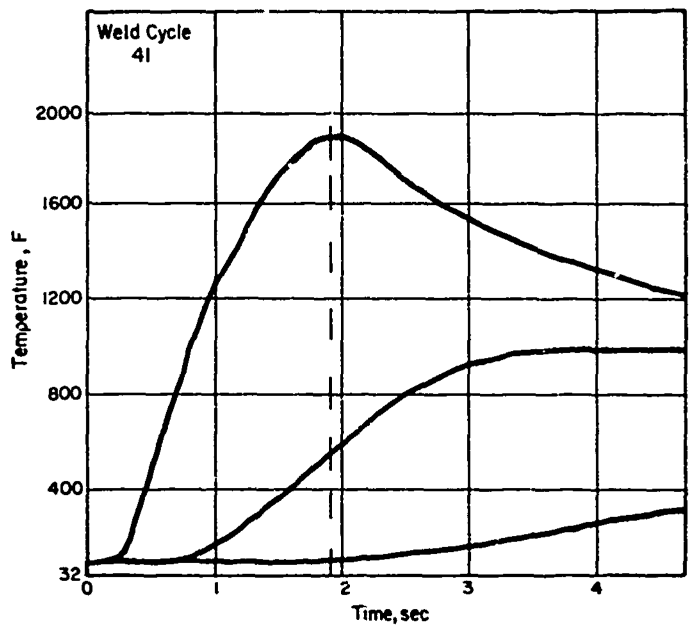
Weld Cycle
41
2000
1600
1200
800
400
32
Temperature, F
0
1
2
3
4
Time, sec

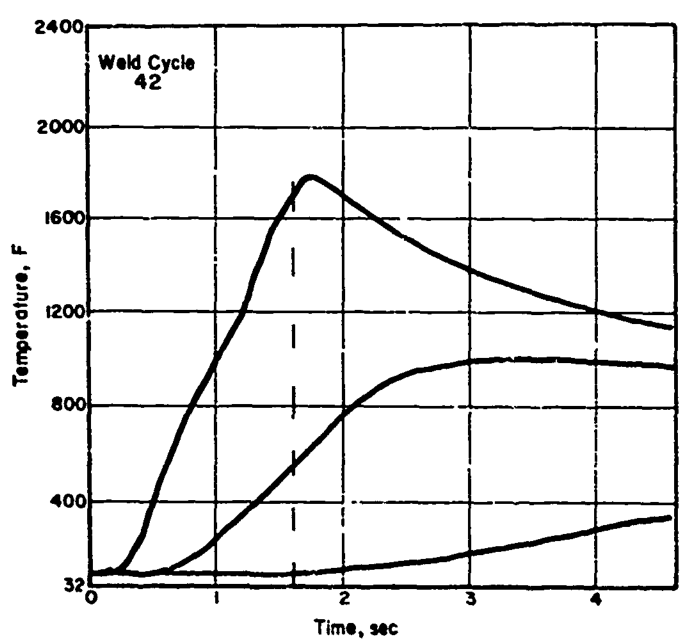
2400
Weld Cycle
42
2000
1600
1200
800
400
32
Temperature, F
0
1
2
3
4
Time, sec

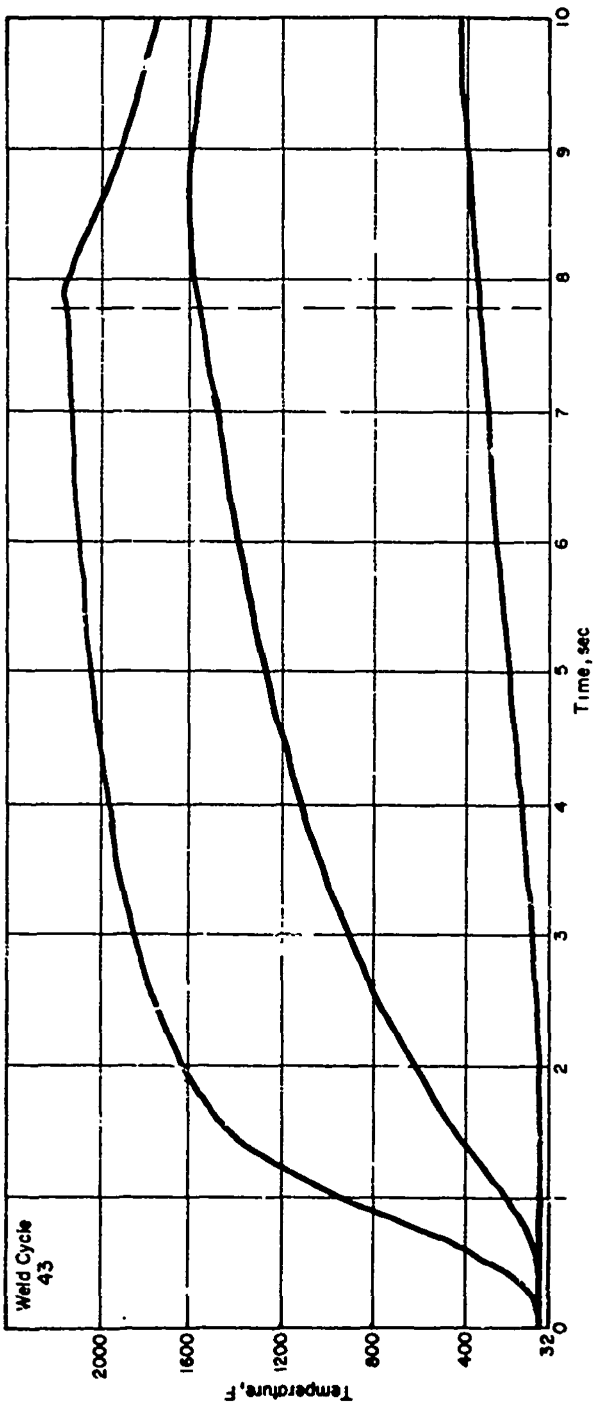

Weld Cycle
43
Temperature, F
2000
1600
1200
800
400
32
Time, sec
0
2
3
4
5
6
7
8
9
10

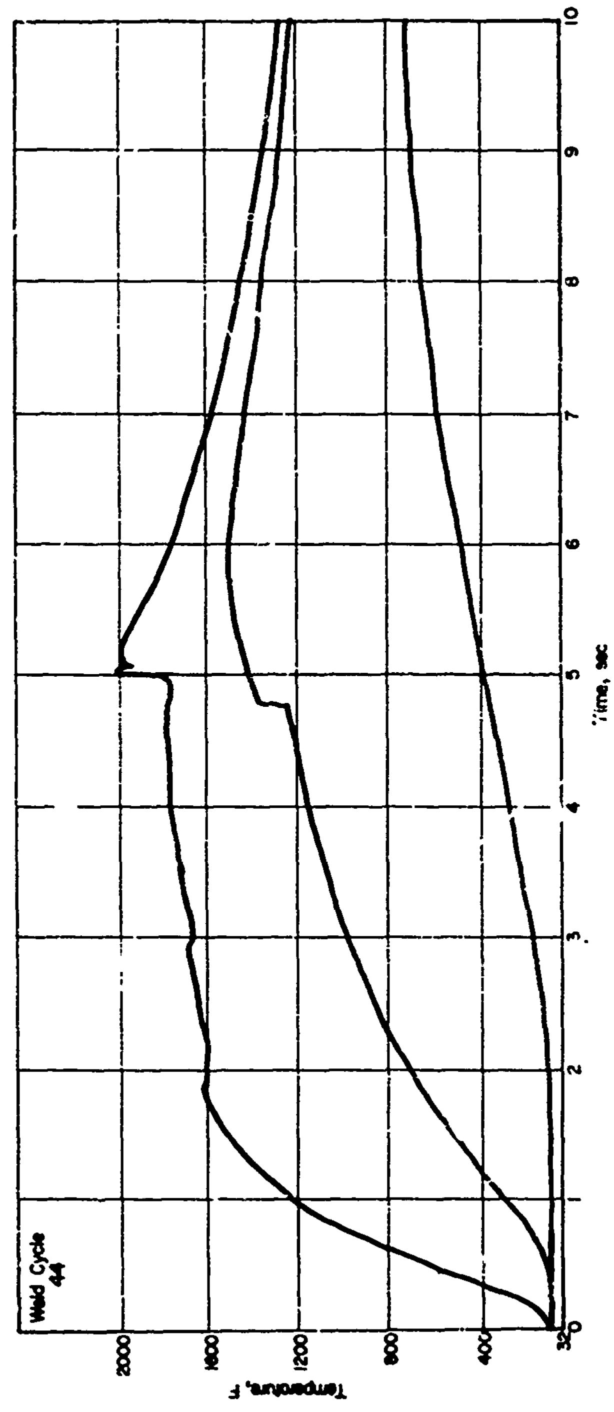
Weld Cycle
44
Temperature, F
2000
1600
1200
800
400
32
0
1
2
3
4
5
6
7
8
9
10
Time, sec

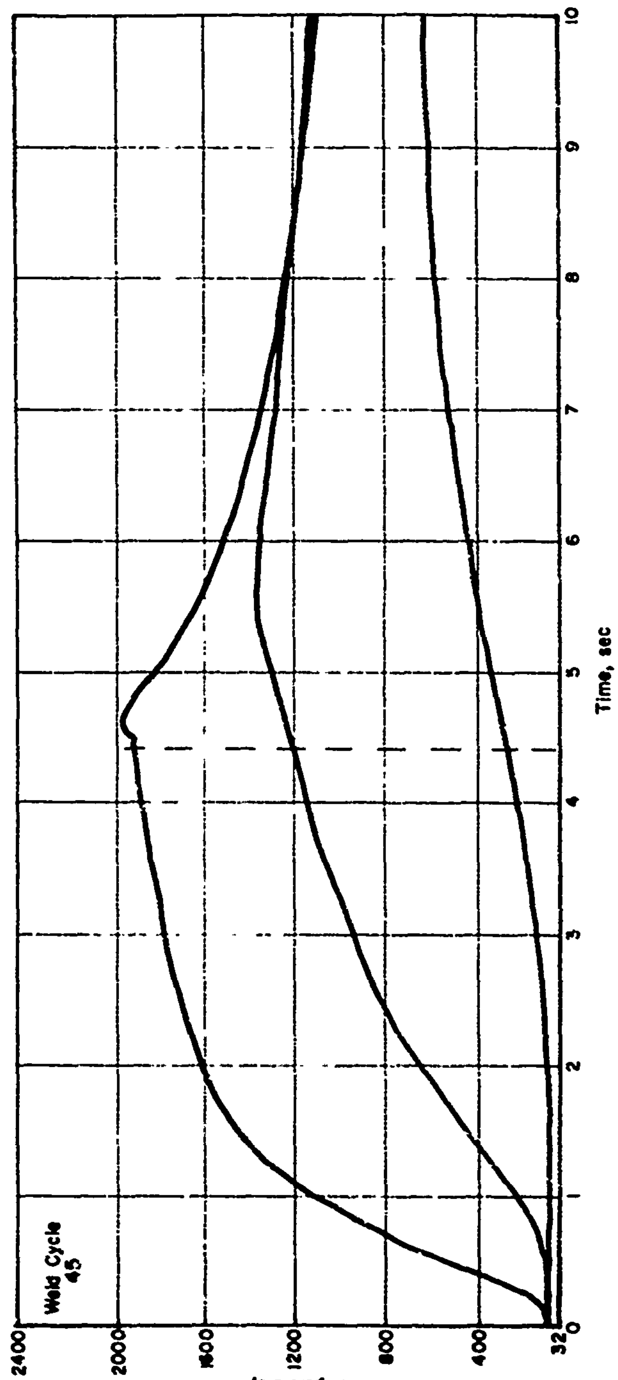
Weld Cycle
45
Temperature, F
2400
2000
1600
1200
800
400
32
Time, sec
0
1
2
3
4
5
6
7
8
9
10

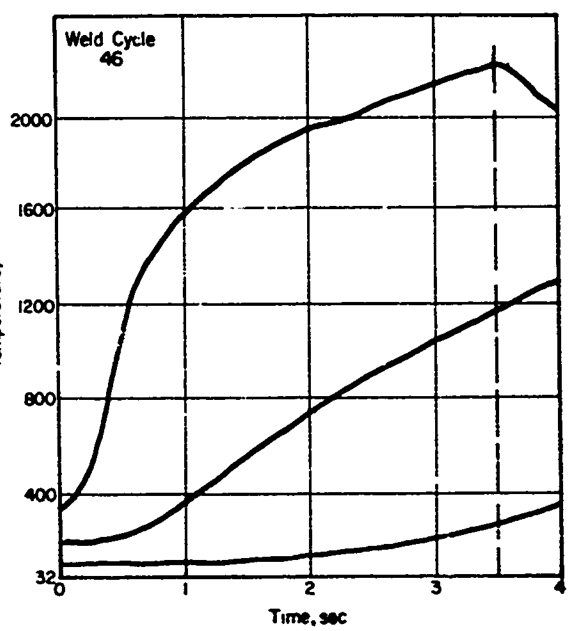
Weld Cycle
46
2000
1600
1200
800
400
32
Temperature, F
0
1
2
3
4
Time, sec

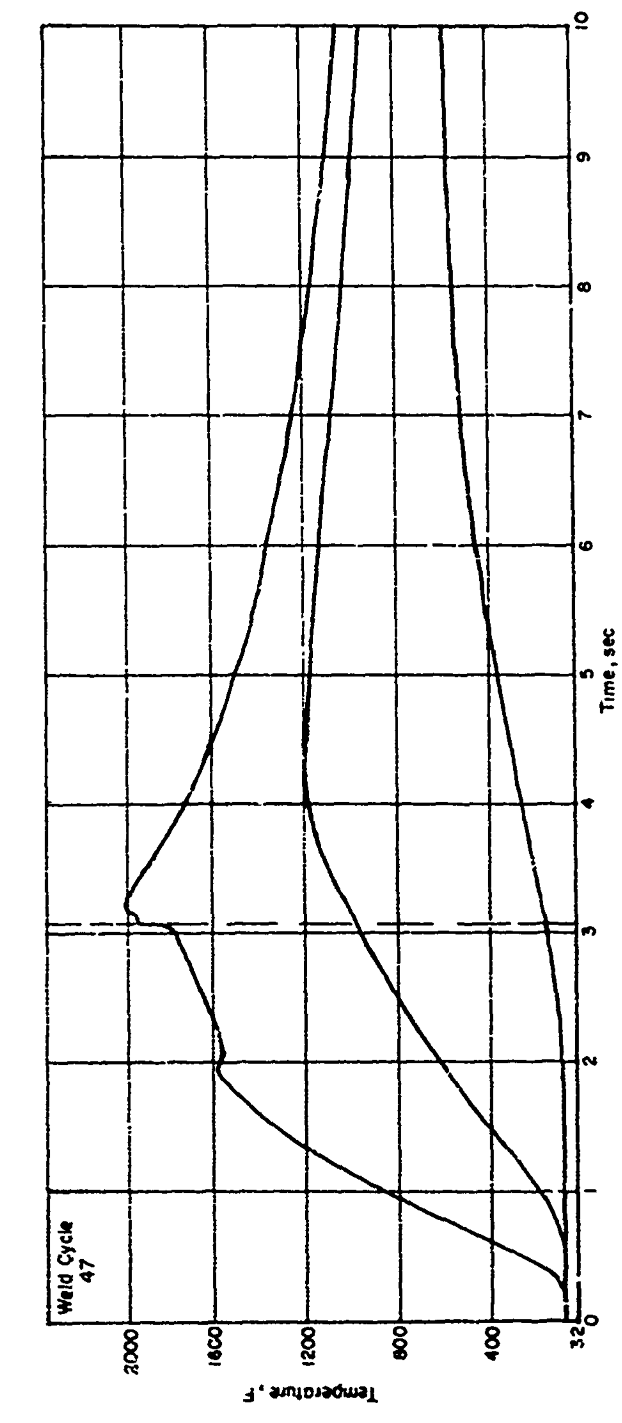
Weld Cycle
47
Temperature, F
2000
1600
1200
800
400
32
0
1
2
3
4
5
6
7
8
9
10
Time, sec

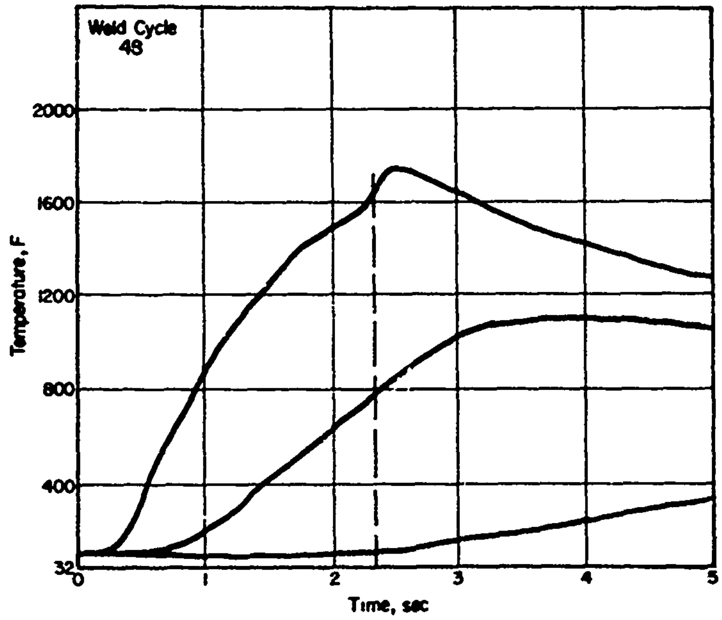
Weld Cycle
48
Temperature, F
2000
1600
1200
800
400
32
0
1
2
3
4
5
Time, sec

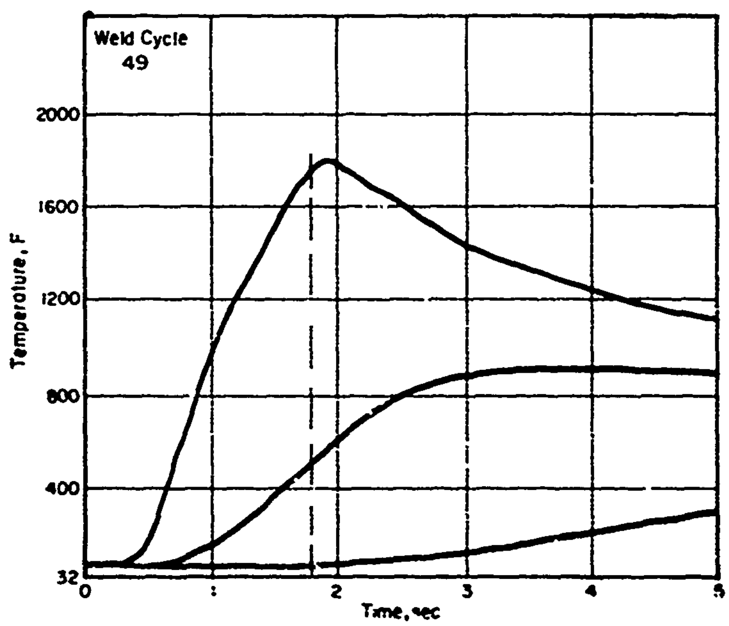
Weld Cycle
49
Temperature, F
2000
1600
1200
800
400
32
0
2
3
4
5
Time, sec

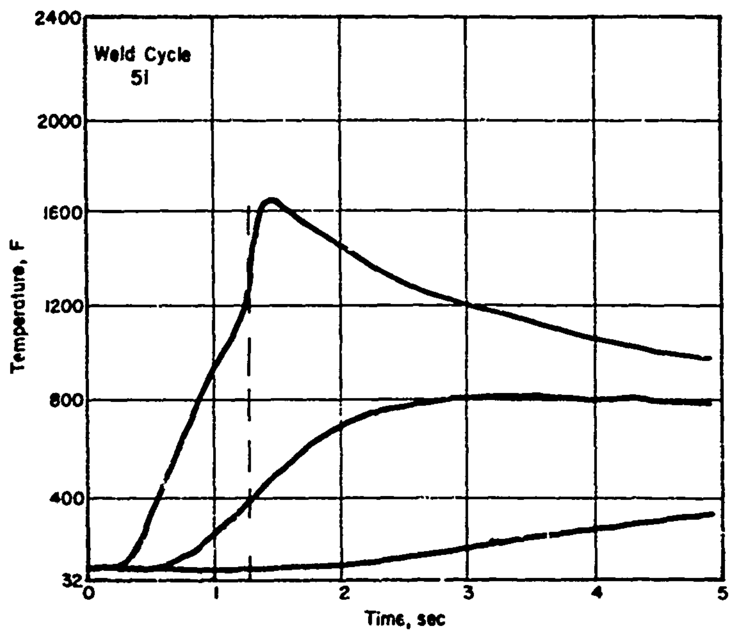
Weld Cycle
51
2400
2000
1600
1200
800
400
32
Temperature, F
0
1
2
3
4
5
Time, sec

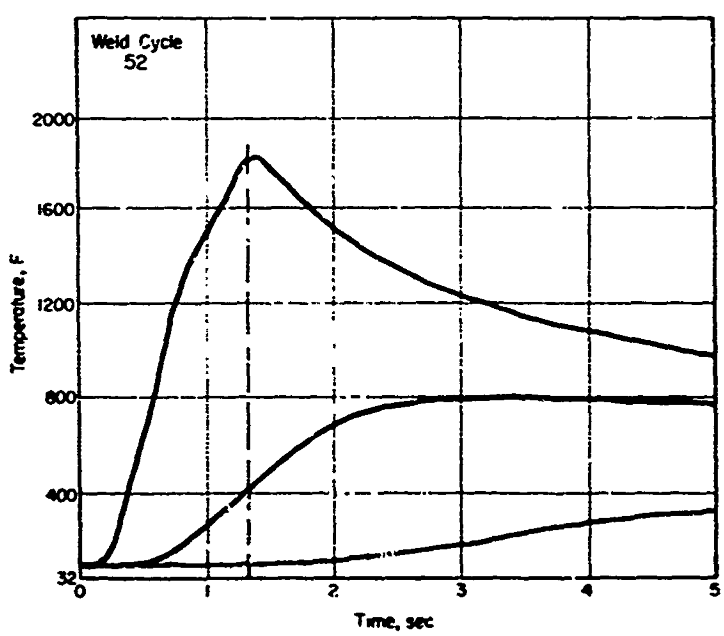
Weld Cycle
52
2000
1600
1200
800
400
32
Temperature, F
0
1
2
3
4
5
Time, sec

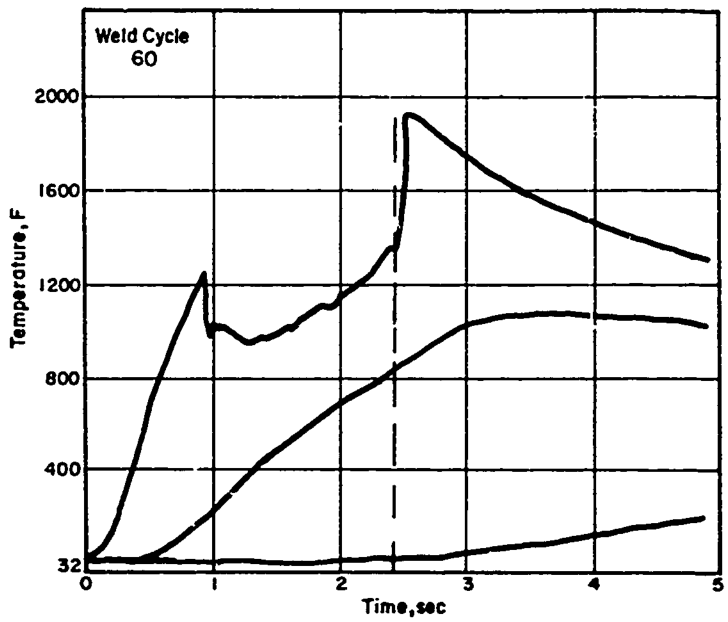
Weld Cycle
60
Temperature, F
2000
1600
1200
800
400
32
0
1
2
3
4
5
Time, sec

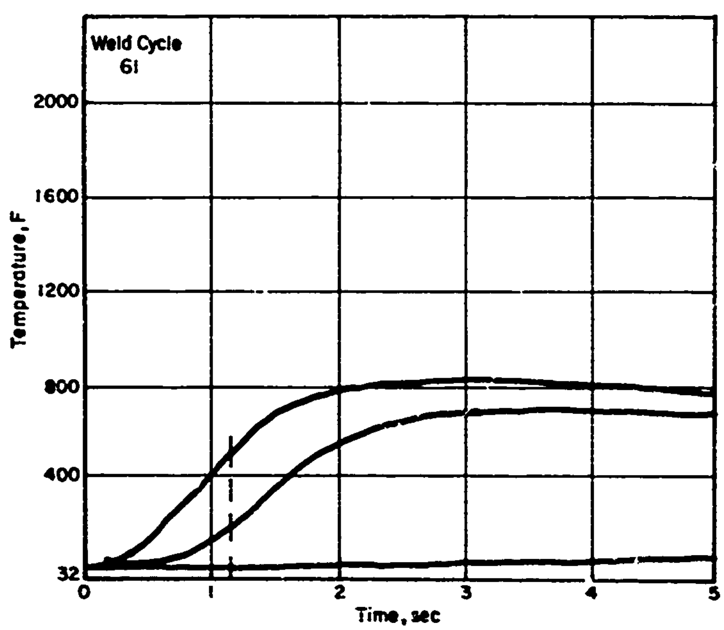
Weld Cycle
61
Temperature, F
2000
1600
1200
800
400
32
0
1
2
3
4
5
Time, sec

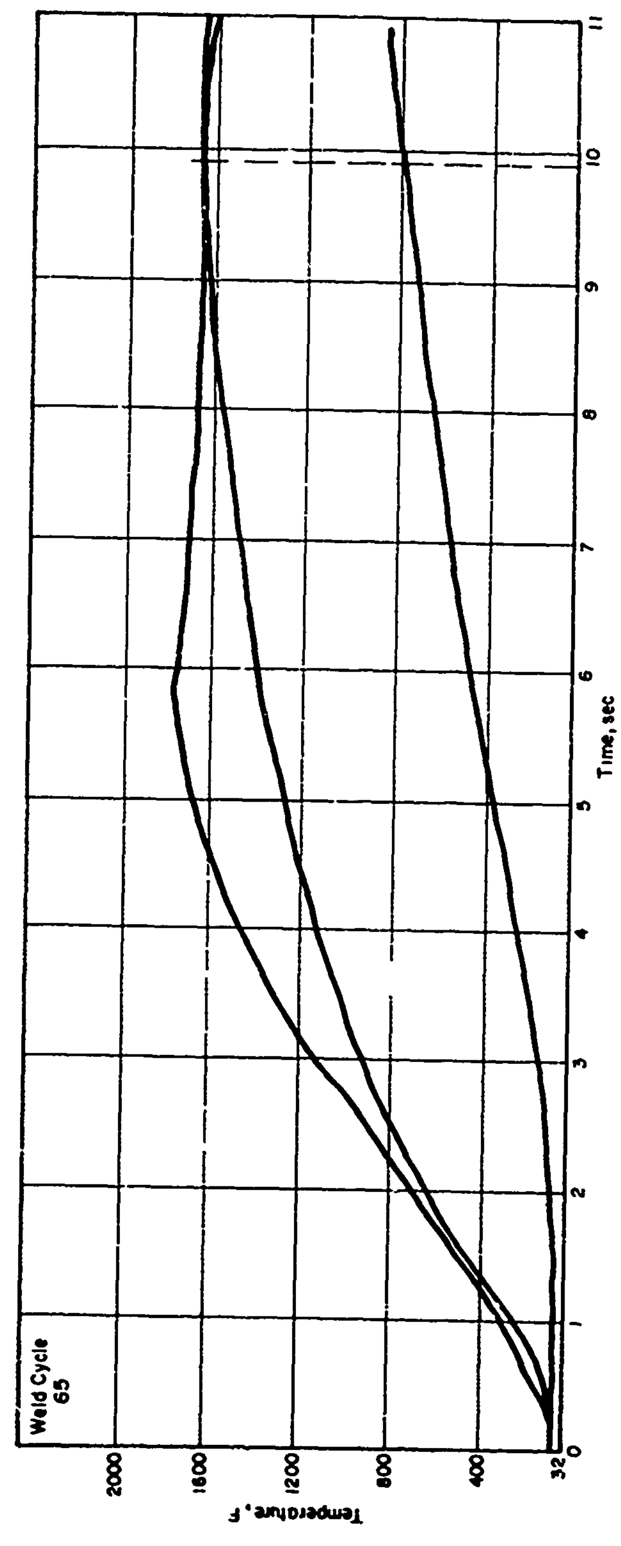
Weld Cycle
65
Temperature, F
2000
1600
1200
800
400
32
Time, sec
0
1
2
3
4
5
6
7
8
9
10
11

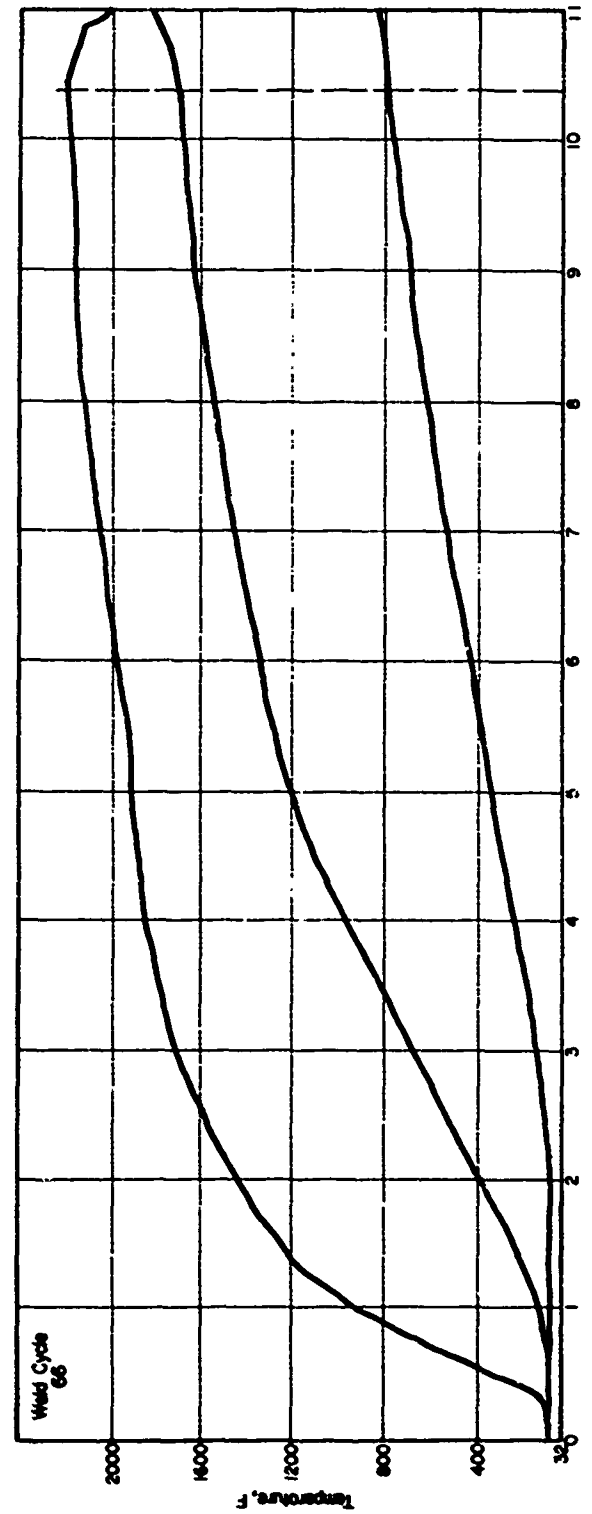
Weld Cycle 66
Temperature, F
Time, sec
2000
1600
1200
800
400
32
0
1
2
3
4
5
6
7
8
9
10
11

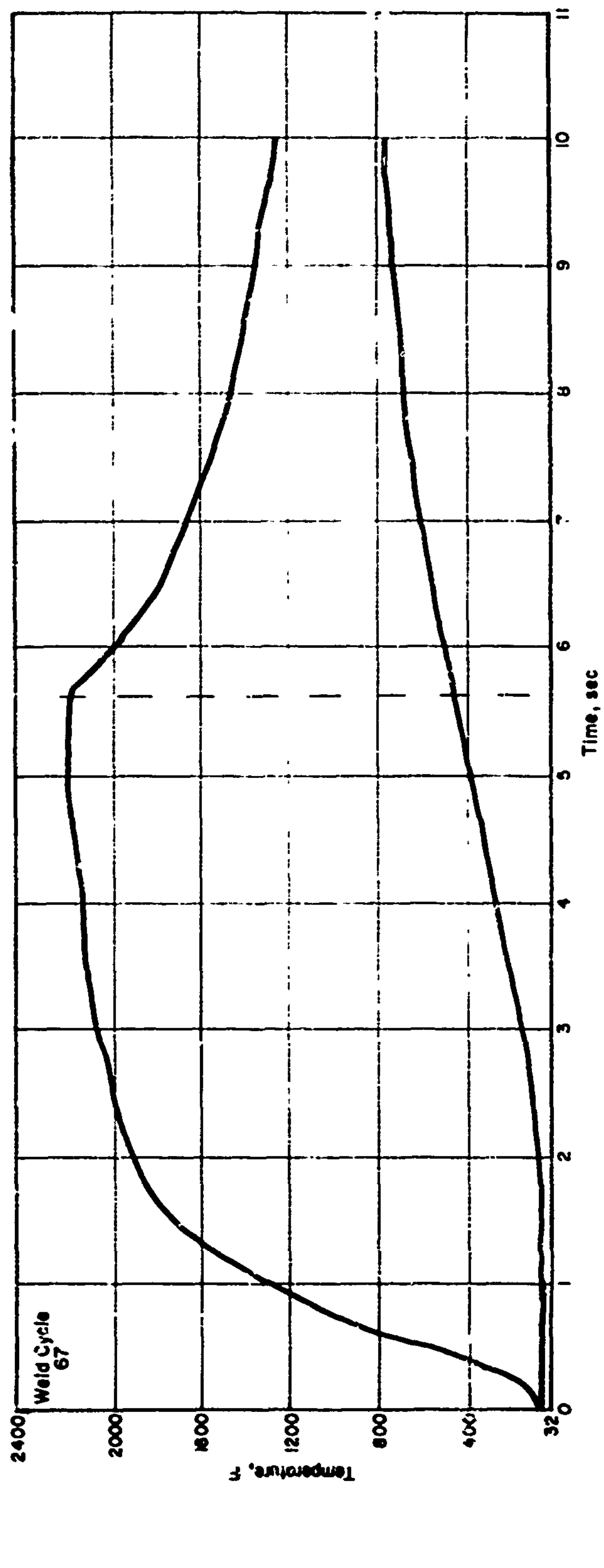
Weld Cycle 67
Temperature, F
2400
2000
1600
1200
800
400
32
Time, sec
0
1
2
3
4
5
6
7
8
9
10
11

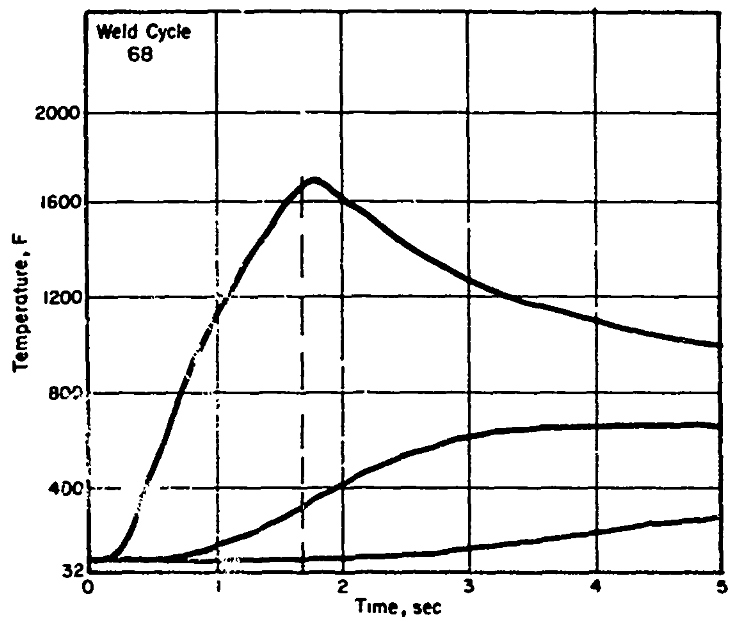
Weld Cycle
68
2000
1600
1200
800
400
32
0
1
2
3
4
5
Temperature, F
Time, sec

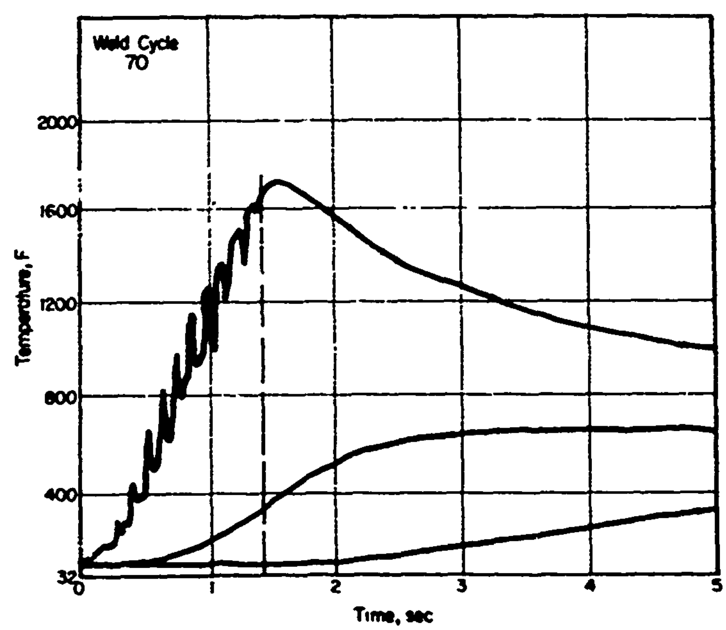
Weld Cycle
70
2000
1600
1200
800
400
32
0
1
2
3
4
5
Temperature, F
Time, sec

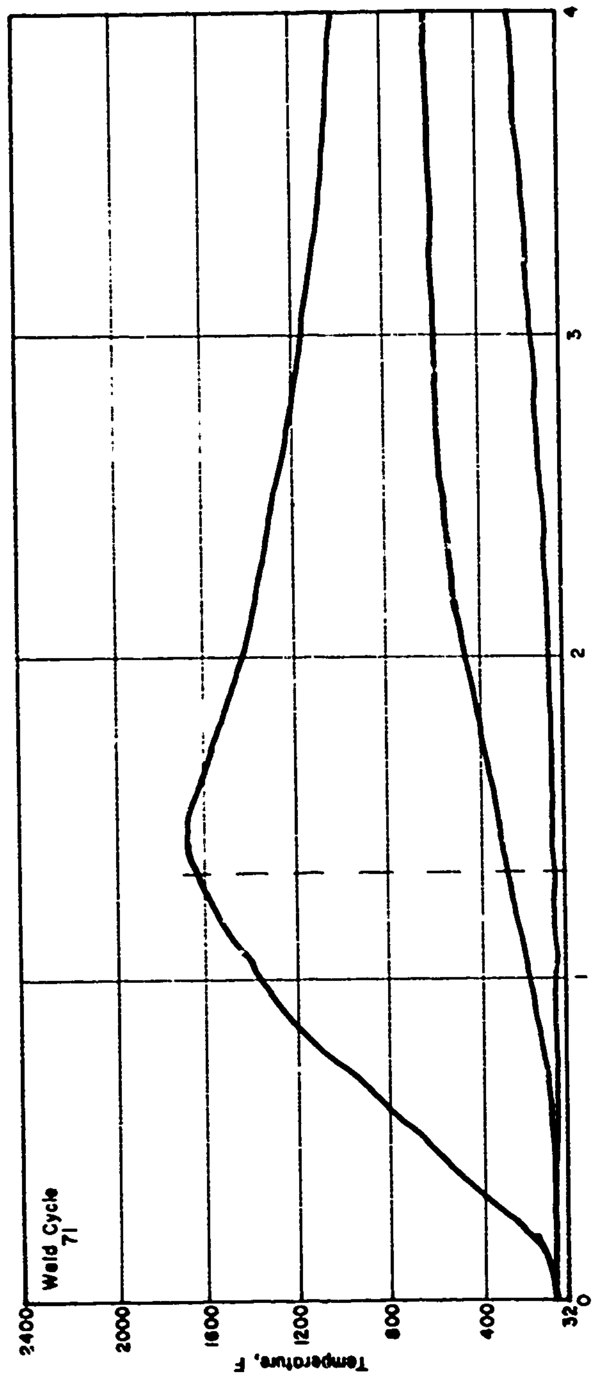
Weld Cycle
71
Temperature, F
2400
2000
1600
1200
800
400
32
Time, sec
0
1
2
3
4

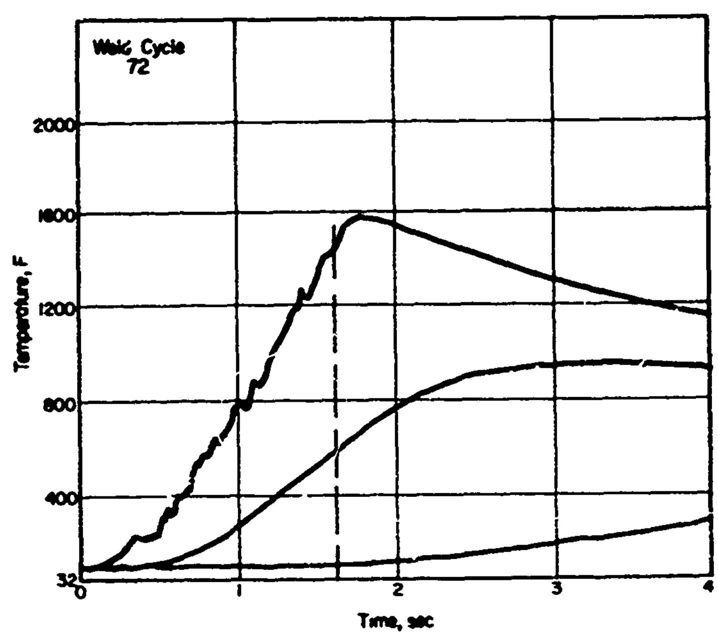

Weld Cycle
72
2000
1600
1200
800
400
32
Temperature, F
0
1
2
3
4
Time, sec

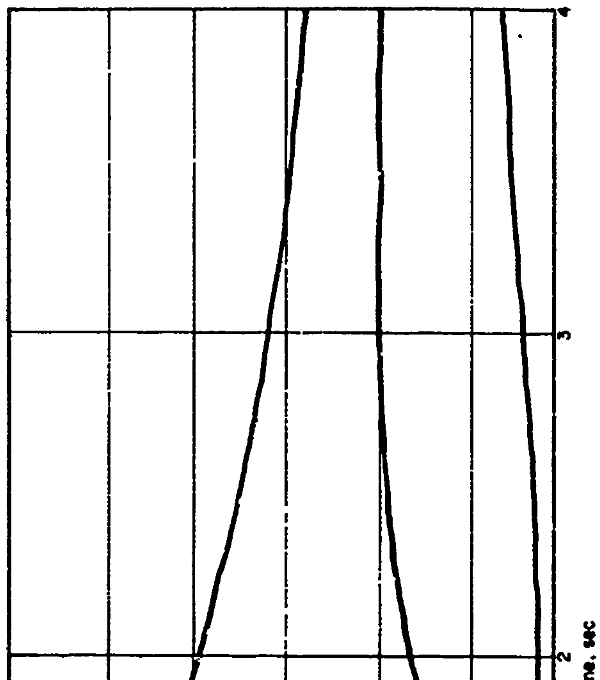

Weld Cycle 73
Temperature, F
2000
1600
1200
800
400
32
0
2
3
4
Time, sec

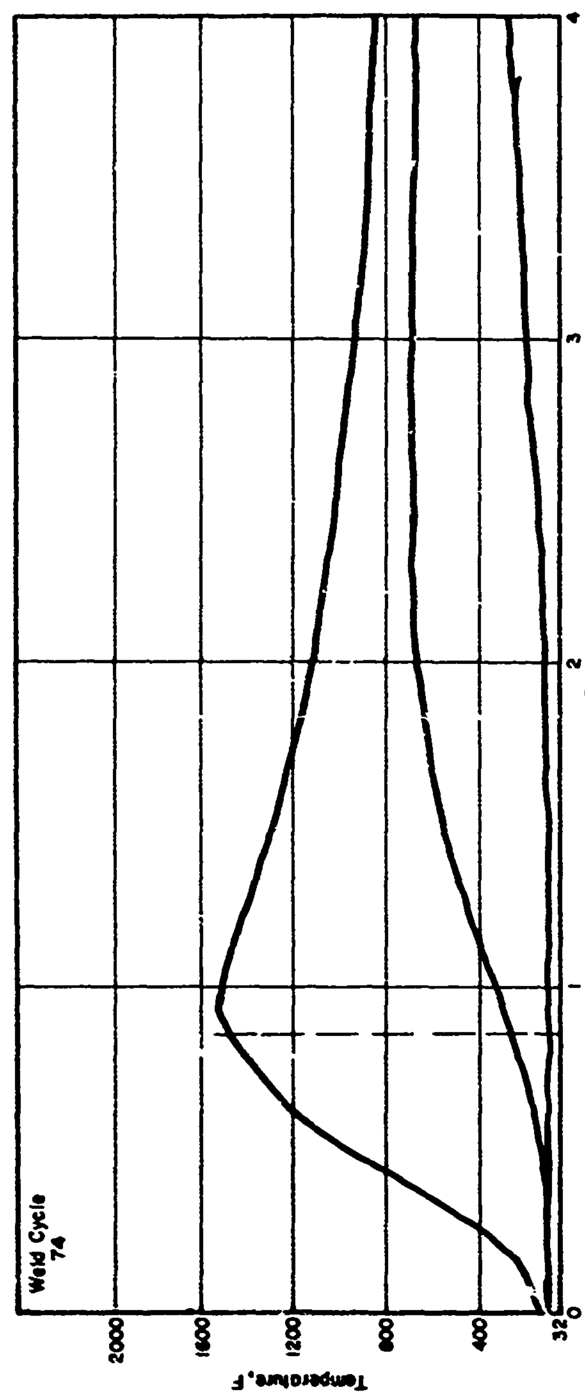
Weld Cycle
74
Temperature, F
2000
1600
1200
800
400
32
0
2
3
4
Time, sec

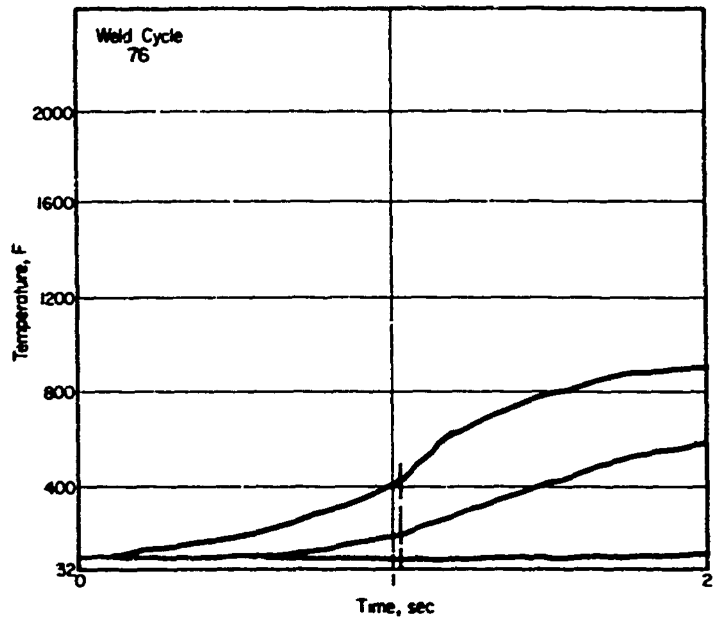
Weld Cycle
76
2000
1600
1200
800
400
32
Temperature, F
0
1
2
Time, sec

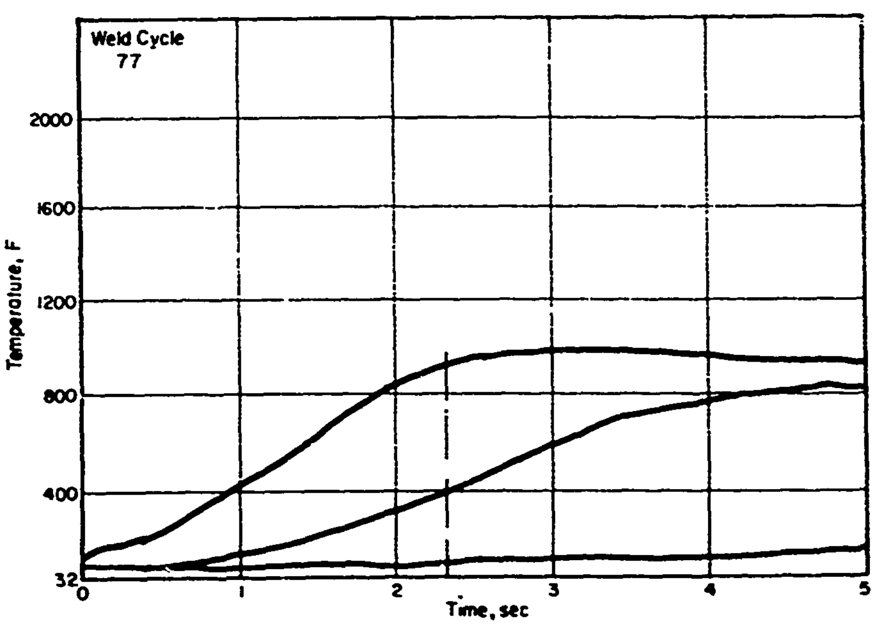
Weld Cycle
77
2000
1600
1200
800
400
32
Temperature, F
0
1
2
3
4
5
Time, sec

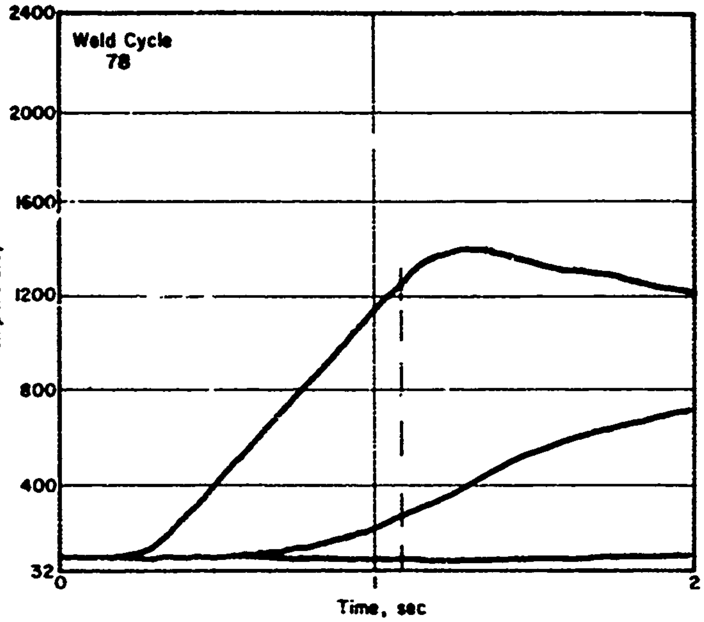
Weld Cycle
78
2400
2000
1600
1200
800
400
32
Temperature, F
0
1
2
Time, sec

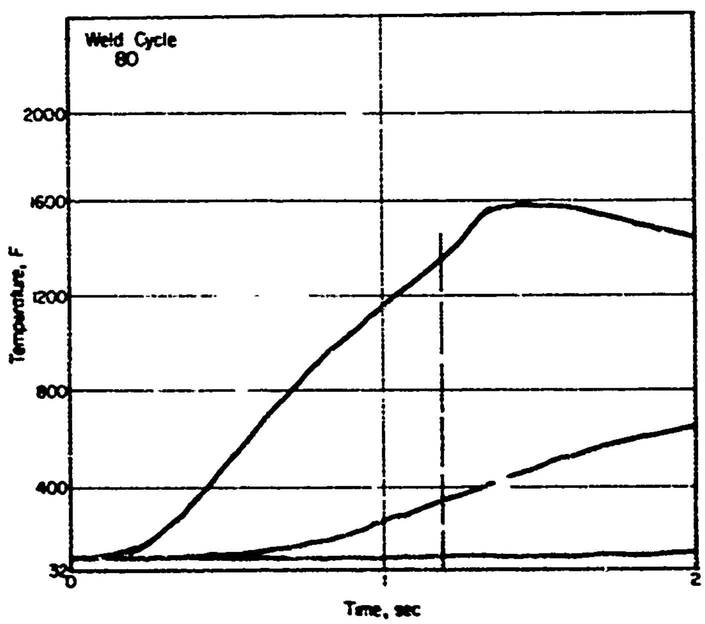
Weld Cycle
80
2000
1600
1200
800
400
32
Temperature, F
0
1
2
Time, sec

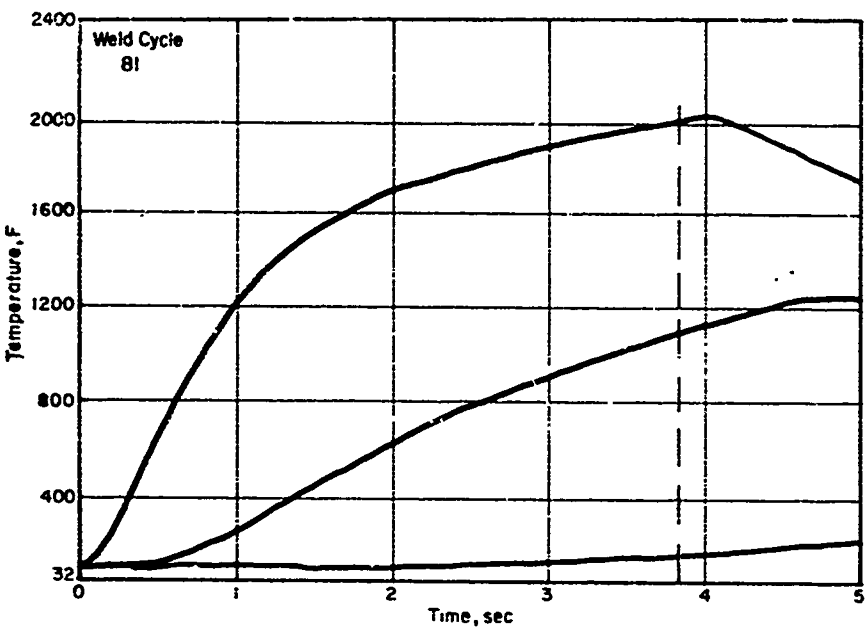

Weld Cycle 81
2400
2000
1600
1200
800
400
32
Temperature, F
0
1
2
3
4
5
Time, sec

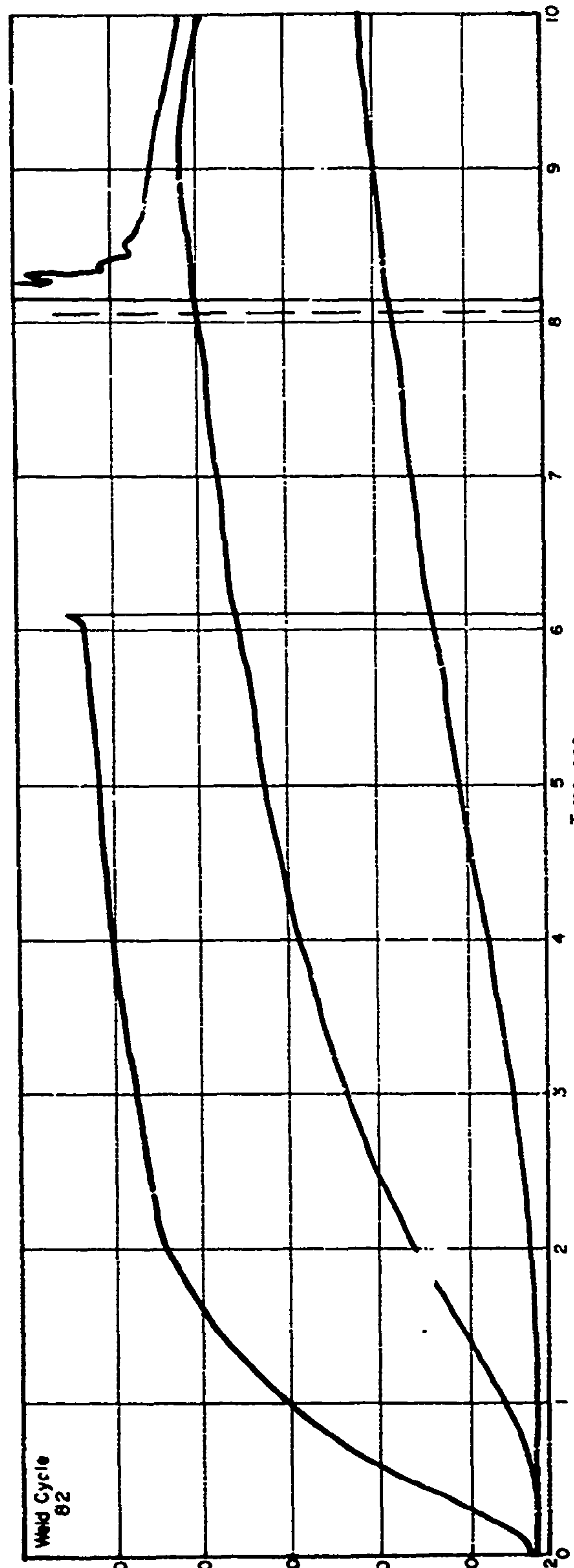
Weld Cycle
82
Temperature, F
32
400
800
1200
1600
2000
Time, sec
0
1
2
3
4
5
6
7
8
9
10

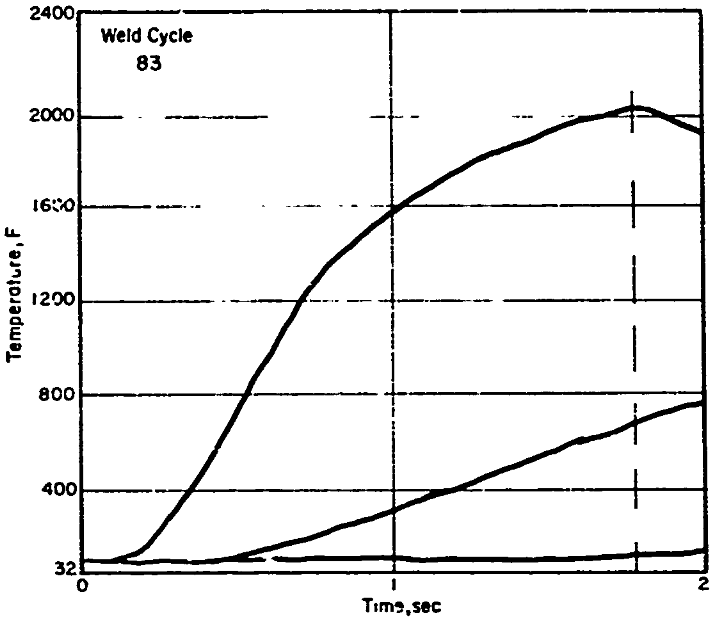
Weld Cycle
83
2400
2000
1600
1200
800
400
32
Temperature, F
0
1
2
Time, sec

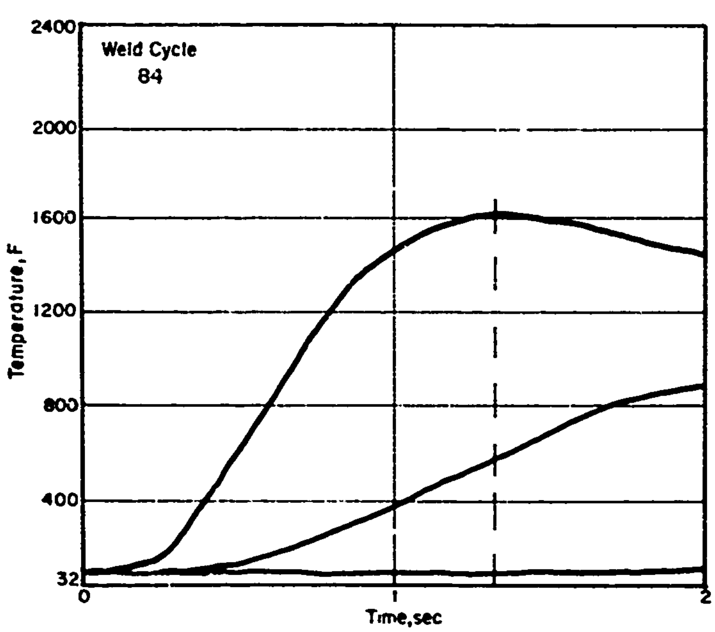
Weld Cycle
84
2400
2000
1600
1200
800
400
32
Temperature, F
0
1
2
Time, sec

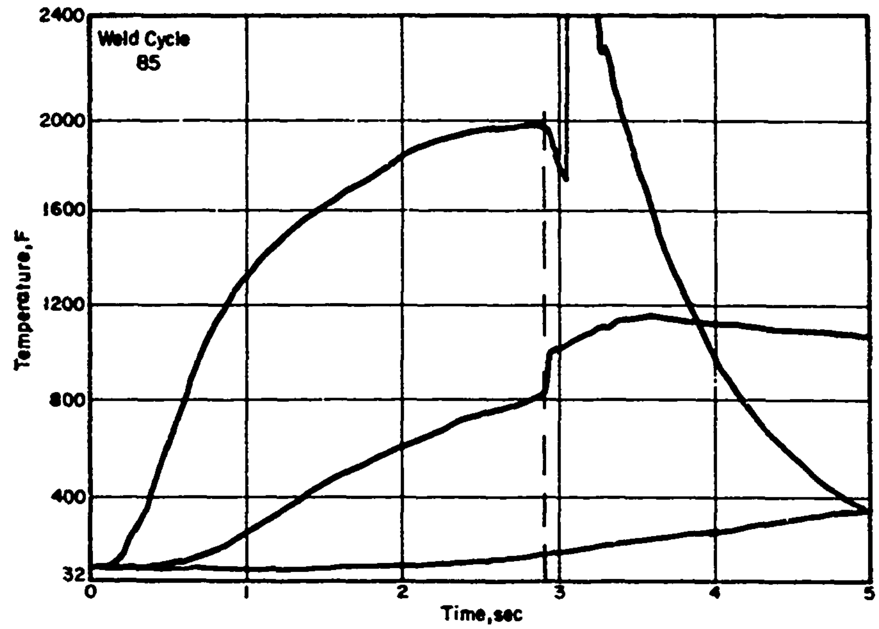
Weld Cycle
85
2400
2000
1600
1200
800
400
32
Temperature, F
0
1
2
3
4
5
Time, sec

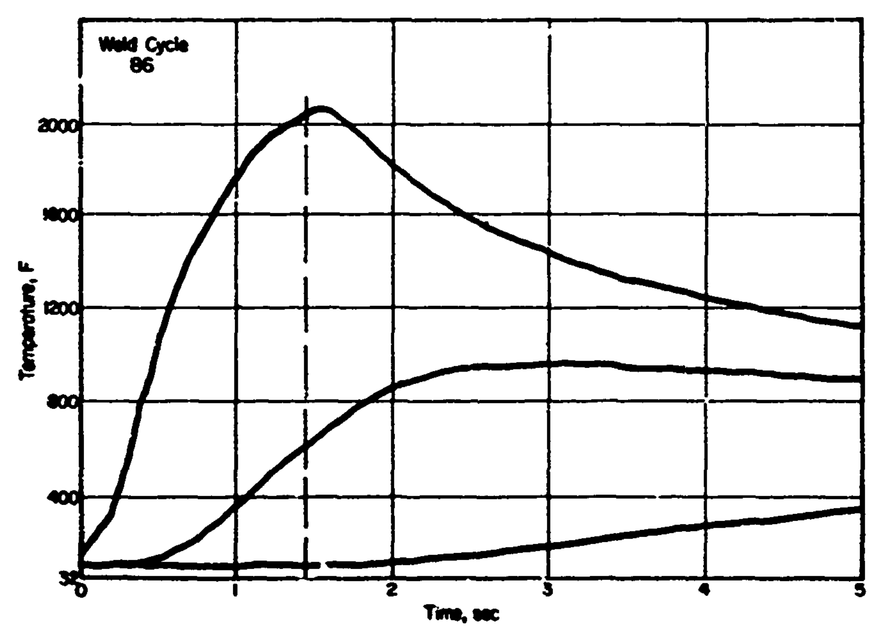
Weld Cycle
86
2000
1600
1200
800
400
Temperature, F
0
1
2
3
4
5
Time, sec

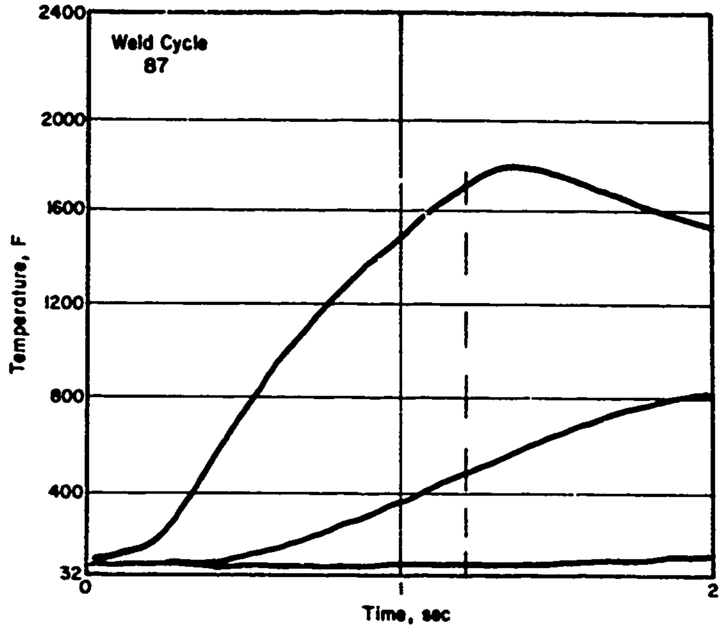
Weld Cycle
87
2400
2000
1600
1200
800
400
32
0
1
2
Temperature, F
Time, sec

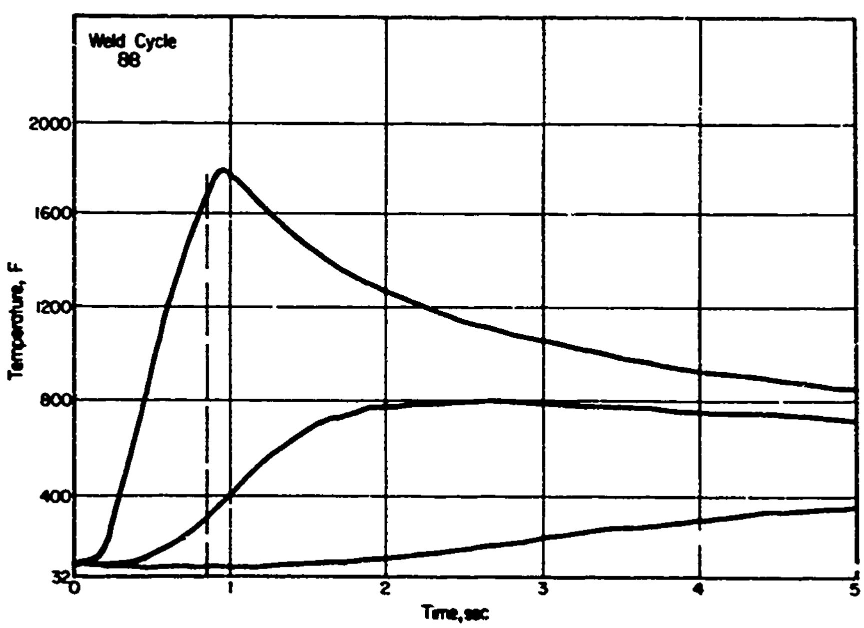
Weld Cycle
88
2000
1600
1200
800
400
32
0
1
2
3
4
5
Temperature, F
Time, sec

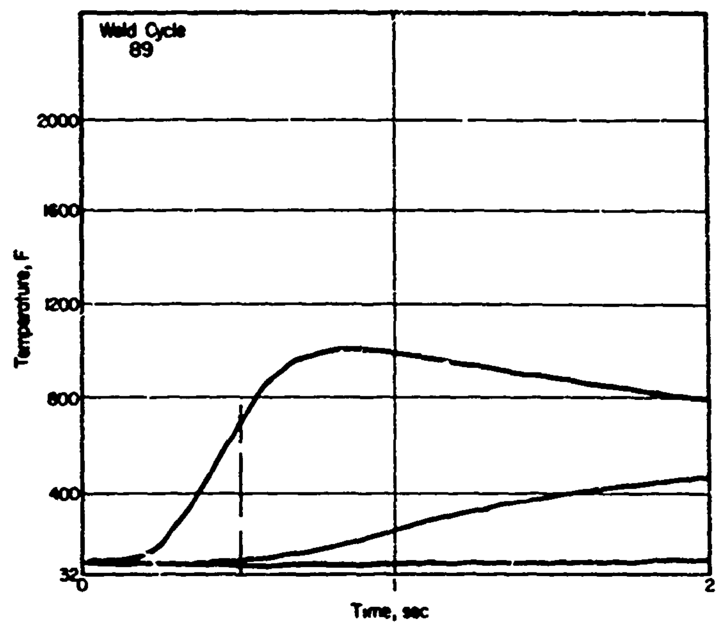
Weld Cycle
89
2000
1600
1200
800
400
32
Temperature, F
0
1
2
Time, sec

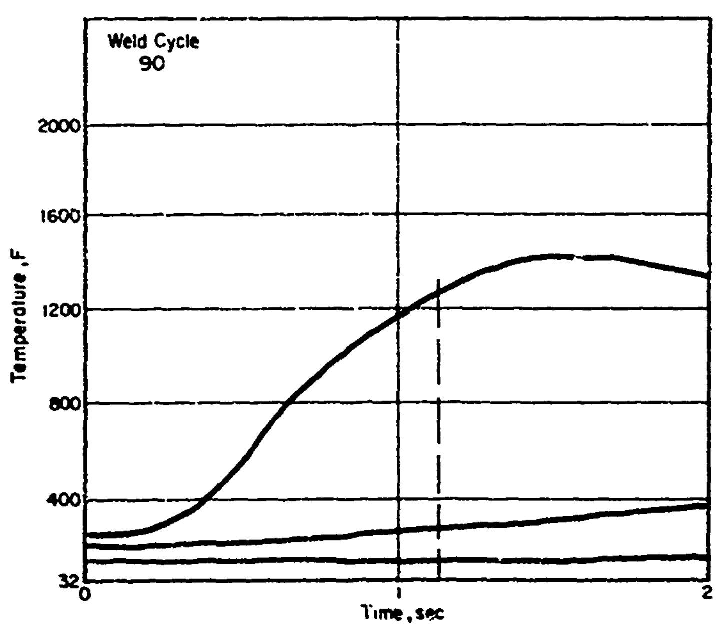
Weld Cycle
90
2000
1600
1200
800
400
32
Temperature ,F
0
1
2
Time, sec

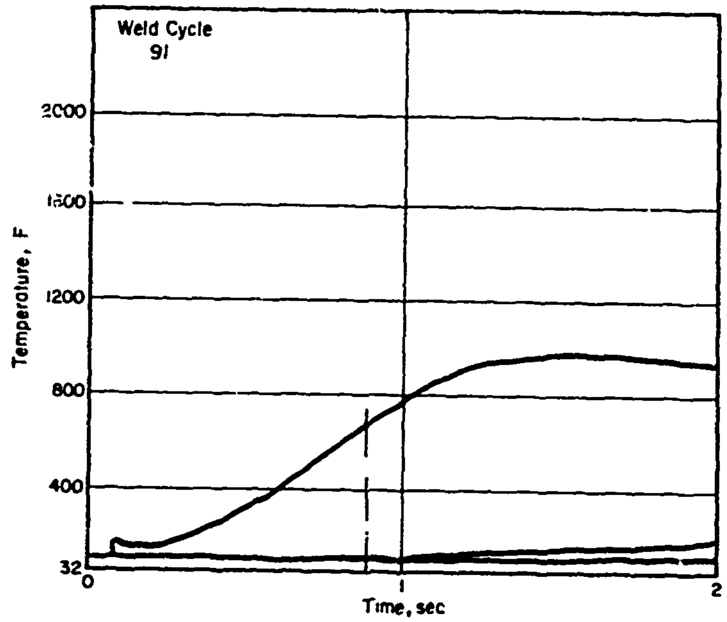
Weld Cycle
91
2000
1600
1200
800
400
32
Temperature, F
0
1
2
Time, sec

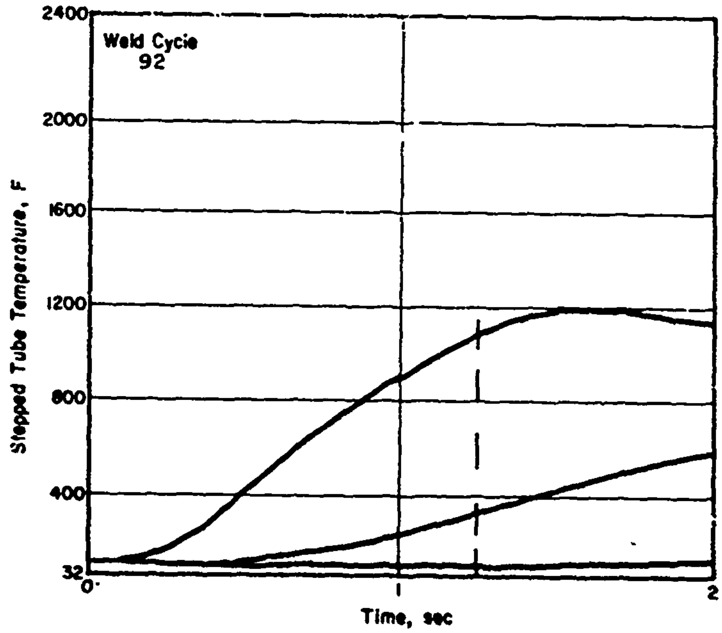
Weld Cycle
92
2400
2000
1600
1200
800
400
32
Stepped Tube Temperature, F
0
1
2
Time, sec

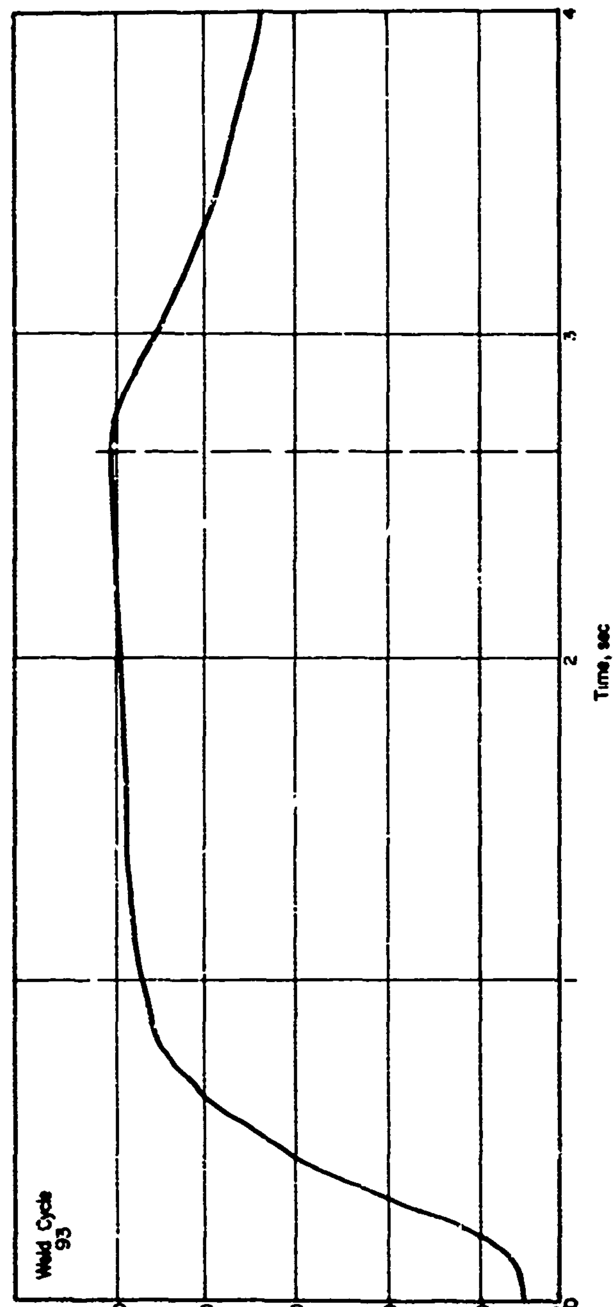
Weld Cycle
93
Thin Tube Temperature, F
2000
1600
1200
800
400
32
Time, sec
0
2
3
4

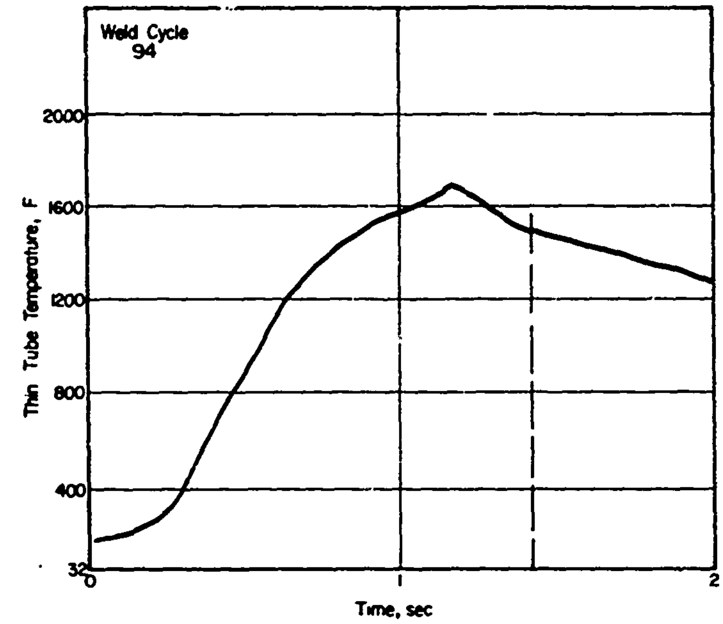
Weld Cycle
94
2000
1600
1200
800
400
32
0
1
2
Thin Tube Temperature, F
Time, sec

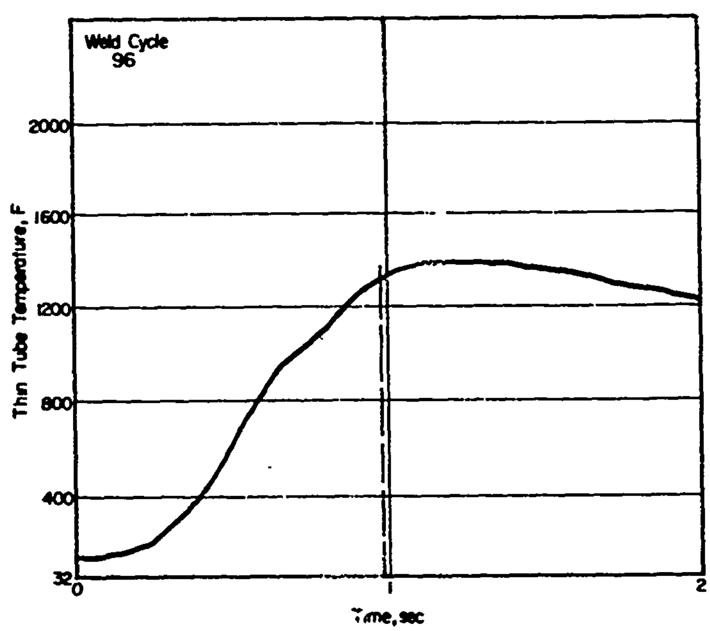
Weld Cycle
96
2000
1600
1200
800
400
32
0
1
2
Thin Tube Temperature, F
Time, sec

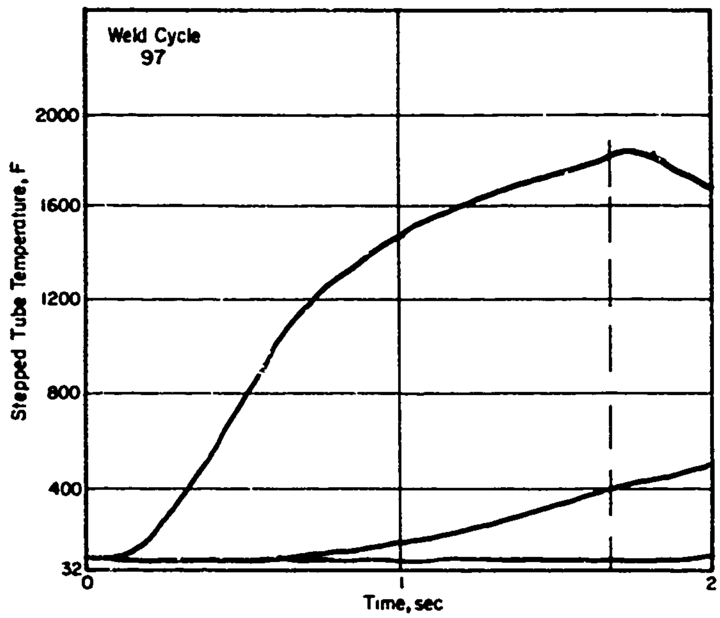

Weld Cycle 97
2000
1600
1200
800
400
32
Stepped Tube Temperature, F
0
1
2
Time, sec

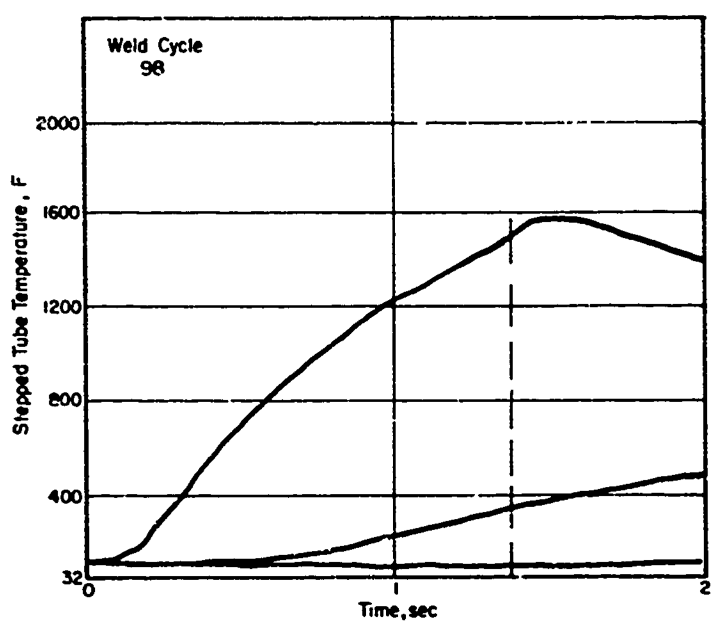

Weld Cycle 98
2000
1600
1200
800
400
32
Stepped Tube Temperature, F
0
1
2
Time, sec

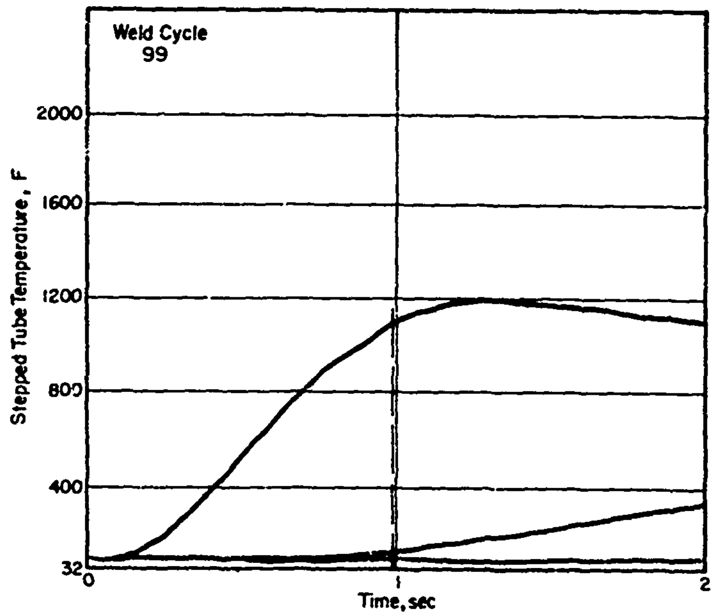

Weld Cycle
99
Stepped Tube Temperature, F
2000
1600
1200
800
400
32
0
1
2
Time, sec

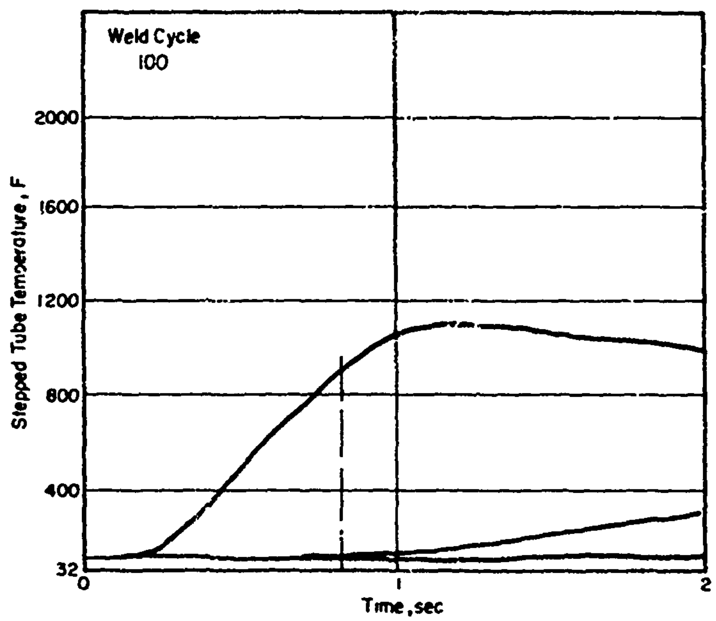

Weld Cycle
100
Stepped Tube Temperature, F
2000
1600
1200
800
400
32
0
1
2
Time, sec

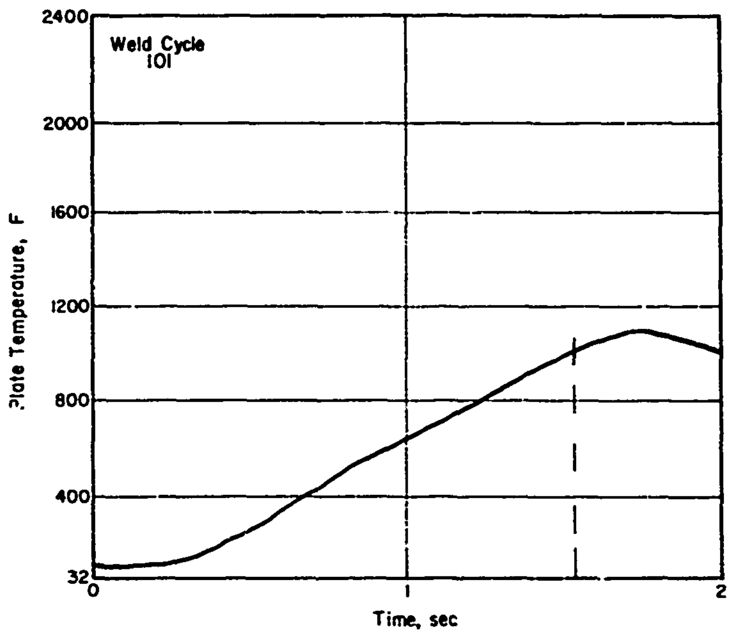

Weld Cycle 101
Plate Temperature, F
2400
2000
1600
1200
800
400
32
0
1
2
Time, sec

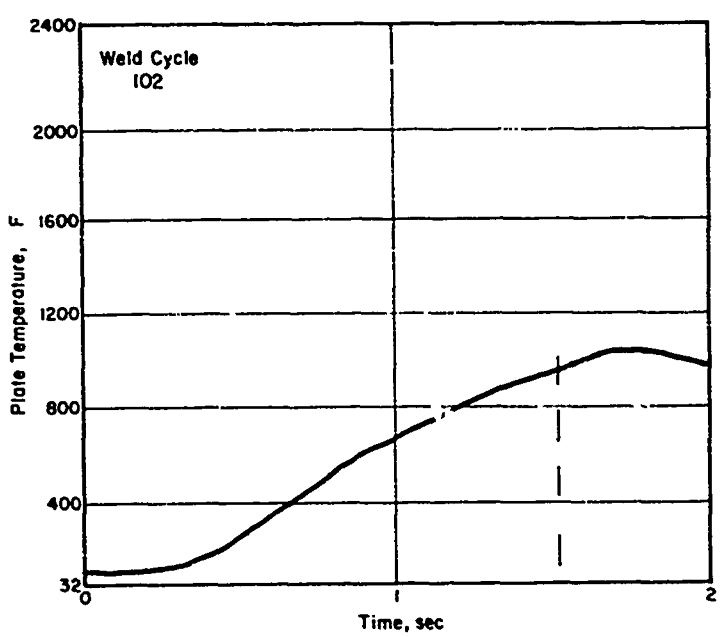

Weld Cycle 102
Plate Temperature, F
2400
2000
1600
1200
800
400
32
0
1
2
Time, sec

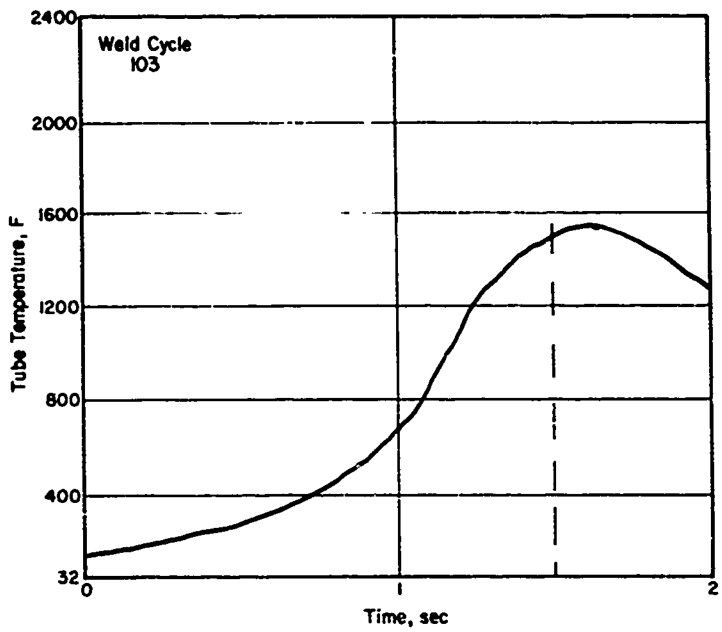
Weld Cycle
103
2400
2000
1600
1200
800
400
32
Tube Temperature, F
0
1
2
Time, sec

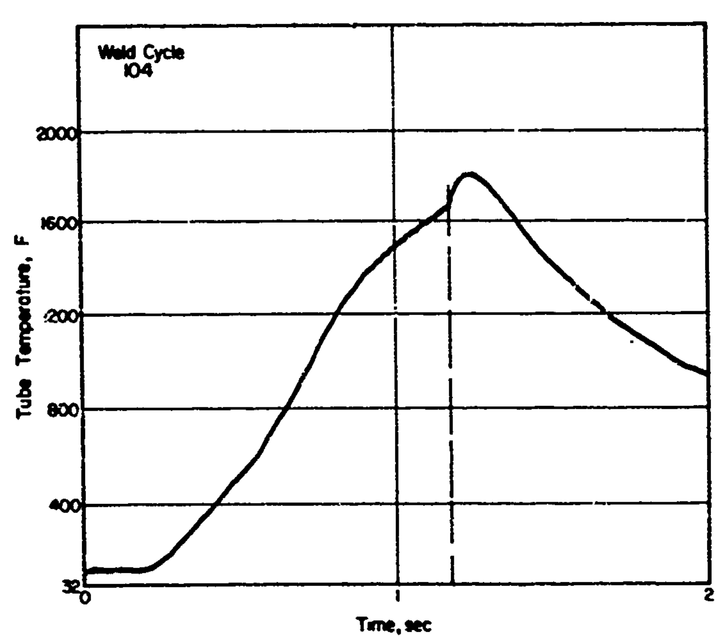
Weld Cycle
104
2000
1600
1200
800
400
32
Tube Temperature, F
0
1
2
Time, sec

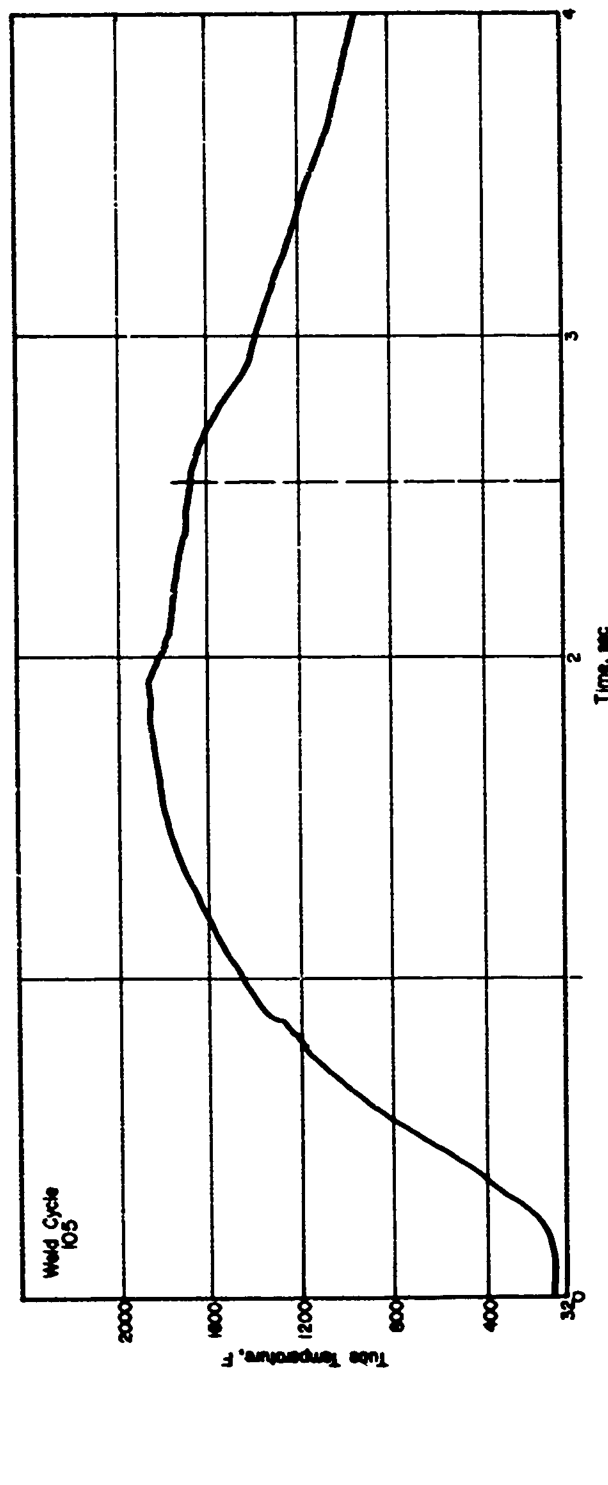
Weld Cycle
105
Tube Temperature, F
2000
1600
1200
800
400
32
0
2
3
4
Time, sec

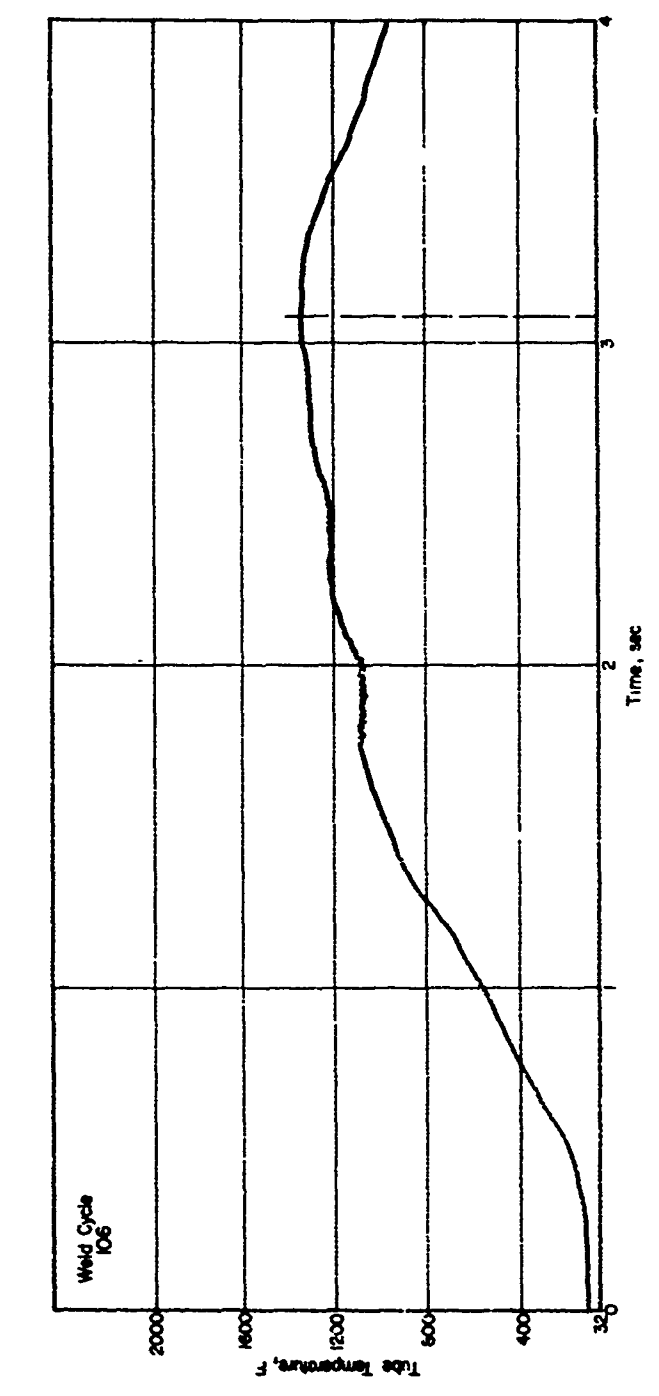
Weld Cycle
106
2000
1600
1200
400
32
0
2
3
4
Time, sec
Tube Temperature, F

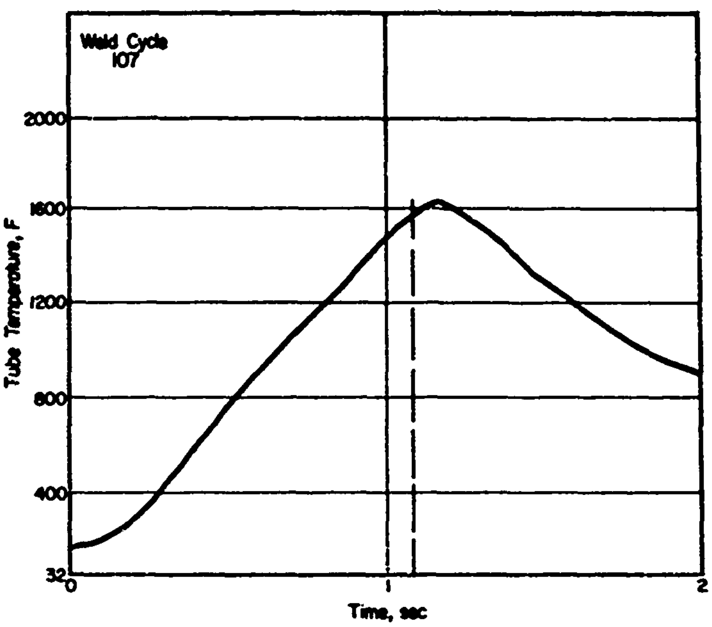
Weld Cycle
107
2000
1600
1200
800
400
32
Tube Temperature, F
0
1
2
Time, sec

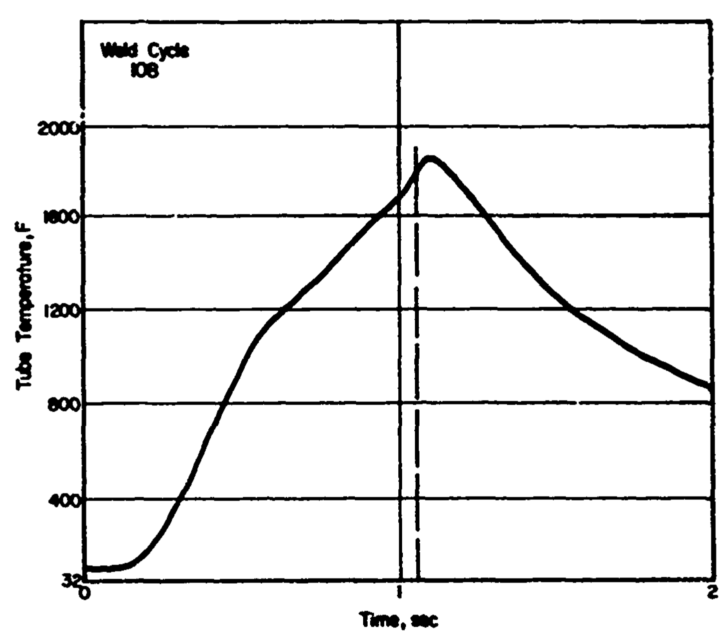
Weld Cycle
108
2000
1600
1200
800
400
32
Tube Temperature, F
0
1
2
Time, sec

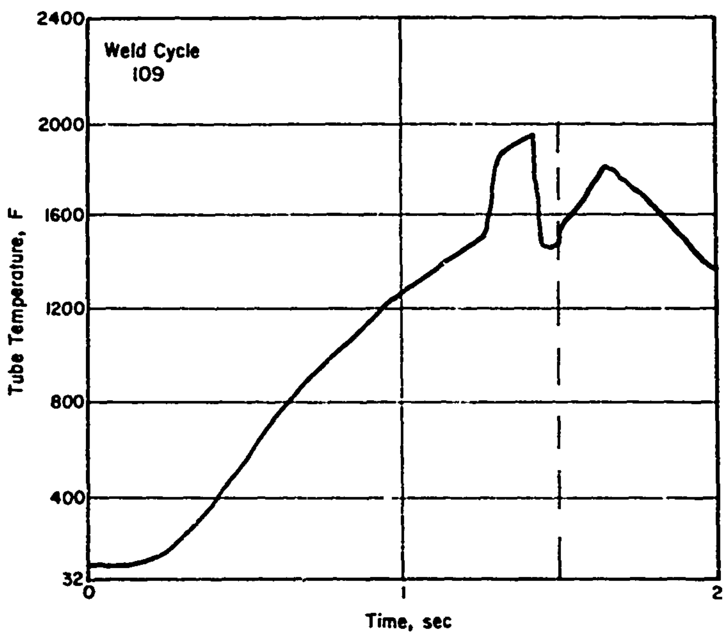

Weld Cycle
109
2400
2000
1600
1200
800
400
32
Tube Temperature, F
0
1
2
Time, sec

APPENDIX E

SUMMARIES OF MECHANICAL PROPERTIES

APPENDIX E

SUMMARIES OF MECHANICAL PROPERTIES

TABLE E-1. MECHANICAL PROPERTIES OF MARAGING STEEL SPECIMENS FROM PHASE II STUDIES

	Properties in the As-Welded Condition				Properties After 3-Hour, 900 F Maraging Treatments		
Weld Cycle	0.2% Offset Yield Strength, 10^3 psi	Ultimate Tensile Strength, 10^3 psi	Fracture Strain, percent	Maximum Bend Angle, degrees	0.2% Offset Yield Strength, 10^3 psi	Ultimate Tensile Strength, 10^3 psi	Fracture Strain, percent
26	136.0	153.5[a]	6.96	180	N.D.	N.D.	N.D.
35	--	111.5	0.79	15	--	195.0	0.43
36	133.0	153.0	5.33	180	260.0	261.0	1.14
37	128.5	149.5[a]	6.35	180	268.0	274.0[a]	3.71
38	--	91.8	0.13	15	--	211.0	0.24
39	--	115.5	0.76	5	--	112.0	0
40	124.5	150.0[a]	5.33	180	260.0	263.0	2.15
41	131.5	155.0	6.14	180	266.0	270.0	2.71
42	132.1	152.0[a]	7.41	180	272.0	278.0[a]	4.48
43	122.4	145.2	1.67	180	247.0	250.0	2.0
44	132.0	147.0	1.0	70	--	205.0	1.0
45	134.0	152.6[a]	5.0	70	245.0	250.0[a]	3.33
46	130.8	147.3[a]	2.33	180	258 5	270.0[a]	5.0
47	133.0	151.0[a]	5.66	180	248.0	254.5[a]	4.0
48	134.3	156.0[a]	8.34	180	238.0	246.0	4.0
49	129.5	147.0[a]	6.34	180	254.0	266.0	5.0
51	134.8	155.5[a]	7.44	180	--	244.0	1.35
52	124.8	150.0[a]	6.34	180	263.0	268.0	4.7
60	130.5	147.0[a]	5.39	180	--	214.0	0.34
61	128.5	146.0	5.05	180	273.0	276.0	1.35
65	126.0	148.0	6.06	71	258.0	261.0	1.68
66	132.5	148.5	6.06	180	260.0	272.0	5.39
67	131.0	149.0	6.06	180	269.0	270.0[a]	4.04
68	129.0	148.0[a]	7.74	6	--	206.0	1.01
69	127.0	147.0[a]	6.73	180	261.0	266.0	4.71
70	125.0	153.5[a]	8.08	135	262.0	255.0	5.05
71	126.0	150.0[a]	8.08	34	--	250.0	1.35
72	115.5	146.5[a]	7.74	56	261.0	266.0	5.39
73	116.5	148.5[a]	7.74	53	267.0	273.0	1.35
74	109.2	147.0[a]	8.75	29	--	231.0	0.67
75	--	80.5	0.5	5	--	38.3	0
76	123.2	144.8[a]	2.6	21	245.0	259.0[a]	1.8
77	144.5	158.0	1.5	11	232.0	253.0	5.5
78	120.0	149.2[a]	3.0	180	266.0[a]	270.0	1.1
80	127.0	147.0[a]	3.4	180	266.0	267.0[a]	2.6
81	127.3	149.0	2.0	180	248.0	250.0	3.5
82	133.5	154.0	8.0	180	264.0	268.0	1.3
83	112.4	133.5[a]	4.0	180	256.0	263.0	6.0
85	125.9	147.5[a]	3.6	180	265.0	268.0	5.5
86	120.5	145.0[a]	4.2	180	263.0	266.0	7.0
87	126.5	146.8[a]	4.2	180	264.0	269.0	7.5
88	155.0	166.5[a]	3.6	180	265.0	266.0	4.0
Control 1	112.0	152.0	3.7	N.D.	270.0	276.0	5.72
Control 2	112.0	152.5	11.45	N.D.	268.0	277.0	5.72
Control 3	N.D.	N.D.	N.D.	N.D.	270.0	281.0	6.06

(a) Fracture occurred outside of weld area.

TABLE E-2. MECHANICAL PROPERTIES OF 7075 ALUMINUM SPECIMENS FROM PHASE II STUDIES

Weld Cycle	0.2% Offset Yield Strength, 10^3 psi	Ultimate Tensile Strength, 10^3 psi	Fracture Strain, percent	Maximum Bend Angle, degrees
54	--	37.3	1.5	3
54	--	35.6	2.0	
55	--	13.4	2.0	8
55	--	13.1	2.5	
57	--	38.8	2.0	8
57	--	36.6	2.0	
58	50.2	50.5	2.5	5
58	--	50.3	2.0	
59(a)	--	46.0	2.0	8
59(a)	--	44.0	1.5	
Control 1	82.0	89.0	11.5	
Control 2	81.3	88.3	13.5	
Control 3(b)	80.0	88.5	16.0	
Control 4(b)	81.2	89.4	15.0	

(a) Specimens stress relief annealed 870 F, 50-minute, water quenched prior to welding; precipitation treated 24 hours, 250 F after welding.

(b) Control specimens given same heat-treat sequence as welded specimens.

TABLE E-3. MECHANICAL PROPERTIES OF MARAGING STEEL SPECIMENS FROM PHASE III STUDIES

	Properties in the As-Welded Condition			Properties After 3-Hour 900 F Maraging Treatment		
Weld Cycle	0.2% Offset Yield Strength, 10^3 psi	Ultimate Tensile Strength, 10^3 psi	Fracture Strain, percent	0.2% Offset Yield Strength, 10^3 psi	Ultimate Tensile Strength, 10^3 psi	Fracture Strain, percent
		Tube-To-Tube Half-Lap Joint Configuration				
92	--	122.0	0.58	--	192.0	0.58
93	162.0	170.0	1.68	288.0	291.0	--
94	162.0	169.5	1.75	--	282.0	0.97
95	150.0	163.0	1.23	294.0	299.0	1.68
96	155.2	168.5	1.75	--	238.0	0.77
97	156.0	166.5	2.57	271.0	273.0	1.08
98	153.5	167.0	3.00	--	262.0	0.94
99	--	139.0	0.69	--	127.2	0.45
100	160.5	168.0	1.18	--	268.0	1.00
		Tube-To-Plate Half-Lap Joint Configuration				
101		138.0		67.8		
102		158.5		279.0		
103		153.8		122.5		
104		153.4		202.5		
105		136.5		144.5		
106		148.0		53.1		
107		138.5		142.5		
108		120.0		150.0		
109		150.0		169.0		

APPENDIX F

FRICTION WELDING MARAGING STEEL TO ALUMINUM

APPENDIX F

FRICTION WELDING MARAGING STEEL TO ALUMINUM

Even though this program has demonstrated that extruded tubes of 7075 aluminum alloy could not be satisfactorily friction welded, it was desired to investigate the possibility of friction welding 18Ni(250) maraging steel tubes to another, more weldable, aluminum alloy of interest to the Missile Command. The 2014 alloy, widely used in missile systems, was found to be unavailable in any form from commercial warehouses. It was therefore decided that this cursory investigation of the feasibility of friction welding aluminum to maraging steel should be conducted using the 6061 aluminum alloy which is readily obtainable in a variety of shapes and sizes.

Three friction-welding experiments were carried out between maraging steel and aluminum alloy tubes having mean diameters of 2.79 in., but significantly different cross sectional areas. Diameter-to-wall thickness ratios (D/T) of the maraging steel components were approximately 30:1 while those of the mating aluminum-alloy components were approximately 14.3:1. The greater wall thickness of the aluminum alloy components was designed to reduce the probable occurrence of simple mechanical heading or extrusion of the aluminum component by the much harder steel component during the heating portion of the friction welding cycle.

The first friction-welding experiment was, as indicated in Table F.1, carried out at a relative rotational velocity of 2000 rpm (1470 sfm) and an axial heating pressure of 3600 psi. Rotation was stopped and a forging pressure of 12,400 psi applied after the axial displacement had reached about 0.220 in. Although this specimen appeared to be welded, the components separated during sectioning for metallographic inspection. Two explanations for this behavior can reasonably be considered. First, it is possible that little or no metallurgical bonding occurred at these welding conditions and the specimen components were only mechanically held together by the residual stresses created by differential thermal contraction between the components after the weld cycle was completed. Sectioning of the specimen for metallographic inspection would then have provided a mechanism for relieving these stresses, thus allowing the components to separate. Alternatively, a significant layer of Fe-Al and/or Ni-Al intermetallic compound may have formed and been retained at the weld interface, possibly as a result of the relatively low heating pressure employed. The intermetallic compound layer would lead to a weak, brittle bond that is, in addition, highly stressed by differential thermal contraction subsequent to welding. Sectioning of the specimen would, again, provide a mechanism for relief of these stresses which might be sufficient to rupture the bond.

TABLE F-1. SUMMARY OF CONDITIONS USED TO FRICTION WELD MARAGING STEEL TO ALUMINUM TUBES

Weld Cycle	Mean Specimen Dia., in.	Faying Area, in.^{2}	Rotational Velocity, rpm	Pressurization Rate, psi/sec	Heating Pressure, psi	Conditions of Cycle Termination: Torque, ft-lb	Conditions of Cycle Termination: Upset, in.	Forging Pressure, psi	Cycle Time, sec
118	2.786	0.661	2000	Impulsive	3630	40	~0.220	12,400	2.42
123	2.787	0.652	270	Impulsive	4450	175	0.051	14,700	2.82
124	2.789	0.661	270	7500	4540	170	0.052	15,400	3.17

The remaining two friction-welding experiments were carried out at a relative rotational velocity of 270 rpm (197 sfm), axial heating pressures of approximately 4500 psi, axial forging pressures of approximately 15,000 psi, and total axial displacements of about 0.075 in. These welding conditions were determined by applying the appropriate scale factors to those conditions previously found to produce satisfactory friction welds between 1/4-in.-diameter rods of Type 304 stainless steel and 6061 aluminum.[a] The axial heating pressure was applied impulsively during one of these experiments and at a rate of 7500 psi/sec during the other. Both of these welds appeared, superficially, to be sound as shown by the representative microstructure of Figure F.1. Although no mechanical-property determinations were attempted, both welded segments remained tightly joined after removal of the metallographic specimens and the resultant mechanical stress relief.

18Ni(250) Maraging Steel

6061-T6 Aluminum

505X As-Polished

FIGURE F-1. MICROSTRUCTURE OF FRICTION WELDED JOINT BETWEEN ALUMINUM ALLOY AND MARAGING STEEL TUBES

Welding Conditions: 270 rpm; 4540 psi heating pressure; 15,400 psi forging pressure; ~ 0.075 in. upset; 3.15 sec.

(a) Meiners, K. E., Smith, E. G., Jr., and Gripshover, P. J., "Final Report to Lawrence Radiation Laboratory on Project SANL 102/18 and 102/28", BMI-X-301 (July 24, 1964). (SRD).

As anticipated, essentially all of the axial deformation occurring during these three welding experiments was from upsetting of the aluminum component with no noticeable changes in the maraging steel components. This is evidenced in Figure F-1 by the scalloped appearance of the weld interface. The scallops resulted from the cutting tool used to face off the maraging steel component faying surfaces during specimen fabrication.

It is interesting to note (see Table F-1) that high rotational speed (2000 rpm) yielded a much larger axial displacement than that achieved by a slower rotation at 270 rpm. Further, the increased axial displacement achieved at 2000 rpm occurred under lower heating pressure and in a shorter time than those experienced at 270 rpm. This, again, is in direct contrast to the results of other investigators[b] who indicate that the time to reach a given axial displacement decreases with decreasing peripheral velocity.

Based on this most superficial study, it can be concluded that maraging steel can be successfully friction welded to some aluminum alloys in tubular form under the proper conditions of speed, pressure, and displacement. It must be noted, however, that the conditions studied here may not be those needed to produce optimum quality welds between these two materials and it is recommended that further, more detailed investigations be conducted before considering production friction welding of maraging steel to aluminum components. The results of this study also suggest that the quality of aluminum to maraging steel tubular friction weld joints might be enhanced or the range of conditions producing acceptable joints might be increased by using a tapered rather than a flat-butt joint design to take advantage of the thermal contraction-induced stresses created during post-weld cooling.

(b) Vill, V. I., Friction Welding of Metals, American Welding Society (1962), Page 27.